

Aus dem Institut für Immunologie
im Biomedizinischen Centrum
der Ludwig-Maximilians-Universität München
Vorstand: Prof. Dr. Thomas Brocker



How central tolerance shapes the polyclonal CD4
T cell repertoire specific for the central nervous
system antigen myelin proteolipid protein 1

Dissertation
zum Erwerb des Doktorgrades der Naturwissenschaft
an der Medizinischen Fakultät der
Ludwig-Maximilians-Universität zu München

vorgelegt von
Tobias Johannes Haßler
aus Amberg
2020

Mit Genehmigung der Medizinischen Fakultät
der Universität München

Erster Gutachter:

Prof. Dr. Ludger Klein

Zweiter Gutachter:

Prof. Dr. Gerhild Wildner

Dekan:

Prof. Dr. med. dent. Reinhard HICKEL

Tag der mündlichen Prüfung:

18.03.2021

In Erinnerung an meine Großeltern

ACKNOWLEDGMENTS	6
SUMMARY	8
ZUSAMMENFASSUNG	9
1 INTRODUCTION	11
1.1 Thymus	11
1.2 Maturation of $\alpha\beta$ T cells in the thymus	12
1.2.1 DN Phases	12
1.2.2 Positive and negative selection in the cortex	14
1.2.3 Negative and agonist selection in the medulla: the final maturation steps	17
1.3 Peripheral tolerance mechanisms	21
1.4 Signal strength-based models of thymocyte selection	25
1.5 The endogenously expressed model antigen myelin proteolipid protein 1	27
2 AIM OF THE SUBMITTED THESIS	30
3. MATERIALS & METHODS	31
3.1 Materials	31
3.1.1 Chemicals, Enzymes and Media	31
3.1.2 Cell lines and Bacteria	31
3.1.3 Antibodies	32
3.1.4 PLP1 peptides	33
3.1.5 Vectors	33
3.1.6 Animals	34
3.1.7 Oligonucleotides	34
3.1.8 Commercial Kits	36
3.2 Methods	37
3.2.1 Bioinformatic methods	37
3.2.2 Immunization	37
3.2.3 Molecular Biology	38
3.2.4 Flow Cytometry	46
3.2.5 Cell culture	48
4 RESULTS	49
4.1 Generation of PLP1:I-A^b tetramers	49

4.2 PLP1-specific T cells within the polyclonal T cell repertoire	52
4.3 PLP1-specific T cells in a repertoire of reduced diversity	54
4.3.1 Characterization of Fixed- β mice	54
4.3.2 T _{reg} phenotype of peripheral Tet-1 ⁺ T cells in PLP1-sufficient mice	55
4.3.3 Anergic phenotype within the Tet-1 ⁺ T cell population in the presence of tolerizing-antigen	56
4.3.4 Central tolerance clonally diverts and deletes self-reactive T cells	58
4.3.5 Mature autoreactive thymocytes express anergy markers	59
4.3.6 Clonal deletion and clonal diversion require PLP1 expression by TECs and depend on AIRE	60
4.3.7 CD11c expressing cells are responsible for peripheral T _{reg} cell induction	63
4.4 TCR repertoire of Tet-1⁺ T cells	64
4.5 Characterization of selected PLP1-specific TCRs in transgenic mice	68
4.5.1 Hierarchy of functional avidity to PLP1	71
5. DISCUSSION	73
5.1 Establishment of the tetramer technology	73
5.2 Polyclonal T cell repertoire reveals clonal diversion as major tolerance mechanism	74
5.3 Tolerance mechanisms in a repertoire of reduced complexity	75
5.4 Tolerance-inducing factors in a repertoire with reduced diversity	77
5.5 How central tolerance affects individual PLP1-specific T cell clones	78
5.6 Characterization of selected TCR candidates	80
6. CONCLUSION	85
7. APPENDIX	103
7.1 Table of figures	103
7.2 Abbreviations	105
7.3 Eidesstattliche Versicherung	107

Acknowledgments

At first I would like to express my gratitude to everybody who has contributed to the work in this thesis.

The first one to name is Prof. Ludger Klein. **Ludger**, thank you very much for the appreciation and trust you have shown me. Not only have you enabled me to work on a promising and exciting topic, but you have also given me the opportunity to prove myself at numerous congresses, retreats and in the labs of our collaboration partners worldwide. Thanks to your guidance I was able to develop immunologically, but above all personally.

Dear **Christine**, you also have contributed a lot to this development. Not only did you take over the supervision of Maria, you supported me at any time with advice (professionally and life related) and practical assistance. Without your help this doctoral thesis and our publication would have never been possible. You are one of the lab members with whom I enjoyed my time in the lab so much and who make it hard for me to leave.

Dear **Maria**, unfortunately our professional relationship was only of short duration but nevertheless very intense. Thank you for not only convincing me to work with you and Christine on this topic and in this group, but also for always supporting me with words and deeds.

Manu, Sebi und Barbara through your help we were able to answer further questions on the PLP1 topic, which pushed not only our publication but also this doctoral thesis forward - Thank you very much. Furthermore, together with **Madlen**, you made the time in the lab more enjoyable.

Dear **Ursula**, thank you very much for everything. You always took care of my worries and needs and also made sure that I was able to travel around the world safely - not least, thanks to your precious car, we will treat it with care.

Another important person for my (all our) well-being in the lab was **Sonja**. Thanks for the technical help in the beginning, but even more I enjoyed your little encouragements over the years.

Ali, Thomas, Dileepan, Marc and Eric - through the collaboration with you many open questions could be clarified. With your help we were able to push the project forward and achieve some successes. Many thanks.

To all the group members of the whole Klein lab - who have joined and left over the years - thanks for your suggestions and help at any time.

I would also like to express my appreciation to people outside the laboratory who have contributed no less to this work. A big thank you to **Christian** and his team from Comunico for their cooperation over the past years. I hope for many more great events (on a professional or private level) with you in the future.

Datzi, Matze, Philipp and Ursi thanks for the brilliant study - without you I would have never written these lines. To many more amazing years together. Noteworthy, Philipp thanks for the extra portion of motivation.

To my **family**, especially my unfortunately already deceased grandparents, a heartfelt thank you for your support over the last years.

Infine, la persona più importante, **Betta**, e la principale ragione della mia felicità in questi ultimi anni. Mi considero davvero fortunato ad averti avuto al mio fianco dal primo momento in laboratorio e ancora di più perché, grazie alla tua ingegnosa trappola, ci rimarrai. Grazie per il tuo instancabile impegno nell'introdurmi al mondo dell'immunologia e alla dolcezza della vita italiana con **Giorgio**. Non vedo l'ora di scoprire il nostro futuro insieme e sono curioso di vedere cos'altro ci riserverà.

Summary

The fate of a developing T cell is dependent on the interaction of its T cell receptor (TCR) and the self-peptide MHC complex on thymic antigen presenting cells. According to the classical affinity/avidity model of thymocyte selection, the degree of auto-reactivity determines if potentially harmful T cells are diverted into regulatory T cells (intermediate affinity/avidity) or clonally deleted (high affinity/avidity). Nevertheless, how central tolerance induction to a physiological self-antigen is set in the polyclonal repertoire is still poorly understood.

In the presented thesis, we are focusing on the naturally-expressed tissue-restricted antigen myelin proteolipid protein 1 (PLP1), the main component of the myelin sheath, as it is discussed to be one of the putative target antigens in multiple sclerosis (MS) in humans. Upon PLP1 immunization, non-tolerant murine strains develop experimental autoimmune encephalomyelitis (EAE), a MS-like disease, whereas C57BL/6 mice are resistant to EAE and lack recall responses, due to the expression of PLP1 in thymic epithelial cells. Klein *et al.* previously showed that, upon immunization of PLP1-deficient C57BL/6 mice, CD4 T cells react to three epitopes within the PLP1 protein (PLP1₁₁₋₁₉, PLP1₁₇₄₋₁₈₂ and PLP1₂₄₀₋₂₄₈) [1]. To further investigate the mechanisms of central tolerance induction to PLP1, we generated two PLP1:I-A^b tetramers to follow the destiny of PLP1₁₁₋₁₉ and PLP1₂₄₀₋₂₄₈-specific T cells in the polyclonal CD4 compartment. Initially, we identified regulatory T cell induction upon self-recognition as the dominant tolerance mechanism for both PLP1₁₁₋₁₉ and PLP1₂₄₀₋₂₄₈-specific T cells. We then focused on endogenous PLP1₁₁₋₁₉-specific CD4 T cells and we detected differences between the T cell repertoires of PLP1-deficient and PLP1-sufficient C57BL/6 mice, with regard to abundance and T_{reg} cell induction. Furthermore, we could describe in more detail to which extent TRA critical factors such as AIRE, mTECs and also DCs influence the tolerance processes and we collected evidence for T cell anergy induction as a third alternative pathway to tolerize PLP1 specific T cells in the thymus.

Finally, single cell sequencing of tolerant and naïve PLP1₁₁₋₁₉-specific TCR repertoires uncovered TCR candidates that were deleted, whereas others underwent diversion into the T_{reg} cell lineage upon antigen encounter. The characterization of selected TCRs in TCR transgenic mice partially favors the (affinity)/avidity model, although one PLP1-specific TCR does not fit into the model and leaves space for an alternative interpretation of thymocyte selection rules.

Zusammenfassung

Das Schicksal einer heranreifenden T-Zelle hängt von der Interaktion des T-Zell-Rezeptors (TZR) und den körpereigenen Peptid-MHC-Komplexen der Antigen-präsentierenden Zellen im Thymus ab. Gemäß dem klassischen Affinitäts-/Aviditätsmodell der Thymozytenselektion bestimmt der Grad der Autoreaktivität, ob potentiell gesundheitsschädliche T-Zellen in regulatorische T-Zellen umgewandelt (gemäßigte Affinität/Avidität) oder durch das Einleiten der Apoptose (hohe Affinität/Avidität) aus dem System entfernt werden. In wieweit diese Mechanismen der zentralen Toleranzinduktion, ausgehend von einem physiologisch exprimierten körpereigenen Antigen, sich auf ein polyklonales T-Zellen-Repertoire auswirken wurde jedoch bis dato nur unzureichend beschrieben.

In der hier vorgestellten Arbeit konzentrieren wir uns daher auf das natürlich exprimierte und gewebespezifische Myelin-Proteolipid-Protein 1 (PLP1), welches als Hauptkomponente der Myelinscheide als eines der mutmaßlichen Zielantigene bei der humanen Multiplen Sklerose (MS) in Betracht gezogen wird. Interessanterweise, ruft die PLP1-Immunisierung von intoleranten Mauslinien eine MS-ähnliche Erkrankung, die sogenannte experimentelle autoimmune Enzephalomyelitis (EAE), hervor. C57BL/6 Mäuse hingegen sind aufgrund der Expression von PLP1 in den thymischen Epithelzellen gegen EAE resistent und reagieren nicht auf Stimulierungsversuche. Klein *et al.* konnte in PLP1-defizienten C57BL/6-Mäusen durch PLP1-Immunisierung zeigen, dass CD4 T Zellen gegen drei Epitope innerhalb des PLP1-Proteins reagieren (PLP1₁₁₋₁₉, PLP1₁₇₄₋₁₈₂ und PLP1₂₄₀₋₂₄₈) [1]. Die Konstruktion zweier PLP1:I-A^b-Tetramere ermöglichte uns die PLP1-abhängigen Mechanismen der zentralen Toleranzinduktion weiter zu untersuchen und das Schicksal von PLP1₁₁₋₁₉ und PLP1₂₄₀₋₂₄₈-spezifischen T-Zellen im polyklonalen CD4 Kompartiment genauer zu definieren. So konnten wir zu Beginn die Induktion regulatorischer T-Zellen als dominanten Toleranzmechanismus in toleranten PLP1₁₁₋₁₉ und PLP1₂₄₀₋₂₄₈-spezifischen T-Zell-Fraktionen beschreiben. Im weiteren Verlauf war es uns durch die Fokussierung auf endogene PLP1₁₁₋₁₉-spezifische CD4 T-Zellen in *Plp1*^{KO} und *Plp1*^{WT} C57BL/6 Mäusen möglich Unterschiede in der Abundanz und der Fähigkeit regulatorische T-Zellen zu induzieren genauer darzustellen. Ferner konnten wir aufzeigen, in welchem Maße die für die Expression von gewebespezifische Autoantigenen kritischen Faktoren, wie AIRE, mTECs und DCs die Toleranzprozesse nachhaltig beeinflussen. Zudem sammelten wir Indizien für die Induktion von T-Zell

Anergie als dritten alternativen Mechanismus der Toleranzinduktion von PLP1-spezifischen T-Zellen im Thymus.

Abschließend wurde durch Sequenzierung von einzelnen CD4 T-Zellen des toleranten und naiven PLP1₁₁₋₁₉-spezifischen TZR-Repertoires Kandidaten entdeckt, welche infolge der spezifischen Antigenbegegnung eliminiert, während andere in regulatorische T-Zellen umgewandelt wurden. Die selektive Charakterisierung ausgewählter TZRs in TZR transgenen Mauslinien unterstützt zum Teil das (Affinitäts-)/Aviditätsmodell, obwohl ein PLP1-spezifischer TZR nicht der Definition des Modelles entspricht und dadurch Raum für eine alternative Interpretation des Modells ermöglicht.

1 Introduction

1.1 Thymus

The necessity of the thymus gland has long been a mystery to researchers and scientists. Although the ancient Greek philosophers already appreciated the thymus and described it as the source of vital force in human kind [2], it took until the 1960s for the bi-lobed gland to receive the attention it deserved. In 1961, Jacques Miller discovered that thymectomized newborn mice were profoundly lymphopenic and unable to mount effective immune responses against tumors, infections and allogenic skin grafts [3-6]. Interestingly, the immunocompetence of these mice could be restored by thymic transplantation and, moreover, when the thymus transplant came from a different donor strain, the recipients turned out to be immunologically tolerant to antigens of both the donor and the recipient strain. This led Jacques Miller to the hypothesis that the thymus supports the release of functional and self-tolerant lymphocytes into the periphery [5]. 60 years later this theory is still accepted by scientists worldwide and the maturation of T lymphocytes (also known as T cells) in the thymus is generally appreciated as a fundamental process for the generation of an effective adaptive immune response.

The initial patterning of the bi-lobed thymus gland starts with the gene expression onset of the transcription factor *Foxn1* (Forkhead box N1) from the third pharyngeal pouch endoderm including the surrounding neural crest cells. FoxN1 is the key factor for thymic epithelial cell development and regulates the function, morphology and homeostasis of the thymus - but also the differentiation of keratinocytes and hair follicles - throughout life. FoxN1 deficiency causes severe thymic development defects, leading to an impaired T cell compartment [7], and the famous nude phenotype. To ensure a functional immune response even in newborns, the thymus formation starts around embryonic day 10 - 11 in mice and continues growing after birth till puberty [8, 9]. From this point on, the size of the thymus gradually decreases in a process known as thymic involution [10], leading to the transformation of the parenchyma into adipose tissue over time, which is discussed to play a role in age-related immunosenescence. Although the thymus changes greatly during life, its basic structure remains the same. Once the organogenesis is completed, the postnatal bi-lobed thymus - which is located behind the sternum and above the heart [11] - can morphologically be divided into lobules, each composed of an outer cortex and an inner medulla, where specialized epithelial cells can facilitate unique stages of T cell differentiation. The structure of the thymus reflects the tightly-regulated maturation route of developing T cells (otherwise known as

thymocytes) through this organ. Immature thymocytes start their migration from the inner cortex, subsequently move towards the outer cortex, and finally migrate back to conclude their differentiation journey in the medulla. The interplay of cortical and medullary thymic epithelial cells (cTECs and mTECs), various chemokines and checkpoints ultimately ensures the promotion and selection of CD4⁺ or CD8⁺ committed T cells, with a functional T cell receptor (TCR) able to recognize foreign antigens while remaining tolerant to self (reviewed in [12]).

1.2 Maturation of $\alpha\beta$ T cells in the thymus

T cells derive, as all hematopoietic cell lineages, from hematopoietic stem cells in the bone marrow (BM). Initially, T cell precursors get attracted by CXC-chemokine ligand 12 (CXCL12) and CC-chemokine ligand 25 (CCL25) expressing cTECs and enter the thymus via the bloodstream at the cortico-medullary junction (CMJ), while they are still multipotent (figure 2) [13, 14]. The subsequent maturation of the precursor T cell can be divided into three different stages based on the expression of the co-receptors CD4 and CD8, which facilitate the interactions with the major histocompatibility complex class II (MHCII) and MHCI, respectively: the double negative (DN), the double positive (DP) and the single positive (SP) stages. The DN stage can be further divided into four sub-stages (DN1 -> DN4) based on the expression of CD44 (an adhesion molecule) and CD25 (Interleukin-2 receptor α -chain) [15].

1.2.1 DN Phases

The undifferentiated cells that colonize the thymus possess the potential to give rise, next to the T cell lineage, to other specific cell lineages, such as macrophages, dendritic cells, granulocytes, natural killer cells and also B cells [16-20]. A first trend-setting step towards T cell development is initiated by the interaction of the Notch1 receptor with the corresponding Notch ligand Delta-like 4 (DLL4), expressed on the cortical epithelium, close to the CMJ (figure 2) [21]. This not only induces the expression of T cell specific factors but also blocks a possible development into the B cell lineage [17, 22]. Furthermore, the Notch1: DLL4 interaction, in combination with the cytokines IL-7 [23, 24] and Kit ligand (KitL) [25], favors a vigorous proliferation of the progenitor cells within the first 10 days [26, 27]. The Notch signaling persists in the following developmental stage, DN2, and leads to an up-regulation of CD25 (c-Kit⁺ CD44⁺ CD25⁺) [28] and the migration of the immature thymocytes into the inner cortex. At this stage the cells start to express the recombination activating genes (RAG) 1 and RAG2, two

important recombinases for the T cell receptor (TCR) rearrangements [29]. At the late DN2 stage, in combination with the migration to the outer subcapsular zone, the decrease in c-Kit and CD44 expression and the up-regulation of the *Bcl11b* gene, the thymocytes lose the potential to differentiate into alternative cell fates besides the T cell lineage [30, 31]. This irreversible commitment marks the beginning of the DN3 (c-Kit⁻ CD44⁻ CD25⁺) phase and the entry into one of the critical checkpoints during T cell development, the β -selection.

The TCR is an assembled heterodimer of an α - and a β - (polypeptide) chain (1-10 % of T cells express $\gamma\delta$ -chains). During β -selection, the exons of the variable (V), diversity (D) and joining (J) genes of the *Tcrb* locus undergo stochastic DNA rearrangement, a process called VDJ recombination (figure 1). Each of the three segments is composed of several separated exons, each of which encodes a complete gene by itself. A heterodimeric complex composed by RAG1 and RAG2 introduces a random double-strand break next to one of the D and J segments, brings them together and imprecisely ligates the ends. Subsequently, also one of the V segments is inaccurately added to the DJ segment. This random recombination of the individual sub-segments and the variability at the joining sites, where individual nucleotides are deleted or added with the help of the terminal deoxynucleotidyl transferase (TdT), guarantees a tremendous variability of the antigen-binding domain within the β -chain [32]. Simultaneously, the transcripts of *Ptcra* and the *Cd3* genes increase and lead to the expression of the CD3 signaling complex and the pre-TCR α -chain. The invariant pre-TCR α -chain forms a pre-TCR with the expressed β -chain. At this point, a lack of signaling downstream of the pre-TCR results in programmed cell death and the digestion by F4/80 expressing thymic macrophages. Instead, the efficient formation of a pre-TCR complex results in survival and migration into the subcapsular zone. Of note, a safety mechanism of chromatin condensation, known as allelic exclusion, prevents VDJ rearrangements on the second TCR β -chain allele. At the beginning of the DN4 or pre-DP stage (CD44⁻ CD25⁻ CD4^{low} CD8^{low}), a combination of pre-TCR and Notch signaling leads to another strong proliferation round, before CD4 and CD8 co-receptors are slightly up-regulated and the thymocytes differentiate into the DP stage. During the DP phase, the precursor T cells migrate back into the inner cortex, become unresponsive to cytokines and start the rearrangement of the V and J segment of the *Tcra* locus on both alleles, until one of the α -chains is able to form a stable TCR with the β -chain (reviewed in [33, 34]). The lack of allelic exclusion at this point causes around 10 % of mature T cells to express two α -chains on the cell surface [35].

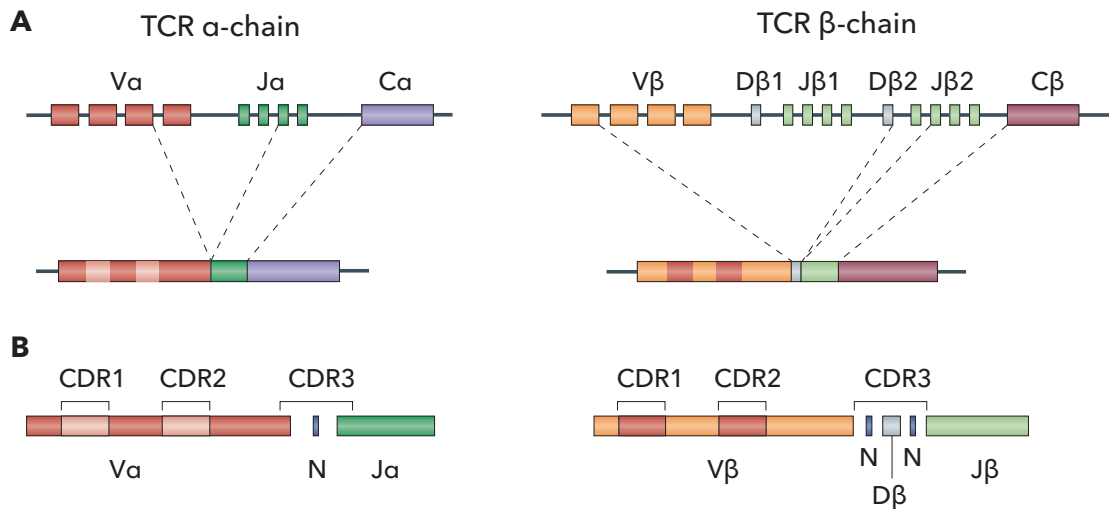


Figure 1: V(D)J recombination of TCR loci in developing thymocytes

The V(D)J recombination is a random process that enables the generation of an immensely variable T cell receptor (TCR) repertoire, with the aim of recognizing all possible pathological antigens. (A) The TCR gene loci consist of many independent gene segments, which are stochastically rearranged and fused to generate each receptor. The upper row shows the DNA configuration, whereas the lower one represents the spliced mRNA. The TCR α -chain locus (left) consists of V (variable) and J (joining) segments, while the TCR β -chain locus has an additional D (diversity) gene segment in between V and J. Both TCR loci also consist of constant regions (Ca or C β), which encode the transmembrane domain and are fused to the V(D)J part during splicing. (B) The most variable region of the TCR is the complementarity-determining region (CDR) 3, as it lies exactly at the junction between the V(D)J segments and interacts directly with the antigen embedded in the MHC groove. Addition (N) and/or deletion of nucleotides at the V(D)J ends ensures additional diversity. The germ line encoded CDR1 and CDR2, instead, establish the interaction with the MHC itself. The figure was adapted from [36].

1.2.2 Positive and negative selection in the cortex

It is estimated that the thymus cortex generates - out of 10 to 100 multipotent precursor cells - roughly 50×10^6 DP (CD4⁺ CD8⁺) T cells per day, therefore producing over time a tremendous amount of different $\alpha\beta$ TCR specificities able to recognize a virtually infinite number of self- and foreign-molecules presented by self-MHCs [37]. However, the random somatic recombination of the α - and β -chain loci does not result only in useful TCR entities, but also in potentially non-functional or harmful receptors, which must be tested before the T cells' maturation process is complete. In order to ensure functionality and self-tolerance, the following selection mechanisms depend on the strength of the interaction between the TCR and the peptides embedded in the self-MHCs. The resulting signaling cascade defines, in combination with various cytokines and co-stimulatory factors, the fate of the immature thymocyte.

The ability of the TCRs to recognize self-MHC molecules is initially tested in the cortex. For this purpose, the cTECs use an exclusive set of enzymes to process intracellular proteins and present them on the respective MHCs: the protease cathepsin L (CTSL) and the thymus specific serine protease (TSSP) for presentation of peptides on MHCII and the thymoproteasome with the specialized subunit $\beta 5t$ (*Psmb11*) for presentation on MHCI (figure 2) [38-40]. Unlike conventional antigen-presenting cells (APCs), cTECs show constitutively enhanced levels of macroautophagy, a degradative pathway, which allows them to load endogenous proteins on MHCII molecules [41]. The combination of these unique mechanisms supports the idea of a specialized library of peptides, embedded in the self-MHCs, for positive selection on cTECs. Indeed, thymocytes expressing functional TCRs, i.e. able to interact with the cTECs' self-peptide MHCs (self-pMHCs) within a defined low-affinity range of self-reactivity, undergo positive selection, meaning they are rescued from the default pathway of programmed cell death (also known as death by neglect) and they are allowed to proceed with development. However, up to 85% of thymocytes do not interact at all with self-pMHCs [42, 43] and die by neglect. A third fraction of DP thymocytes shows high affinity for self-pMHCs and is therefore removed from the repertoire in a process known as negative selection, in order to prevent self-tissue destruction and autoimmunity. As cTECs are relatively inefficient in initiating negative selection and rather specialized in inducing positive selection, it was suggested that rare cortical dendritic cells (DCs) - most likely $CD11c^+ CD8\alpha^{low} SIRP\alpha^+ CD11b^+$ conventional DC2 (cDC2) - implement this process of deletion in the cortex [44, 45] (reviewed in [46, 47]).

Pre-selected DP thymocytes are highly sensitive compared to SP or mature T cells [48], due to the up-regulation of molecules involved in the TCR signaling cascade (such as *Themis*, *Tespa1*, *miR-181-a* and *Scn4b*) [49-53]. They also express extremely low levels of TCR molecules on the surface, which will increase only as a consequence of successful positive selection. Besides the up-regulation of the TCR, positively selected thymocytes induce also CD3, CD5 and CD69 and initiate the SP differentiation program [54, 55]. According to our current knowledge, the differentiation into SP T cells follows the "kinetic signaling" model [56]. This model suggests that, regardless of the MHC restriction, the CD8 expression is down-regulated after positive selection into a $CD4^+ CD8^{low}$ intermediate stage [57]. T cells that express TCRs able to establish a prolonged signaling with one of their counterpart MHCII molecules, expressed by cTECs, up-regulate the transcription factor ThPOK and commit to the CD4 SP lineage [58]. Due to the down-regulated expression of CD8, MHCI-restricted T cells are only able to produce

a short or weak signal. However, they respond to the presence of six lineage-specific cytokines (IL-6, IL-7, IL-15, IFN- γ , TSLP and TGF- β) and can thus up-regulate the transcription factor Runx3d [59], reverse the expression of CD4 and irreversibly commit to the CD8 SP lineage (reviewed in [60]).

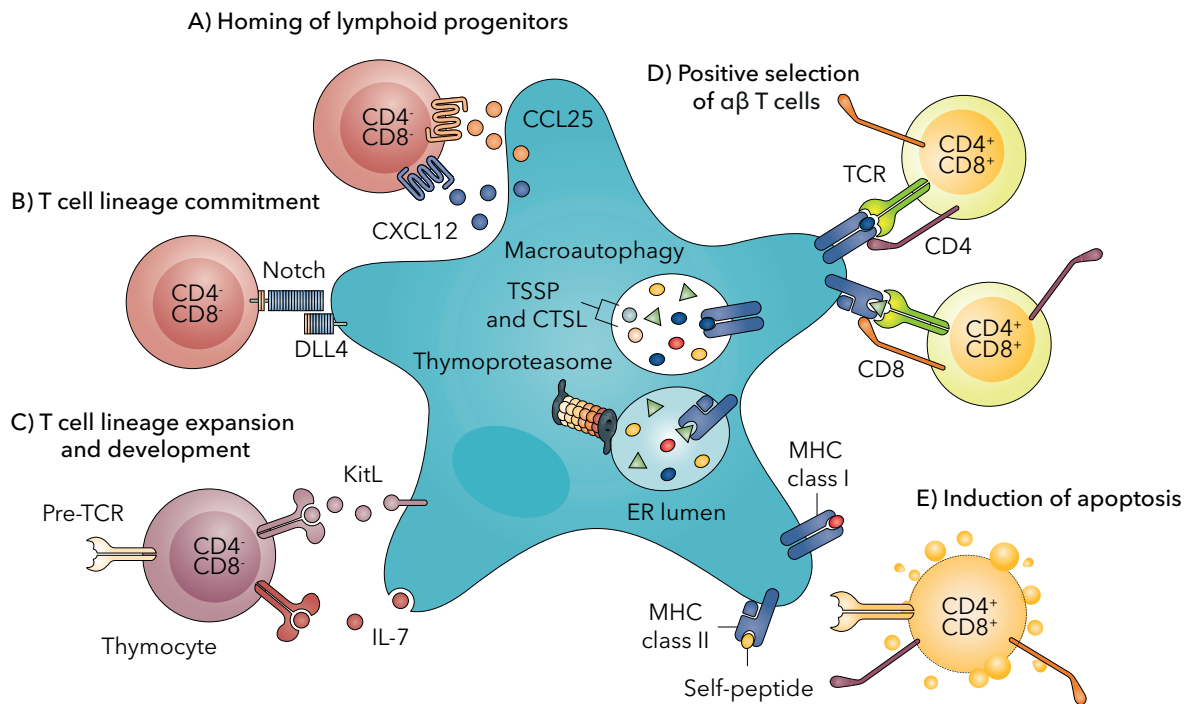


Figure 2: Role of cTECs in T cell development

Functional diversity of cortical thymic epithelial cells (cTECs) promoting T cell maturation. (A) cTECs attract hematopoietic T cell precursors by releasing chemokines CXCL12 and CCL25 into the thymus. (B) Interaction between the Notch1 receptor on the thymocytes and DLL4 on cTECs initiates the commitment to the T cell lineage. (C) IL-7 and KitL released by cTECs promote the proliferation of DN T cells. (D) Positive selection guarantees the survival of DP T cells, whose TCR binds to self-pMHC with an appropriate affinity/avidity. Intracellular proteins are digested by the thymoproteasome and loaded on the MHC I of cTECs. Unlike conventional antigen-presenting cells, cTECs constitutively shuttle intracellular proteins to the MHCII loading compartments via macroautophagy, and generate self-peptides thanks to the expression of the thymus-specific serine protease (TSSP) and cathepsin L (CTSL). (E) TCRs whose affinity to the self-pMHC is either excessive or absent undergo apoptosis. The figure was adapted from [61]. ER: endoplasmic reticulum

Thymocytes assigned to their specific lineage induce the expression of the chemokine receptors CCR4 and CCR7. The corresponding ligands for the former (CCL17 and CCL22) are expressed by cDC2, whereas the ligand for the latter (CCL21Ser) is

produced by mTEC^{lo} (AIRE⁻ CD80^{lo} MHCII^{lo}). These expression patterns attract the SP T cells into the medulla [62-65].

1.2.3 Negative and agonist selection in the medulla: the final maturation steps

To limit the emigration of mature self-reactive T cells into the periphery, in the medulla the positively selected and self-MHC-restricted thymocytes test their potential to interact with a broad range of self-antigens, which they may be confronted with in the periphery. The antigen repertoire is displayed on the respective MHCs expressed by APCs such as mTECs, BM-derived conventional and plasmacytoid dendritic cells (cDCs and pDCs) and, more recently discovered, also by B cells (reviewed in [46]). In the medulla, TCR stimulation through self-recognition instructs the alternative fates of clonal deletion (recessive tolerance) or clonal diversion (in the presence of IL-2 and TGF- β) into suppressive forkhead box P3 (FoxP3)⁺ CD25⁺ regulatory T (T_{reg}) cells (dominant tolerance) [66-71]. To which extent the individual APCs affect the selection outcome is still under debate. Experiments with mice lacking DCs [72], or lacking MHC molecules on hematopoietic APCs [73], or mice with diminished expression of MHCII on mTECs - the so-called C2TAkd mice [74] - attempted to define the roles of medullary APCs in self-tolerance induction. Regardless of the setup, an increase in CD4 SP T cells was monitored across the experiments, providing evidence for a significant role of the respective APCs in clonal deletion [72-74]. This perspective changed with a TCR high throughput analysis of conventional T (T_{conv}) cells and T_{reg} cells from C2TAkd animals and from mice lacking MHCII on BM-derived APCs. In both experimental settings, Perry *et al.* identified a lack of T_{reg} cell TCR specificities at single-cell level and their appearance in the T_{conv} cell repertoire, arguing for an important role of mTECs and BM APCs in clonal diversion next to clonal deletion [75]. Overall the influence of different medullary APCs on self-tolerance induction seems to be, at least partially, non-redundant, as the self-peptidome presented by individual APCs is believed to be partly divergent (reviewed in, [46, 76]).

In mature mTEC^{hi} (Aire⁺ MHCII^{hi} CD80^{hi}), for example, it is possible to detect the mRNA of more than 19,000 different genes (reflecting about 90 % of the entire genome), which is so far the highest amount of transcribed genes ever measured in any cell type [77]. In addition, mTECs can use autophagosomal degradation to shuttle intracellular proteins to MHCII loading compartments, as well as extensive RNA editing and alternative-splicing mechanisms to enlarge the complexity of self-antigens that are presented to

developing thymocytes (figure 3) [78, 79]. Extraordinary and unique in this respect is the intrinsic competence of promiscuous gene expression (PGE) of tissue-restricted antigens (TRAs), whose expression is usually strictly controlled and limited to specific tissues or cells outside the thymus [80]. The presence of TRAs within the thymus fosters a self-tolerant thymocyte repertoire. A lack of individual TRAs, on the other hand, can cause organ-specific autoimmune reactions, as shown for the multiple sclerosis mouse model - experimental autoimmune encephalomyelitis (EAE) [1] - or diabetes and Graves diseases in humans [81, 82]. Interestingly, to generate a tolerant T cell repertoire it is sufficient that less than 3 % of mTEC^{hi} express specific TRAs - in a mosaic-like pattern - at a given time [83-85]. Recently, it was demonstrated in two independent experiments that neo-self-antigens expressed in this TRA-like pattern convert a significant fraction of polyclonal CD4⁺ T cells, specific for the respective neo-self-antigen, into T_{reg} cells [86, 87]. In contrast, the same antigen under the control of promoters for ubiquitously expressed genes resulted in a reduced number of tetramer-positive T cells and a lack of specific T_{reg} cells [87].

The transcription of around 2300 TRA genes (and around 1600 ubiquitous genes [63]) is regulated by the autoimmune regulator (AIRE) (figure 3), whose loss of function is linked to a breakdown in self-tolerance associated with multiple organ failure, lymphocytic infiltration and autoantibodies in mice [88-90] and humans [91, 92], a clinical condition known as APECED (autoimmune polyendocrinopathy, candidiasis and ectodermal dystrophy). It is now broadly accepted that Aire-expressing mTEC^{hi} (at least in part) are responsible for the organ-specific tolerization of immature thymocytes via clonal deletion and clonal diversion. The negative selection of autoreactive thymocytes was initially investigated in TCR transgenic (tg) mice expressing cognate neo-self-antigens, such as hen egg lysozyme (HEL) or ovalbumin (OVA), under the control of AIRE-dependent organ-specific promoters. These studies revealed an AIRE-based reduction of the monoclonal TCR tg CD4 SP population [93-95]. More recently, AIRE-dependent intrathymic deletion of CD4 SP thymocytes was also confirmed in the TCR polyclonal repertoire. Using the tetramer technology, researchers detected in the absence of AIRE an increase of self-reactive CD4 SP thymocytes - specific either for the TRA interphotoreceptor retinoid-binding protein (IRBP) or the model antigen GFP expressed under the TRA insulin promoter [87, 96]. Combined, the above-mentioned experiments support the possibility that the transcription of AIRE-dependent TRAs in Aire-expressing mTECs favors deletion of self-reactive thymocytes. On the other hand, the extent to which AIRE-dependent PGE in mTECs contributes to the development of regulatory

T cells is rather well described. Patients suffering from APECED provided first indications, whose symptoms were traced back to a mutation in the *Aire* gene leading to an ablation of regulatory T cells [97]. At the same time, Aschenbrenner *et al.* described that the clonal diversion - next to clonal deletion - of TCR tg CD4 SP thymocytes specific for the influenza hemagglutinin (HA) model antigen into T_{reg} cells is dependent on AIRE expressing mTECs [98]. Furthermore, high throughput TCR analysis of AIRE-sufficient and -deficient mice revealed that some T_{reg} cell populations are dependent on the expression of certain TRAs on mTECs, otherwise they enter the T_{conv} cell lineage [75, 99]. However, the expression of TRAs is not exclusively dependent on AIRE, as the presence of PGE in AIRE-deficient mice suggests [77, 88]. Only recently, another transcription factor, FEZF2, was described in mTECs to initiate the expression of TRAs (figure 3). Although both transcription factors are co-expressed by the same cell type, the majority of genes they are activating seem to be largely non-overlapping. Interestingly, FEZF2-deficient mice (similarly to *Aire* knockout mice) suffer from multi-organ autoimmunity and display an altered T cell repertoire [100, 101]. Further investigations are still required to describe the exact tolerogenic functions of FEZF2-expressing mTECs.

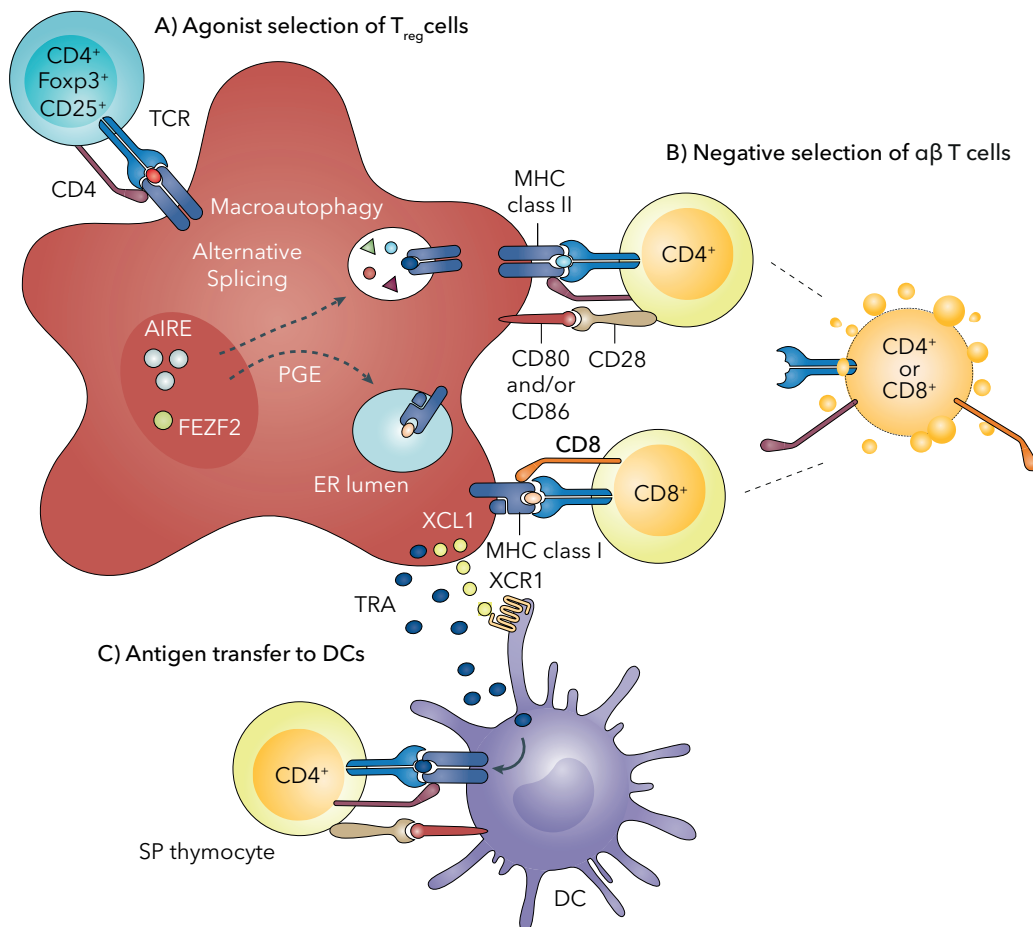


Figure 3: Medullary thymic epithelia cells (mTECs) and their function in central tolerance

Mature mTECs are capable of presenting the majority of self-antigens, even those that are restricted to specific tissues. This promiscuous gene expression (PGE) of tissue-restricted antigens (TRAs) is partly initiated and controlled by the transcription factors AIRE and FEZF2. To broaden the range of self-antigens presented for central tolerance induction, mTECs exploit, among other mechanisms, alternative splicing. Similarly to cTECs, mTECs possess an enhanced ability to shuttle self-proteins to MHCII compartments via macroautophagy. SP thymocytes, whose TCR reacts too strongly with pMHC presented by mTECs, are either converted into suppressor T_{reg} cells (A) or negatively selected (B). The secretion of XCL1 by mTECs attracts DCs in close proximity to mTECs, promoting TRA transfer and tolerance induction by DCs (C). The figure was adapted from [61].

During the transit of thymocytes through the medulla, a heterogeneous DC population, which constitutes around 0.5 % of the total cells in the thymus, also plays a crucial role in the induction of central tolerance [102]. The main hematopoietic APC fraction is the thymic resident conventional DC1 (cDC1) subset, which is distinguished from the aforementioned cDC2 population by the expression of CD11c, CD8 α and the chemokine receptor XCR1 [103]. The heterogeneity is completed by the thymus immigrating CD11c^{low} B220⁺ CCR9⁺ pDCs. The main difference between the DC populations is the nature of the presented antigens. For instance, attracted by the AIRE-dependent expression of XCL1, the cDC1 localize close to mTEC^{hi} (figure 3). This condition enables the well documented transfer of mTEC^{hi}-derived antigens to cDC1 for cross-presentation [75, 104-107]. A different scenario applies to the extrathymically originated cDC2 and pDC populations, which acquire blood-derived self-antigens in the periphery and transfer them (cDC2 guided via CCR2 and pDCs via CCR9) back to the thymus [44, 108]. Although the contribution of the individual fractions to central tolerance induction is not yet clarified in detail, there are substantial indications of the influence of the whole DC population on the thymocytes. A lack of DCs in CD11c-Cre:loxP-STOP-loxP-DTA or LT β R-deficient mice, indeed, leads to an increase of the thymic CD4 SP population, accompanied by CD4⁺ organ infiltrating lymphocytes in the periphery, most presumably due to the absence of negative selection of autoreactive entities [72, 109]. Other studies in the polyclonal TCR repertoire indicate that DCs induce suppressor T_{reg} cells by presenting either AIRE-dependent or -independent (model)-antigens, taken up from mTECs [87, 96, 107]. Although some hallmarks of clonal deletion and clonal diversion have been clarified, further experiments are needed to better understand the complex interaction of the individual DC populations with their thymic environment.

This applies equally to the B cell population, which might either immigrate from the periphery or already reside in the thymic medulla. Despite their APC-characteristic up-regulation of CD40, CD80, CD86 and MHCII, their influence on the alteration of the immature TCR repertoire is not described in detail [110]. However, recently an AIRE-expressing B cell subpopulation within the medulla was reported to promote negative selection of self-reactive thymocytes by the presentation of a neo-self-antigen [111]. The extent to which B cells influence the diversion of self-reactive thymocytes into regulatory T cells has not (yet) been described. Nevertheless, initial experiments in which B cells were removed, thereby reducing the T_{reg} cell fraction in the thymus, indicate a possible role in regulatory T cell generation [112].

Regardless of the APCs with which the positively selected SP thymocytes interact during their path of development in the medulla, their maturation follows a certain expression profile of CD69 and MHCI [113]. The specific stages can be classified into three distinct populations: recently immigrated semi-mature $CD69^+ MHCI^-$ SP thymocytes which are not able to proliferate convert into mature $CD69^+ MHCI^+$ cells and terminate in mature $CD69^- MHCI^+$ thymocytes ready to emigrate into the periphery. Of note, the up-regulation of MHCI defines the state in which the thymocytes acquire the ability to proliferate. To finalize the emigration process into the periphery, the mature thymocytes follow a chemical sphingosine-1-phosphate (S1P) gradient. The expression of S1P lyase in the thymus ensures a low concentration of S1P within the thymic epithelium, resulting in an increasing gradient towards the S1P-rich blood or lymph. Concomitantly with the down-regulation of CD69, the S1P receptor (S1PR) gets up-regulated, eventually ensuring the emigration of the fully developed thymocytes in the periphery [114] (reviewed in [115]).

1.3 Peripheral tolerance mechanisms

Despite these strictly-regulated maturation steps in the thymus, some self-specific T cells are able to escape the positive and negative selection processes. The threat of peripheral T_{conv} cells triggering an autoimmune response is increased by the fact that not all TRAs are displayed in the thymus - at least not in the peripheral structure - for self-tolerance induction. This is due not only to the fact that some TRAs are not presented in the medulla, but also that mutations, post-translational modifications and the interaction of various proteins contribute to the appearance of neo-antigens in the periphery, to which the T cells were not able to establish tolerance during their

maturation [116, 117]. To overcome these circumstances, further peripheral tolerance strategies exist to avoid self-destructive immune responses (figure 4).

For instance, rare antigens or those in immune privileged areas are partially ignored by the immune system and the activation of T_{conv} cells within these regions is kept to a minimum. Indeed, anatomical barriers (e.g. blood-brain barrier [118], blood-testis barrier [119], blood-retina barrier [120] or the placenta [121]) protect - at least in part - such antigens from a misdirected immune response.

Nevertheless, DCs have the ability to capture self-antigens in the periphery and present them to potentially autoreactive T cells, although under steady state conditions they seem to have an IL-10 expressing tolerogenic phenotype ($CD40^{low}$, $CD80/86^{low}$ and MHC^{low}) to maintain different tolerance mechanisms, such as the induction of peripheral T_{reg} cells (pT_{regs}), T cell anergy or deletion [122-124].

In the presence of the cognate antigen, TGF- β together with IL-2 and retinoic acid (RA) instruct naïve $CD4^+$ T cells aware of self to become CD25 and FoxP3 expressing pT_{reg} cells in mice [125, 126]. This is enhanced by DCs expressing either BTLA [127], CD80/86 [128], ICOS-L [129] or PD-L1/L2 [130] or secreting one of the anti-inflammatory cytokines such as IL-10 [131], IL-27 [132], IL-35 [133] or RA [134]. Peripheral-derived T_{reg} cells coexist next to the thymus-derived T_{reg} (tT_{reg}) cells and it seems that they complement one another in controlling immune homeostasis and limiting unnecessary inflammations (reviewed in [135]). A change in the $CD4^+$ T_{reg} cell composition, for instance due to a loss of function in either FoxP3 or CD25, initiates severe autoimmunity observed in scurfy mice [67, 136, 137] and in immune dysregulation, polyendocrinopathy, enteropathy, X-linked (IPEX) syndrome in humans [138, 139]. It appears that a large proportion of tT_{reg} cells expresses Neuropilin-1 (Nrp1) [140, 141] and Helios [142] compared to pT_{reg} cells. Besides, it seems that the first of three conserved non-coding DNA sequences at the FoxP3 locus, which displays specific chromatin marks to bind TGF- β , Smad3 and the nuclear factor of activated T (NFAT) cells, is essential for peripheral but not for thymic FoxP3 expression [143]. There is also some evidence in favor of pT_{reg} cells occurring more frequently at mucosal surfaces, due to the presence of the microbiota [144]. However, although these initial pieces of evidence suggest differences between the two populations, individual functions of the distinct subgroups have not been fully characterized yet.

Overall, CD4⁺ regulatory T cells developed a huge variety of mechanisms to preserve peripheral tolerance (figure 4). In order to suppress activated CD4⁺ T_{conv} cells, they are able to secrete inhibitory molecules, such as IL-10 [145], IL-35 [133] and TGF-β [146], or inhibit their differentiation into effector or memory T cells by actively removing local IL-2 [147]. They can also withdraw another energy source, ATP, within an autoimmune environment through the expression of CD39 and CD73. In a first step CD39 triggers the hydrolysis of ATP or ADP to AMP. CD73 subsequently dephosphorylates AMP into the immune suppressive adenosine molecule [148], which in turn stimulates the signaling cascade of the immune checkpoint A2aR on active CD4⁺ T_{conv} cells [149]. Furthermore, it was suggested that unintended immune responses against self are suppressed by contact-dependent suppression. Normally, for a successful immune response against foreign-antigens, CD4⁺ T_{conv} cells experience the first stimulus of activation by binding the pMHCII complex of an APC through their TCR in cooperation with the CD4 co-receptor. To achieve successful activation, the TCR aggregates with the CD3γ/δ/ε/ζ subunits and in parallel an additional co-stimulatory immunological synapse is formed between the T cell's CD28 co-receptor and the CD80 or CD86 (CD80/86) molecules on the APC [150]. By expressing CTLA-4 and LAG-3, T_{reg} cells disrupt these connections and neutralize the activating effect. Indeed, due to their higher affinity, LAG-3 binds the pMHCII complex and CTLA-4 takes over the interaction with CD80/86 [151]. In addition, CTLA-4 has been shown to reduce the expression of CD80/86 on DCs [152] or promote the expression of the enzyme indoleamine 2,3-dioxygenase-1 (IDO1) in humans [153] (TGF-β in mice [154]). IDO1 expressed by DCs removes tryptophan as energy source by metabolism, in addition the metabolites act as a positive feedback loop for T_{reg} cell induction (reviewed in [155]). In turn, IL-10 and TGF-β produced by regulatory T cells appear to promote the tolerogenic state of the DC population [156]. At the same time, activated self-reactive CD4⁺ T cells are suppressed by co-inhibitory signals initiated by the immune checkpoint receptors (e.g. A2aR [149], BTLA [157], CTLA-4 [158], LAG3 [159], PD-1 [160], TIGIT [161], TIM-3 [162] or VISTA [163]) expressed on the T cell surface. The binding of the respective ligand increases, for instance, the T cell dependent production of the anti-inflammatory cytokines (such as IL-10 [149, 161, 164, 165] or TGF-β [149, 165, 166]), counteracting the activation or arresting the production of key pro-inflammatory cytokines (such as IFN-γ [149, 163, 164, 167-169]) to prevent the onset of auto-proliferation and immunopathology.

Next to the suppressive T_{reg} cell lineage, T cells that come across self-pMHC molecules have also the possibility to convert to anergic CD4⁺ FR4⁺ CD73⁺ T cells (figure 4). This

status is initially favored by the chronic stimulation of the TCR and a lack of CD28 co-stimulatory signals. In general, anergy is defined as the lack of response of T_{conv} cells to their cognate antigen, associated to a failure in IL-2 production. Remarkably, regulatory and anergic T cells overlap in the surface expression of FR4, CD73, CTLA-4, ICOS and PD-1. Therefore, it has recently been speculated that the functional arrest of the cells not only protects against unwanted autoimmune reactions but could also provide precursor cells for the pT_{reg} cell lineage [170-172].

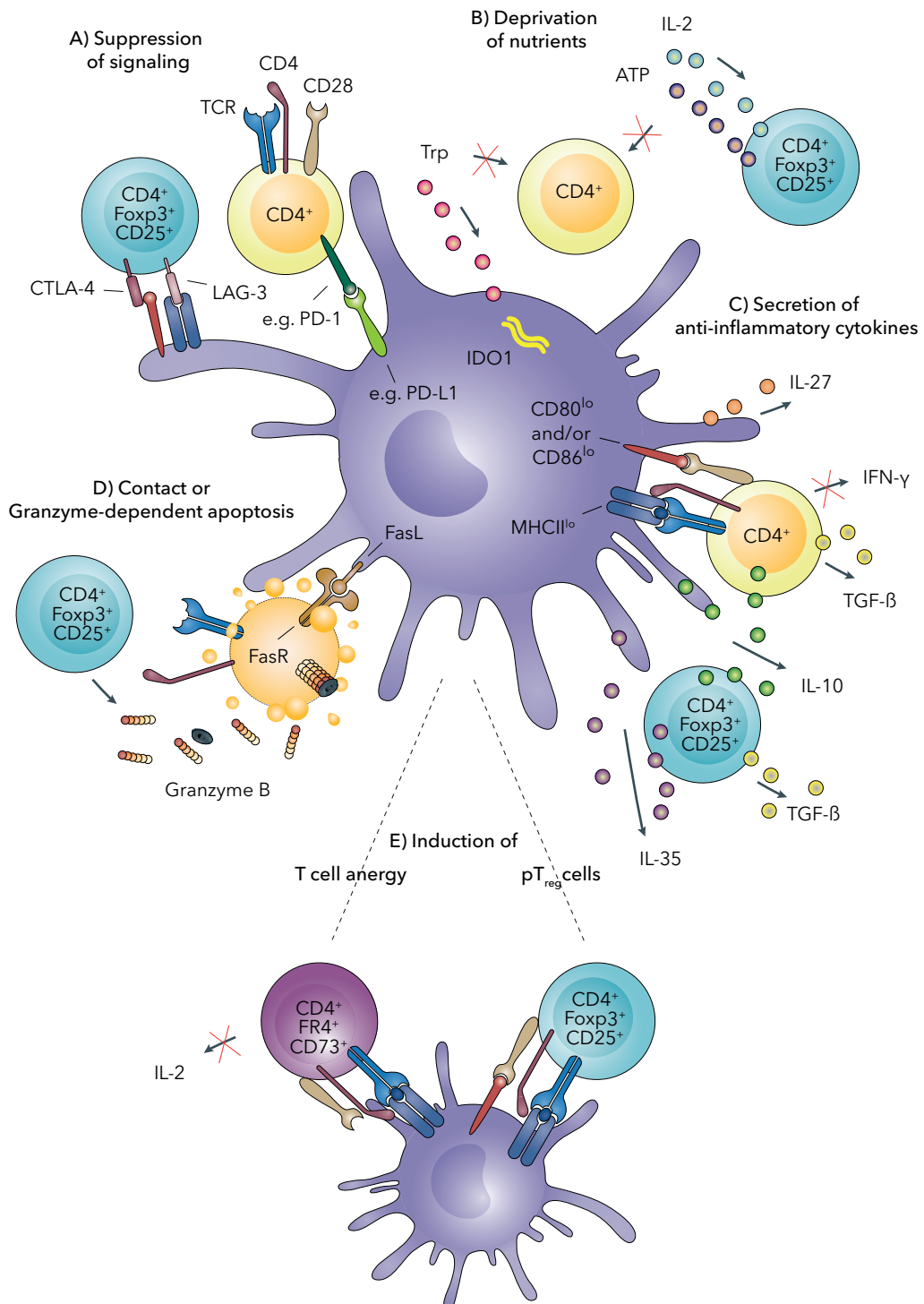


Figure 4: Peripheral tolerance mechanisms

Mechanisms that maintain immune homeostasis in the periphery involve mainly DCs and T_{reg} cells. (A) DCs stimulate immune checkpoint receptors via ligand expression, e.g. PD-L1 to interact with PD-1. T_{reg} cells in contrast prevent autoreactive T cells from binding the MHCII via LAG-3 (which has a higher affinity than the TCR) and CD80/CD86 via CTLA-4 (which has a higher affinity than CD28). (B) Deprivation of nutrients to prevent the activation and differentiation of autoreactive T cells include removal of Tryptophan (Trp) by DCs and IL-2/ATP by T_{reg} cells. (C) In the absence of inflammation, DCs and T_{reg} cells secrete anti-inflammatory cytokines, such as IL-10 and IL-35. Furthermore, stimulation of immune checkpoint inhibitors on self-reactive T cells induces a switch from pro-inflammatory (e.g. IFN- γ) to anti-inflammatory (e.g. IL-10 and TGF- β) cytokine production. (D) Autoreactive T cells can undergo apoptosis, as a result of contact-dependent FasL:FasR interaction with DCs or following the cytolysis induced by Granzyme B released by T_{reg} cells. (E) DCs can convert self-reactive T cells into regulatory and anergic T cells to maintain immune homeostasis. IDO1: Indolamine-2,3-Dioxygenase.

The last opportunity to inhibit self-aware T cells in an autoimmune response is their deletion (figure 4). Through the expression of FasL, DCs are able to stimulate the death receptor Fas on the surface of self-reactive T_{conv} cells and thereby initiate a caspase chain reaction inside the cell, resulting in cell death [173]. T_{reg} cells, on the other hand, initiate apoptosis by producing granzyme A and B in humans [174] and granzyme B in mice to lyse self-reactive T cells [175].

1.4 Signal strength-based models of thymocyte selection

It is now widely accepted that the alternative fates of self-reactive T cells significantly depend on the intensity of the interaction between TCR and the expressed pMHC on the APC, in both the thymic and peripheral environment. However, in the thymus, due to the random TCR gene rearrangement in the early stages of thymocyte maturation, the thymocyte pool expresses an infinite number of different $\alpha\beta$ TCR specificities, which in theory are all capable of interacting with the same pMHC complex at a broad spectrum of intensity. Two models that are very often used to describe the decision-making process of alternative fates are the so-called affinity and avidity models (figure 5). The first model defines, for a given antigen concentration, affinity as the strength of an individual TCR:pMHC contact, whereas in the second one avidity is described by the total of all TCR:pMHC connections of a given thymocyte. In detail, this means that the affinity model suggests that, above a certain affinity threshold thymocytes are removed from the thymic T cell repertoire via deletion; otherwise the risk of a self-reactive response of these T cells is unpredictable. T cells with intermediate affinity, instead, are converted into T_{reg} cells and those with lower affinity leave the thymus as T_{conv} cells. The

avidity model, on the other hand, must be extended to include the number of possible TCR:pMHC connections of an entire cell. Based on a reduced TCR density on the cell surface or a limited amount of self-antigen, a fraction of the thymocytes intended for deletion would shift to the T_{reg} cell compartment. Similarly a part of the T_{reg} cells would exit the thymus as T_{conv} cells. Finally, it is important to mention that the thymocytes in both models require a certain low self-awareness in the cortex to be positively selected (reviewed in [176]).

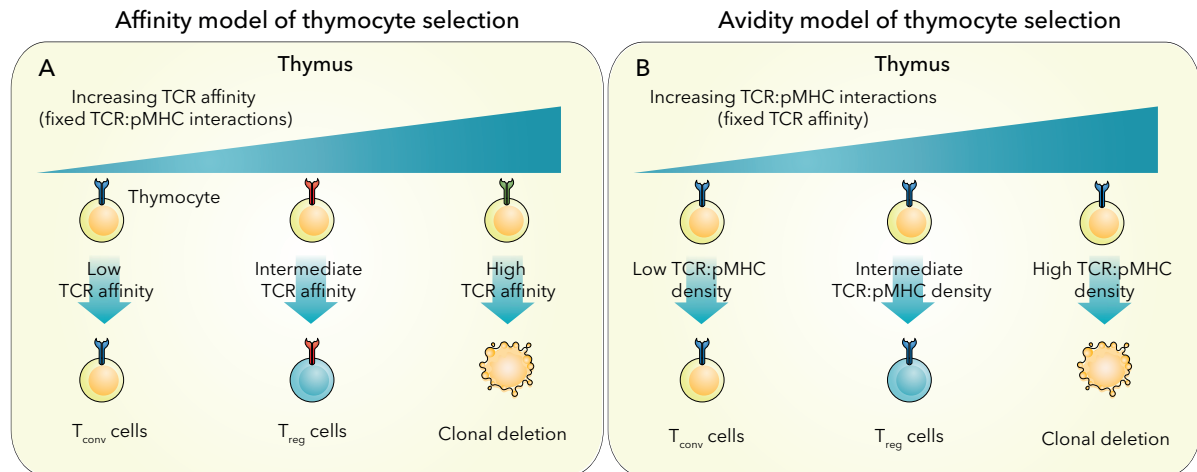


Figure 5: Affinity and avidity-dependent models of thymocyte selection

(A) According to the affinity model of thymocyte selection, for a given ratio of TCR:pMHC interactions the T cell fate is influenced by the affinity of the TCR. Thymocytes expressing TCRs with low affinity to the cognate self-pMHC escape central tolerance mechanisms and leave the thymus as T_{conv} cells; TCRs with intermediate affinity lead to T_{reg} cell induction; high-affinity TCRs are removed from the mature repertoire through negative selection. (B) According to the avidity model of thymocyte selection, for a given TCR (and therefore for a given TCR affinity) the density of TCR:pMHC interactions is crucial in determining the T cell fate. At a low TCR:pMHC density, which could mean low levels of TCR per thymocyte or low expression of pMHC in the medulla, thymocytes are allowed to mature and exit the thymus as T_{conv} cells. Increasing the TCR:pMHC density would instead lead to T_{reg} cell induction or, at the highest TCR:pMHC densities, to negative selection of the same TCR entity. The figure was adapted from [176].

The overall affinity/avidity model is based on the antigen-dependent deletion and T_{reg} cell induction of monoclonal TCR thymocytes elucidated in TCR transgenic mice exposed to neo-self ligands [177-180]. Furthermore, early studies with immature thymocytes from fetal thymic organ culture (FTOC) - specific for a LCMV-peptide - indicated that an increase in agonist concentration induces the deletion of immature thymocytes *in vitro* [181]. Other FTOC experiments using NOD TCR tg mice extended this view and indicated that thymocytes destined for deletion can be partially converted

into agonist-induced T_{reg} cells by reducing the antigen concentration [182]. Variable concentrations of model antigens in TCR transgenic mice confirmed these observations *in vivo*, where a decrease or a gradient in neo-self-antigens was obtained either through the expression under different promoters or by the reduction of the MHCII molecules in C2TAkd animals. In both cases a lowered antigen concentration favored the conversion of immature thymocytes to T_{reg} cells and reduced the potential for deletion as observed at high antigen concentrations [74, 183]. Using a broad range of TCR transgenics with different affinities for an OVA-peptide, Lee *et al.* wanted to describe the range of self-reactivity below the deletion threshold. Their findings suggest that a rise in self-recognition results in an affinity-dependent linear increase of the thymic T_{reg} cell generation [184].

So far, the affinity model is mainly based on results of TCR transgenic model systems, which have the disadvantage of a limited and non-physiological T cell repertoire. The overexpression of specific TCR characteristics prevents the natural development by overloading the selection niches [185, 186]. In order to avoid these circumstances and to understand how alternative fates are determined by the expression of a natural antigen, first attempts in the polyclonal system have been made. The findings of Kieback *et al.* revealed that, after encountering the endogenous myelin oligodendrocyte glycoprotein (MOG), MOG-specific tT_{reg} cells possess a higher affinity to the cognate antigen compared to T_{conv} cells [187]. Although these findings suggest affinity/avidity-dependent T_{reg} cell diversion of self-reactive thymocytes, many aspects remain to be clarified. It needs to be confirmed to what extent clonal deletion and clonal diversion on a single T cell level alters the TCR repertoire and how the characteristic properties of these TCRs are defined.

1.5 The endogenously expressed model antigen myelin proteolipid protein 1

In order to define specific TCR identities shaped by thymic selection mechanisms in a physiological setting, our preference was given to the naturally expressed model protein called myelin proteolipid protein 1 (PLP1). PLP1 is a hydrophobic integral transmembrane protein with four hydrophobic α -helices and highly conserved among mammals. The full-length form consists of 276 amino acids (aa) and co-exists with an alternatively spliced form, called DM20, lacking an intracellular loop including the 116 - 150 aa. Both forms are encoded on the X-chromosome and form together with myelin basic protein (MBP) and MOG the main protein-components of the myelin layer, which is

built up by oligodendrocytes in the central nervous system (CNS) and by Schwann cells in the peripheral nervous system (PNS). Due to a multi-layered arrangement, the myelin membrane operates as an insulator and guarantees loss-free and fast signal transmission of the nerve axons (reviewed in [188]).

PLP1 is a promising model protein, as it is an embedded membrane protein and a potential target of severe autoimmune demyelinating diseases such as multiple sclerosis (MS) [189]. It is suggested that autoreactive T cells infiltrate the CNS and attack myelin-based antigens to trigger an immunopathological cascade, resulting in the destruction of the myelin layer [190]. Interestingly, in a number of mouse lines the disease model of MS, experimental autoimmune encephalomyelitis (EAE), is caused by the injection of PLP1. For instance, SJL/L mice show distinct MS-like disease symptoms and histological characteristics [191], whereas the C57BL/6 strain appears to be highly tolerant to PLP1 injection, which confirms strong tolerance mechanisms for the latter [192]. We can now understand the circumstances that create such divergent susceptibilities thanks to the findings of Klein *et al.* In $Plp1^{WT} \rightarrow Plp1^{KO}$ thymus chimeras (C57BL/6 background), irradiated and reconstituted with bone marrow from $Plp1^{KO}$ mice, they revealed a reduction of peripheral T cell response upon PLP1 injection - arguing for the establishment of T cell tolerance via ectopically expressed PLP1 on radio resistant thymic epithelia cells. The specific immunogenic epitopes were subsequently defined more precisely in an *in vitro* re-stimulation assay (figure 6). Following PLP1 immunization *in vivo*, primed T cells from $Plp1^{KO}$ mice demonstrated a strong proliferation upon stimulation with the epitopes PLP1₁₁₋₁₉, PLP1₁₇₄₋₁₈₂ and PLP1₂₄₀₋₂₄₈, which was absent in cells from $Plp1^{WT}$ mice (except a weak response upon PLP1₁₇₄₋₁₈₂ stimulation) [1, 193]. In comparison with the already identified SJL/L epitopes embedded in H-2^s MHCs no overlap was detected, possibly due to the different haplotypes (C57BL/6 expresses H-2^b) [191, 194, 195]. This might be the crucial difference. Since the shortened DM20 variant is mainly expressed in the thymus, tolerance induction to one of the five epitopes of the SJL/L mouse is missing [196]. Consequently, autoreactive T cells develop and proliferate within recall experiments and in general the mice are more susceptible to EAE. However, due to the expression of all three immunodominant epitopes in the thymus of C57BL/6 mice, tolerance induction is very efficient towards PLP1 [1]. Therefore PLP1-deficient and -sufficient C57BL/6 mice represent the perfect model systems to describe central tolerance mechanism in the presence or absence of a naturally expressed antigen.

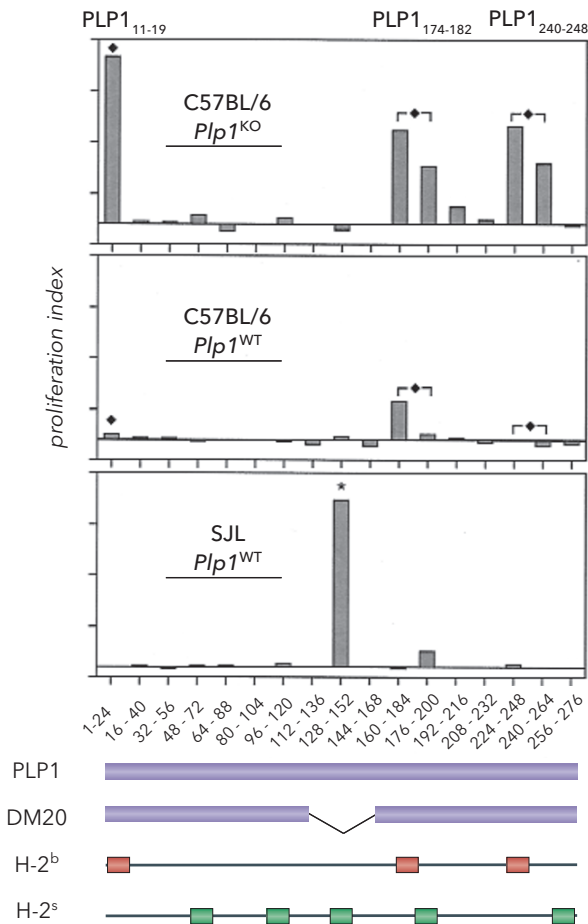


Figure 6: T cell epitopes of PLP1 in C57BL/6 and SJL mouse strains

After immunization with the entire PLP1 protein, T cells harvested from the draining lymph nodes of C57BL/6 *Plp1*^{KO} (upper row), C57BL/6 *Plp1*^{WT} (middle row) and SJL *Plp1*^{WT} (lower row) were re-stimulated *in vitro* with overlapping 24-mers spanning the PLP1 protein [1]. In the C57BL/6 strain (H-2^b haplotype) three main T cell epitopes were identified (♦), based on the proliferation of *Plp1*^{KO} T cells. Further experiments narrowed down the effect of the 24-mers to the specific core epitopes PLP1₁₁₋₁₉, PLP1₁₇₄₋₁₈₂ and PLP1₂₄₀₋₂₄₈ [193]. The proliferation in the *Plp1*^{WT} counterpart is barely visible. As opposed to the C57BL/6, the SJL strain (H-2^s haplotype) showed, even on a *Plp1*^{WT} background, an extensive proliferative response to one particular epitope (*), which is absent in the DM20, the thymic version of PLP1. This explains the EAE susceptibility of this strain. The panel at the bottom shows the overlap between the whole PLP1 protein, the DM20 thymic version of PLP1 and the T cell epitopes described for H-2^b and H-2^s haplotypes. The figure was adapted from [1].

2 Aim of the submitted thesis

The recognition of self in the thymus leads to the diametrically opposite outcomes of deletion and T_{reg} cell diversion. Based on the affinity/avidity models of thymocyte selection, these different outcomes rely on the strength of the TCR:pMHC complex interactions. So far this was mainly tested with TCR transgenics specific for neo-self-antigens. Therefore, the question remains open as to how an endogenously expressed self-antigen shapes a polyclonal TCR repertoire. Using novel tetramers specific for two immunogenic epitopes of PLP1, we set out to determine whether central tolerance mechanisms are effective towards PLP1-specific T cells and, if so, how different epitopes of the same protein affect the fate of these self-reactive specificities. Consequently, we asked whether the decision between deletion and diversion depends on TRA critical factors such as AIRE, mTECs and DCs. Ultimately, we wanted to characterize the effect of central tolerance on the size of the respective alternative fates, at the level of individual TCRs, in order to test if the characteristic properties of specific TCRs fit into the affinity/avidity model.

3. Materials & Methods

3.1 Materials

3.1.1 Chemicals, Enzymes and Media

Common chemicals were acquired from Roth, Merck and Sigma unless otherwise mentioned. Cell culture media and their supplements were obtained from Gibco™ and Biochroma AG. Oligonucleotides for mouse genotyping, TCR α -chain single cell sequencing and core epitope design during tetramer generation were purchased from IDT. Enzymes and related Kits were received from BioRad, Roche, Promega, Invitrogen and ThermoFisher. DNA and Plasmid purification kits were obtained from Qiagen.

3.1.2 Cell lines and Bacteria

Standard protocols were used to prepare LB (lysogeny broth) media, which contained 0.1 $\mu\text{g/ml}$ of either Ampicillin or Kanamycin. For selection plates 1 % (w/v) agar was added to the LB media. Stratagene provided the competent *Escherichia Coli* (*E.coli*) strains One Shot TOP10 for sequencing experiments and SoloPack Gold for plasmid transformation during cloning steps.

Schneider Drosophila Cells for tetramer expression were cultivated in Schneider Drosophila Medium (SDM) containing 10 % Fetal Bovine Serum, 100 U/ml of Penicillin and Streptomycin and 20 $\mu\text{g/ml}$ Gentamycin. While upscaling the cells were cultivated in Express Five Serum Free Medium (SFM) including 100 U/ml of Penicillin and Streptomycin and 20 $\mu\text{g/ml}$ Gentamycin. HEK293T cells transfected with modified pTa cassette vectors encoding one of the four TCR α -chain genes (2.2.3.4 Transgenic Mice), were kept in DMEM (Iscove's Modified Dulbecco's Medium) including 8 % (v/v) heat-inactivated FCS. Upon electroporation of A5 cells (derived from BALB/c TCR HA α g 6.5 mice) in the presence of the pTa cassette vectors, cells were kept in DMEM including 10 % (v/v) of heat-inactivated FCS. Thymocytes and primary T cells grew in IMDM (Iscove's Modified Dulbecco's Medium) including the supplements 25 mM HEPES, 8 % (v/v) heat-inactivated FCS, 4 mM L-Glutamine, 1 % (v/v) Non-Essential Amino Acids, 1 mM Sodium Pyruvate, 50 μM β -Mercaptoethanol, 100 U/ml Penicillin and 100 $\mu\text{g/ml}$ Streptomycin. Cells were frozen in freezing medium containing 70 % cell medium, 20 % heat-inactivated FCS and 10 % Dimethyl Sulfoxide (DMSO).

3.1.3 Antibodies

All listed antibodies used for flow cytometry, MACS enrichment/depletion were anti-mouse.

Specificity	Conjugate	Clone	Supplier
B220/CD45R	Pe-Cy7 / BV421	RA3-6B2	BioLegend
CCR6	APC / BV421	29-2L17	BioLegend
CCR7	PerCP-Cy 5.5	4B12	BioLegend
CD11b	Pe-Cy7 / BV421	M1/70	BioLegend
CD11c	Pe-Cy7 / BV421	N418	BioLegend
CD16/CD32	(=Fc block)	2.4G2	In house
CD25	APC-Cy7 / Pe-Cy7	PC61	BioLegend
CD4	BV510	RM4-5	BioLegend
CD44	PB	IM7	BioLegend
CD45.1	BV421	A20	BioLegend
CD45.2	Alexa-647	104	BioLegend
CD5	Alexa-647	53-7.3	BioLegend
CD62L	APC-Cy7	MEL-14	BioLegend
CD69	BV711	H1.2F3	BioLegend
CD73	BV421 / BV605	TY/11.8	BioLegend
CD8a	Per-CP (Cy 5.5) / FITC	53-6.7	BioLegend
FoxP3	FITC / APC	FJK-16s	Invitrogen
F4/80	Pe-Cy7 / BV421	BM8	BioLegend
FR4	PerCP-Cy5.5	12A5	BioLegend
H-2K^b	BV786	AF6-88.5	BD Bioscience
Va3.2	FITC	RR3-16	BioLegend
TCR VB2	FITC	B20.6	BD Bioscience
TCR VB3	FITC	KJ25	BD Bioscience
TCR VB5.1/5.2	FITC	MR9-4	BD Bioscience
TCR VB6	FITC	RR4-7	BD Bioscience
TCR VB8.3	FITC	F23.1	BD Bioscience
CD4	MicroBeads	GK1.5	Miltenyi Biotec
CD8a	MicroBeads	53-6.7	Miltenyi Biotec
CD19	MicroBeads	6D5	Miltenyi Biotec

3.1.4 PLP1 peptides

Peptides analog to the previously identified immunogenic regions of PLP1 (red letters) [1, 193] were synthesized and purified by peptides&elephants or from BioTrend.

PLP₁₋₂₄ GLL ACC ARC **LVG APF ASL** VAT GLC

PLP₉₋₂₀ **CLV GAP FAS** LVA

PLP₂₃₇₋₂₄₈ HLF **IAA FVG AAA**

3.1.5 Vectors

3.1.5.1 Tetramer

The production of MHCII tetramer was described before [197]. To express biotinylated MHCII monomer carrying the peptides PLP1₁₁₋₁₉ (Tet-1) or PLP1₂₄₀₋₂₄₈ (Tet-3), vectors based on the pRMHa backbone [198], kindly provided by Marc Jenkins and his laboratory (University of Minneapolis), were used upon modifying the core peptide region. In summary, pRMHa plasmids included an ampicillin resistance and a metallothionein promoter controlling one of the MHCII chains (I-A^b alpha or I-A^b beta).

A 4x amino acid glycine linker followed by the core epitope [1, 193] of the respective tetramer was encoded at the N-terminal of the I-A^b β-chain and flanked by an *Xma*I and *Spe*I restriction site. Due to the weak binding affinity of the I-A^b chains, an acidic (I-A^b α-chain) and a basic (I-A^b β-chain) leucin zipper motif were encoded at the C-terminal, following the I-A^b chain motifs to facilitate the heterodimerization [198]. In addition, a BirA biotinylation signal sequence (I-A^b α-chain) and a His₆ purification tag (I-A^b β-chain) were fused at the C-terminal of the zipper motifs [199]. *In vitro* biotinylation was completed by co-expression of a BirA protein ligase encoded on the p18BirA vector [200]. Growth of undesired microorganisms was prevented expressing a blasticidin resistance gene (pCo Blast) [201].

3.1.5.2 Transgenic mice

To functionally express defined TCR α-chains of interest as a transgene in mice, gene blocks expressing the characteristic VJ regions (including introns) TCR-F, TCR-A, TCR-H and TCR-E (in detail 3.2.3.4 Transgenic Mice) were introduced between the *Xma*I/*Not*I restriction sites of the pTα cassette vectors previously described by Kouskoff *et al.* [202].

3.1.6 Animals

6 to 10-week-old mice on C57BL/6 background (purchased from Charles River) used in this study were bred and kept under specific pathogen free conditions in individually ventilated cages in the animal facilities of the Institute for Immunology, LMU Munich. All animal studies were performed in strict accordance to local law regulation.

Plp1^{KO} (gift from Klaus Nave from the Max-Planck-Institute for Experimental Medicine, Göttingen) [203], *Aire*^{KO} [204], Δ DC (nicely provided by David Voehringer) [72], FoxN1-cre [205], conditional *PLP1* allele (*Plp1*^{fl} - kindly given by Hauke Werner from the Max-Planck-Institute for Experimental Medicine, Göttingen) [206], FoxP3^{GFP} reporter (referred to as DREG) [207, 208], *Rag1*^{KO} [209] and *Tcra*^{KO} [210] mice have been described before. TCR β -*Plp1*^{tg/-}::*Tcra*^{+/-}::*Dereg*^{tg/-} (Fixed- β) mice for single cell analysis were obtained by crossing the previously in our lab generated TCR-*Plp1*::*Dereg*^{tg/-} transgenic mice [193] with C57BL/6 *Tcra*^{KO} *Plp1*^{WT} or *Plp1*^{KO} animals - resulting in TCR β -*Plp1*^{tg/-} mice harboring a *Plp1*₁₁₋₁₉-specific TCR β -chain (V β 6) whereas the TCR α -chain remains polyclonal.

Tcra^{tg/-} transgenic mouse lines TCR-F, TCR-A, TCR-H and TCR-E were generated via pronuclear injection of linearized pTa cassette vectors into C57BL/6 zygotes (described in 3.2.3.4 Transgenic mice) performed by Ronald Naumann at the Max-Planck-Institute of Molecular Cell Biology and Genetics Dresden. TCR α -chain transgenic mice were crossed with TCR β -*Plp1*^{tg/-} animals to obtain mice expressing a transgenic TCR specific for PLP1.

3.1.7 Oligonucleotides

Oligonucleotides were purchased from IDT. For Tet-1 and Tet-3 tetramer generation overlapping primer pairs were constructed to resemble the core epitopes PLP1₁₁₋₁₉ or PLP1₂₄₀₋₂₄₈ (chapter 3.2.3.2 Novel I-A^b tetramer expression and purification):

Primer	Sequence 5' - 3'
PLP1.4 long (9-20) sense	CCG GGG ACC GAA GGC TGC CTG GTG GGC GCG CCG TTT GCG AGC CTG GTG GCG GGC GGC GGC GGC A
PLP1.4 long (9-20) anti-sense	CT AGT GCC GCC GCC GCC CGC CAC CAG GCT CG AAA CGG CGC GCC CAC CAG GCA GCC TTC GGT C
PLP15.237_C sense	CC GGG ACC GAG GGC CAC CTG TTC ATC GCC GCC TTC GTG GGC GCC GCC GGC TGC GGC GGC A
PLP15.237_C anti- sense	CT AGT GCC GCC GCA GCC GGC GGC GCC CAC GAA GGC GGC GAT GAA CAG GTG GCC CTC GGT C

Primer for polyclonal single cell TCR α -chain amplification and sequencing (specified in chapter 3.2.3.3 Single cell TCR α -chain sequencing):

Primer	Sequence 5' - 3'
TRAC215r	GGT GAA GCT TGT CTG GTT GCT C
TRAC222r	GAT ATC TTG GCA GGT GAA GCT TGT C
TRAC254r	ACT GGG GTA GGT GGC GTT G
Anchor_fw	ACA GCA GGT CAG TCA AGC AGT AGC AGC AGT TCA ATA AGC GGC CGC CAT GGA CCC CCC CCC CC
TRAC6	GTC AAA GTC GGT GAA CAG GC
Adaptor 1	ACA GCA GGT CAG TCA AGC AGT A
TRAC13	GAG ACC GAG GAT CTT TTA ACT G
Adaptor 2	AGC AGT AGC AGC AGT TCG ATA A
TRAC 2 nd nested	CAG GTT CTG GGT TCT GGA TG
M13 for	GTA AAA CGA CGG CCA G
M13 rev	CAG GAA ACA GCT ATG AC

Primers for mouse genotype identification (described in 3.2.3.1 Genotyping)

Gene	Primer	Sequence 5' - 3'
Aire	B6-Aire wt fwd	AAG CCG TCC AGG ATG CTA T
	B6-AIRE-KO int	GTC ATG TTG ACG GAT CCA GGG TA
	B6-AIRE rev	AGA CTA GGT GTT CCC TCC CAA CC
CD11c-cre	CD11c cre fwd	CGA TGC AAC GAG TGA TGA GG
	CD11c cre rev	GCA TTG CTG TCA CTT GGT CGT
Dereg	Dereg (P442)	CCC AGG TTA CCA TGG AGA GA
	Dereg (P443)	GAA CTT CAG GGT CAG CTT GC

DTA	DTA fwd	TAC ATC GCA TCT TGG CCA CG
	DTA rev	CCG ACA ATA AAT ACG ACG CTG
FoxN1-cre	FoxN1 cre fwd	GAC ATA GCC CTC AGT GTT CAG G
	FoxN1 cre rev	CCC TAC ATT CAG GTT CAG
PLP1	PLP com fwd	GAA AGG TTC CAT GGT CAA GG
	PLP wt rev	CTG TTT TGC GGC TGA CTT TG
	PLP ko rev	CTT GCC GAA TAT CAT GGT GG
Rag1	Rag1 com fwd	CCG GAC AAG TTT TTC ATC GT
	Rag1 wt fwd	GAGGTTCCGCTACGACTC T
	Rag1 ko fwd	CCG GAC AAG TTT TTC ATC GT
TCRa wt/ko	TCRa fwd	TGA CTC CCA AAT CAA TGT GC
	TCRa rev (wt)	GGT GAG ATG ACC CAA AGC AG
	TCRa rev (ko)	CCT ACC CGC TTC CAT TGC TCA
TCRβ-PLP1 (Vβ6)	V β 6 fwd	CCC AGA GCC AAA GAA AGT C
	V β 6 rev	AGC CTG GTC CCT GAG CCG AA
WT1*	WT1CF2R	CTT ACC AGG GCT TAC CAG CA
	WT1CF3R	ATG TGG CTT CAA ACC CTC TG
	TRAJ12 rev third SacII	TTC CGC GGC TCC AGC TTG TCC TTC ATT GCA GGG CCA TTT CCT GGA CCA T
223**	223no 37CF1F	CCA GTG CTG GGG ATA CAC TT
	223KO37rev	AAG GCC CAG GCT AAG AAG AG

*WT1 primer set was used to identify the TCR-A, TCR-H and TCR-E transgenes

**223 primers amplified the TCR-F transgene

3.1.8 Commercial Kits

CellTrace™ Violet Cell Proliferation Kit	Invitrogen
Drosophila Expression System Kit	Invitrogen
Herculase II Fusion Enzyme	Agilent
His-Bind® Purification Kit	Novagene
iScript™ Select cDNA Synthesis Kit	Bio-Rad
Pierce™ Monomeric Avidin	ThermoFisher
Terminale Deoxynucleotidyl Transferase	Promega
Zero Blunt™ PCR cloning Kit	Invitrogen

3.2 Methods

3.2.1 Bioinformatic methods

3.2.1.1 Sequences searches and alignments

Protein and nucleotide sequences were searched in the NCBI database (<https://www.ncbi.nlm.nih.gov/protein/> or <https://www.ncbi.nlm.nih.gov/gene/>). Cutting sites of enzymes and the design of oligonucleotides were performed using plasmid editor ApE, CLC Sequence Viewer7 or with NEBuilder. TCR a-chain sequences were accurately annotated via IMGT/V-Quest [211].

3.2.1.2 Statistical Analysis

Statistical analysis was performed with Prism7. The specific statistical tests applied to each experiment are described in the figure legends.

3.2.1.3 In silico peptide:I-A^b binding prediction

The algorithm to predict the binding capability of immunogenic peptides into the I-A^b binding pocket was nicely provided by Marc Jenkins (University of Minneapolis) (unpublished).

3.2.2 Immunization

50 µl PBS based emulsion containing 50 µg peptide of interest (3.1.4 PLP1 peptides) and 50 % (v/v) Complete Freund Adjuvants (Difco) was injected into the footpad of 6 - 10 week old mice 10 days before analysis.

3.2.3 Molecular Biology

3.2.3.1 Genotyping

Mouse tissue was obtained during clipping procedure (ear marks) and used for genotype determination. Tissue was digested in 50 μ l digestion reaction at 55 °C for 5 h, followed by a heat inactivation step at 95°C for 5 min.

	Mouse tissue
Digestion Reaction	0.06 U Proteinase K
	0.5 % (v/v) Triton X-100
	1 % (v/v) Gitocher Buffer
	1 % β -Mercapthoethanol
	sterile dH ₂ O
	670 mM Tris pH 8.8
10x Gitocher Buffer	166 mM (NH ₄) ₂ SO ₄
	65 mM MgCl ₂
	0.1 % Gelatin
	sterile dH ₂ O

Genotype analysis was performed in a PCR reaction mix as depicted:

	5 % (v/v) Digestion Reaction Mix
PCR reaction	250 nM Forward primer
	250 nM Reverse primer
	1 x PCR Reaction buffer
	1 U Taq DNA Polymerase
	sterile dH ₂ O
	250 mM KCl
PCR Reaction buffer	50 mM Tris pH 8.3
	43 % (v/v) Glycerol
	7.5 mM MgCl ₂
	2.0 mM Cresol Red
	sterile dH ₂ O

For the determination of the genes TCR β -Plp1 (V β 6), *Tcra* and *Aire* program TD 54 x 30 was used, whereas for *CD11c-cre*, *Dereg*, *DTA*, *FoxN1 cre*, *Plp1*, *PLP^{fl}*, *Rag1*, *WT1* and 223 program TD 58 x 30.

TD 54 x 30 program			TD 58 x 30 program		
94 °C	3 min		94 °C	3 min	
94 °C	45 sec		94 °C	45 sec	
60 °C	45 sec	2x	64 °C	45 sec	2x
72 °C	1 min		72 °C	1 min	
94 °C	45 sec		94 °C	45 sec	
58 °C	45 sec	2x	62 °C	45 sec	2x
72 °C	1 min		72 °C	1 min	
94 °C	45 sec		94 °C	45 sec	
56 °C	45 sec	2x	60 °C	45 sec	2x
72 °C	1 min		72 °C	1 min	
94 °C	45 sec		94 °C	45 sec	
54 °C	45 sec	30x	58 °C	45 sec	30x
72 °C	1 min		72 °C	1 min	
72 °C	5 min		72 °C	5 min	
4 °C	∞		4 °C	∞	

3.2.3.2 Novel I-A^b tetramer expression and purification

Generation of I-A^b tetramers responding to the immunogenic region PLP1₁₁₋₁₉ (Tet-1) (in collaboration with Marc Jenkins) or PLP1₂₄₀₋₂₄₈ (Tet-3) were obtained by tetramerized peptide:I-A^b biotinylated monomers expressed in *Drosophila melanogaster* S2 cells [197].

In brief, using the *Drosophila* Expression System kit, *Drosophila* S2 cells were co-transfected with modified pRMHA vectors encoding either the I-A^b α - or I-A^b β -chain and two plasmids containing a BirA ligase or a blasticidin resistance gene (3.1.5.1 Tetramer).

sterile dH ₂ O	up to 300 μ l
CaCl ₂	240 mM
I-A ^b alpha	9 μ g
I-A ^b beta	9 μ g
p18 BirA	9 μ g
pCo Blast	1 μ g

Cells were allowed to recover in SFM medium for two days before starting the selection with the SFM medium containing blasticidin. After reaching a total cell number of 2.5×10^8 , cells were passaged to a 3 L spinner shaking flask for up-scaling to a final number of 5×10^6 cells/ml in 500 ml serum free SFM (including blasticidin 25 μ g/ml), at 28 °C and 125 rpm.

The expression of biotinylated peptide:I-A^b monomer was induced by 0.8 mM copper sulfate and 2 mg/ml Biotin. Peptide:I-A^b heterodimers expressed and secreted into the culture supernatant were separated from free biotin nine days upon transfection with a His-Bind Purification Kit (Novagene) according to the manufacturers manual. Eluted fractions were passed over a Pierce Monomeric Avidin UltraLink column to separate unwelcome unspecific His-column bound proteins and biotinylated peptide:I-A^b according to the manufacture's instruction. The biotinylated peptide:I-A^b was displaced and eluted with 12 ml elution buffer (2mM in PBS). Soluble and free biotin was separated within four washing steps using 5 ml PBS and an Amicon Ultra-15 column (Millipore) with a molecular weight cut-off of 30 kD. The final peptide:I-A^b monomer concentration was calculated after measuring the OD280 (Nanodrop) and using an extinction coefficient for BSA as reference.

Peptide:I-A^b monomer was stored at -80 °C. Peptide:I-A^b tetramerization was achieved by adding streptavidin conjugated with APC or PE (Prozyme) in a 4.5:1 ratio for 30 min at room temperature in the dark. Final concentration of 1 μ M was adjusted with PBS.

Purity of protein fractions was checked via sodium dodecyl sulphate polyacrylamide gel electrophoresis (SDS-PAGE). All fractions were loaded with 4x native Lam's sample buffer (200 mM Tris HCl pH 6.8, 60 % Glycerol and 20 μ g/ml Bromophenol Blue) and separated according to their size - SDS 15 % gel at 175 V for 60 min in running buffer. Proteins were either dyed with Coomassie or transferred in an exact replica of the gel on a nitrocellulose membrane during semi-dry western blot. Transfer was realized with

transfer buffer (running buffer + 8% MeOH) at max. 50 V and 160 mA for 2 h. Following the protein transfer, the membrane was incubated with selected antibodies and the SuperSignal® West Pico Chemiluminescent Substrate. Images were developed using a CEA RP NEW medical X-ray film.

Running buffer	400 mM Glycine
	500 mM Tris
	15 mM SDS
	sterile dH ₂ O

3.2.3.3 Single cell TCR α -chain sequencing

The findings by Dössinger *et al.* (depicted in figure 7) describing the amplification of a TCR sequence from a sorted single cell, served as the basis for the single cell TCR α -chain sequencing within this thesis [212].

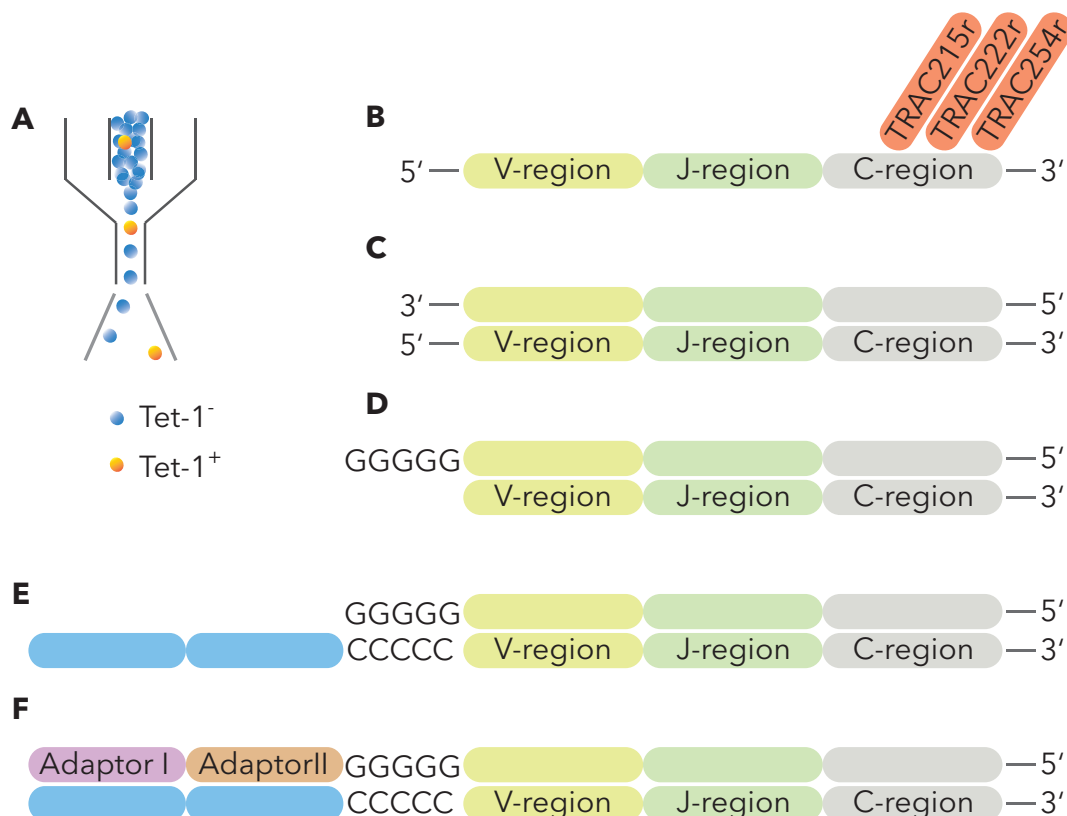


Figure 7: Schematic overview of single cell TCR α -chain sequencing

(A) One CD4⁺ Tet-1⁺ T cell/well was index sorted into wells of a 96 well plate using FACS Aria™ Fusion and a 100 μ m nozzle. (B) Reverse transcription was performed with the iScript cDNA synthesis kit and the specific primers TRAC215r, TRAC22r and TRAC254r (binding C-region - gray). (C) Remaining oligonucleotides were digested by Exonuclease I before (D) dGTP tailing. (E) A unique anchor platform was added via multi guanine cytosine hydrogen bonds using the introduced 3' - guanosin overhang. (F) Nested amplification steps were performed using either Adaptor I and TRAC13 (1st round) or Adaptor II and TRAC 2nd nested (2nd round).

3.2.3.3.1 Reverse Transcription

Synthesis of cDNA from single cell mRNA templates was realized in 96 well plates. One cell/well was sorted and stored at least over night at -80 °C to mechanically disrupt the cell walls. After thawing the plate, reverse transcription was performed using the iScript cDNA Synthesis Kit (figure 7 B). Samples were resuspended in 1x iScript buffer, 0.1 % Triton X-100, 1.25 μ M each of *Tcra* constant region reverse primers (TRAC215r, TRAC222r, and TRAC254r), 0.4 μ l Enhancer, 0.2 μ l iScript reverse transcriptase in a total of 4 μ l/well. Reverse transcription was performed at 25 °C for 5 min, 42 °C for 30 min and an inactivation step at 85 °C for 5 min on a Life ECO cycler from BIOER.

3.2.3.3.2 Exonuclease I digest

Unwelcome single stranded oligonucleotides, which would affect the results of the oligo-dG tailing, were digested with Exonuclease I (figure 7 C). 1 μ l of Exonuclease I digestion mix was added to the reverse transcription mix leading to a final concentration of 1 U/ μ l Exonuclease I and 1x reaction buffer. Digestion reaction was realized at 37 °C for 45 min, with a final inactivation step at 85 °C for 5 min.

3.2.3.3.3 Oligo-dG tailing

Addition of dGTPs to generate a unique binding sequence at the 3' end of the variable *Tcra* region was realized using the Terminal Deoxynucleotidyl Transferase Kit (figure 7 D). A tailing mix of 3.2 μ l resulting in 0.73 U/ μ l Terminale Transferase, 2.0 mM dGTP and 1x Terminal transfer buffer was added. Tailing was performed at 37 °C for 45 min followed by 75 °C for 10 min of inactivation.

3.2.3.3.4 TCR α -chain amplification

Following anchor and nested PCR amplification steps were performed using the cycler protocol:

94 °C	3 min	
94 °C	15 sec	
60 °C	30 sec	24x
72 °C	45 sec	
72 °C	5 min	
4 °C	∞	

The dGTP labeled variable *Tcra* gene region served as a binding platform for the anchor primer during the anchor PCR reaction (figure 7 E). The anchor PCR reaction mix was directly added to the oligo-dG tailing mix, for a final volume of 21 μ l. Therefore, the Herculase II Fusion DNA Polymerase Kit from Agilent was used and resulted in a final concentration of 1x buffer, dNTP each 215 μ M, 4 % DMSO, 0.25 μ l Herculase polymerase and 540 mM of each primer Anchor for and TRAC6.

For the first nested PCR amplification step 1 μ l per well of the Anchor PCR amplification product was mixed with 20 μ l nested PCR reaction mix I (leading to 1x buffer, dNTP each 190 μ M, 4 % DMSO, 0.25 μ l Herculase polymerase and 475 mM of each primer Adaptor I and TRAC13 and) in a new 96 well plate (Figure 7 F violet)

The second nested PCR reaction was performed by mixing 20 μ l nested PCR reaction mix II (resulting in 1x buffer, dNTP each 190 μ M, 4 % DMSO, 0.25 μ l Herculase polymerase and 475 mM of each primer Adaptor II and TRAC 2nd nested) and 1 μ l per well of the first nested PCR amplification product again in a new 96 well plate (figure 7 F brown).

The final DNA products generated during these steps were separated running a 1.5 % TAE agarose gel. Amplification products within a range of 200 - 650 bp were purified in 10 μ l H₂O by using the QiAquick Gel Extraction Kit from Qiagen, according to the manufacturer's protocol.

3.2.3.3.5 Cloning, transformation and sequencing

10 - 100 ng purified PCR product (DNA template) was ligated into the pCR®-Blunt vector using the modified Zero Blunt PCR cloning protocol (Ligation mix: 10 - 100 ng DNA template, 8 ng pCR®-Blunt, 1X ExpressLink™ T4 DNA Ligase Buffer and 5 U/rct T4 DNA Ligase). The plasmid with the gene of interest was transformed into TOP10 *E.coli* bacteria. After 30 min on ice and a heat shock at 42 °C for 45 sec the cells were mixed with 200 µl S.O.C. medium and kept on 37 °C for 1 h at 225 rpm to recover. Cell suspension was plated on LB-agar selection plates including Kanamycin and kept overnight at 37 °C. Two colonies per sorted cell were picked and used for plasmid preparation with the QIAprep Spin miniprep kit from Qiagen.

Sanger sequencing on extracted plasmids was performed by eurofins using the sequencing primer M13 for. Sequenced data were analyzed and annotated using CLC sequence viewer 7, ApE, Vector NTI and IMGT/V-Quest [211].

3.2.3.4 Generation of transgenic Mice

The generation of four unique TCR α-chain transgenic mice, was achieved via pronuclear injection of modified and linearized pTα cassette vectors [202].

3.2.3.4.1 Modification of pTα cassettes

In brief, to generate TCR α-chain gene fragment expressing unique characteristics of either TCR-A, TCR-H or TCR-E (all sharing the same VJC-region and differ only by two amino acids in the CDR3 region), genomic DNA of a CD4⁺ Tet-1⁺ T cell encoding the TCR α-chain (TRAV6D-6*6*02 = V gene segment / TRAJ12*01 = J gene segment / constant gene segment), was subjected to Q5® Site-Directed Mutagenesis (New England Biolabs) experiments. The resulting gene block contained the following CDR3 regions; ALGAPGGYKVV = TCR-A, ALGSTGGYKVV = TCR-H and ALGGPGGYKVV = TCR-E, discriminable due to the newly-introduced silent mutations (figure 8).

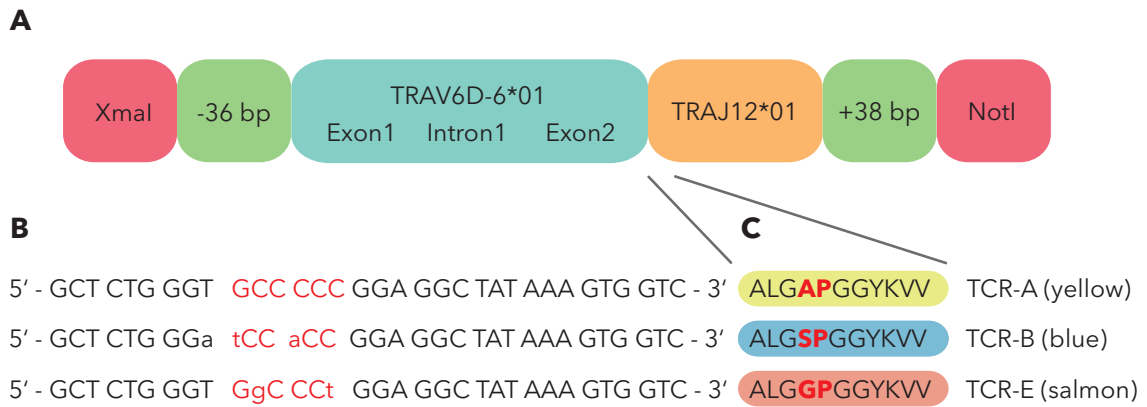


Figure 8: TCR-A, TCR-H and TCR-E gene fragment

(A) The main gene fragments that characterize the TCR-A, TCR-H and TCR-E gene blocks. In red the cleaving site of the respective restriction enzymes (Xmal/NotI) providing overhangs for sticky end ligation into the pTa cassette. The V region (TRAV6D-6*01 in blue) and J region (TRAJ12*01 in orange) are flanked by additional nucleotides expressing the relevant binding sequences for the spliceosome complex. (B) Nucleotide sequences of the respective CDR3 regions, which only differ in the red-labeled nucleotides. In small letters the introduced silent mutations for quick discrimination. (C) The respective amino acid sequence of the three CDR3 regions, with differences highlighted in red and bold.

To clone the TCR-F gene block, we took advantage of a pTa cassette of the previously published TCR-PLP1 tg animal [193]. Both constructs share at the N-terminus a fragment from the Xmal restriction site to the beginning of the CDR3 region. The part from the CDR3 onwards, was exchanged with three overlapping oligonucleotides encoding an Accl restriction site, the CDR3 region (AVSSNTNTGKLT) followed by the J segment TRAJ27*01+108 bp spliceosome binding sequence and N-terminal ending with a NotI cutting site. The Accl restriction site (located close to the CDR3 region C-terminal) was presence in both parts and therefore used for digestion and ligation (figure 9).

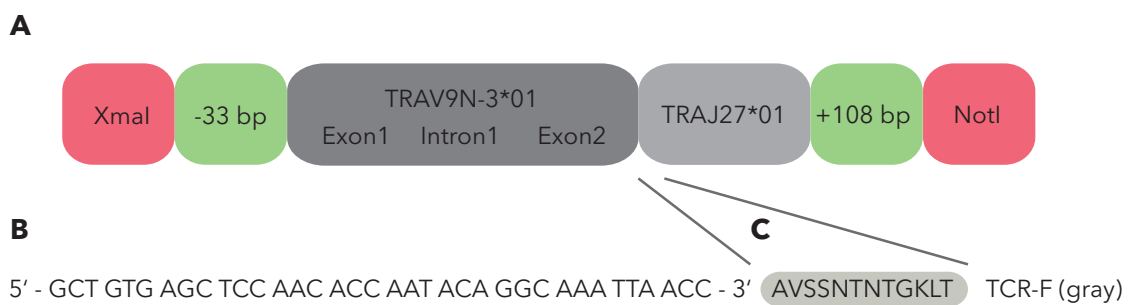


Figure 9: TCR-F gene fragment

(A) In red the restriction enzymes cleaving sites flanking the TRAV9N-3*01 (dark gray) and TRAJ27*01 (light gray) regions including the respective spliceosome complex binding sequence in green. (B) Nucleotide and (C) amino acid sequences of the TCR-F CDR3 region.

Last, the pEMBL18 backbone was removed from all four pTα cassette vectors via Sall digestion. Linearized DNA was used for transfection, electroporation and pronuclear injection experiments.

3.2.3.4.2 Transfection of human embryonic kidney (HEK) 293T cells

HEK293T cells were co-transfected with one of the modified pTα cassette vectors together with the pTβ cassette vector encoding the Vβ6 chain (Fixed-β) via calcium phosphate co-precipitation. 1×10^6 HEK293T cells were seeded 24 h prior transfection. For each construct a mixture (450 μl H₂O, 12.5 μg each cassette vector and 50 μl 2.5 mM CaCl₂) formed precipitates in 5 min at 37 °C. In the next step 37 °C preheated HeBS was carefully added. Pre-seeded HEK293T cells were overlaid and gently mixed with the transfection mix and incubated for 8 h at 37 °C. Transfection mix was exchanged with fresh medium and kept over night (24 - 30 h post transfection) before assaying for TCR transgene expression.

3.2.3.4.3 Electroporation of A5 cells

To test whether the pTα cassette vectors lead to the expression of a TCR α-chain able to form a functional TCR with the Vβ6-chain encoded on the pTβ cassette vector, A5 cells derived from BALB/c TCR HA_{Tg} 6.5 mice were electroporated with 25 μg of each cassette vector and 5 μg linearized NFAT-GFP vector including a puromycin resistance gene with 250 mV at RT. Following an incubation step for 10 min on ice, cells were kept over night in DMEM containing 10 % (v/v) of heat-inactivated FCS before being selected with 3 μg/ml puromycin. Resistant cells were subject of TCR expression and stimulation experiments.

3.2.4 Flow Cytometry

3.2.4.1 Tetramer staining and Tetramer based magnetic-activated cell sorting (MACS enrichment)

Enrichment of rare tetramer (APC and PE labeled) specific CD4⁺ T cells was achieved by incubation with magnetic nanoparticles-coated antibodies against APC and PE and a strong magnetic field [197, 213]. In brief, for each mouse analyzed a single cell suspension of either thymus, spleen or lymph nodes (axillary / brachial / cervical / inguinal / mesenteric) was incubated for 1 h in the dark at 25 °C with 100 μl tetramer staining mixture (1x Fc block, 2 % (v/v) mouse serum, 2 % (v/v) rat serum in tetramer buffer) including 15 nM APC and PE-labeled Tet-1 or Tet-3 I-A^b tetramer, respectively.

After a washing step tetramer labeled cells were incubated with anti-PE and anti-APC MicroBeads (Miltenyi), each 25 µl in a total volume of 300 µl tetramer buffer, in the dark on ice for 30 min.

Subsequently, cells binding to MicroBeads were positively selected using magnetized LS columns according to the manufacturer's instruction. The bound fraction was usually re-suspended in 100 µl antibody mix.

3.2.4.2 Surface and intracellular staining

Standard protocols for staining $5 - 10 \times 10^6$ cells or total MACS enriched cells were performed at 4 °C for 30 min in 100 µl FACS or tetramer buffer. Intracellular FoxP3 staining of mice lacking the expression of the FoxP3^{GFP} reporter (Dereg) was achieved by fixation and permeabilization (Fix/Perm Kit - eBioscience™) according to the description of the manufacturers.

Flow-cytometric analysis was implemented on FACSCanto II, LSRFortessa, while single cell sorts were performed on FACSARIA Fusion sorter. Both instruments were purchased from BD and located in the Core Facility Flow Cytometry of the BioMedical Center. The software FACSDiva used acquisition, recording and sorting, while FloJo9 and 10 were used for analysis.

Tetramer buffer	2.0 % (v/v) fetal calf serum
	0.1 % (w/v) sodium azide
	2.0 mM EDTA
	sterile PBS
FACS buffer	2.0 % (v/v) fetal calf serum
	2.0 mM EDTA
	sterile PBS

3.2.4.3 Calculation of cell numbers of the entire tetramer specific population

To calculate the number of tetramer specific T cell population within one mouse, 5 µl of the bound fraction obtained from MACS enrichment were mixed with pre-diluted AccuCheck Counting Beads (life technologies). The number of counting beads was

measured on a Casy Counter. The total amount of cells was enumerated by calculating the ratio of counting beads to the cells within 5 µl with the following formula:

$$\text{total cells sample} = \left(\frac{\text{cell count}}{\text{bead count}} \right) \times (\text{bead conc.}) \times \left(\frac{\text{bead volume}}{\text{cell volume}} \right) \times (\text{sample volume})$$

Afterwards the percentage of Tet⁺ T cells within the remaining bound sample fraction was multiplied with the total cells of 5 µl to obtain the total number of Tet⁺ T cells per sample.

$$\text{total number Tet}^+ \text{ cells} = \text{total cells sample} \times \text{percentage of Tet}^+ \text{ cell in sample}$$

3.2.5 Cell culture

3.2.5.1 Proliferation assay

PLP1 dependent proliferation of TCR-F, TCR-A, TCR-H and TCR-E TCR transgenic T cells were monitored *ex vivo* during a Cell Trace Violet (CTV) Cell Proliferation assay in the presence of PLP1₁₋₂₄.

5 x 10⁶ peripheral T cells/ml from PLP1-deficient, TCR transgenic, *Rag1*^{KO} mice were washed two times with 15 ml PBS and subsequently re-suspended and incubated in 1 ml 37 °C warm PBS containing 3 µmol CTV for 5 min at 37 °C. Reaction was stopped adding 2 ml FCS. After washing the cells in PBS the pellet was re-suspended in 1 ml IMDM before 5 - 10 x 10⁴ cells/well were seeded in 96 well plates and stimulated with 50.000 - 80.00 BM-derived, LPS-matured and irradiated CD45.1⁺ DCs and a dilution series of PLP1₁₋₂₄ respectively. Cells were stimulated at 37 °C and 7 % CO₂ for 4 days.

4 Results

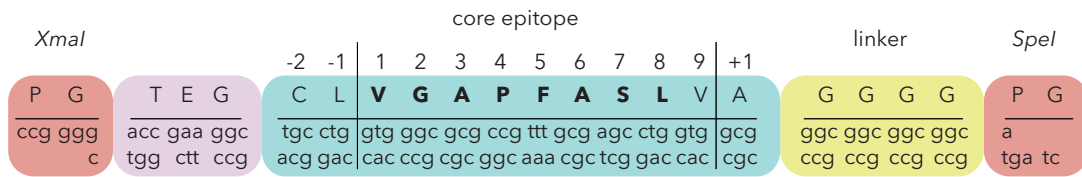
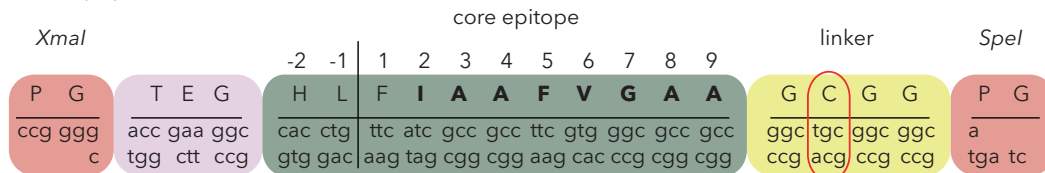
4.1 Generation of PLP1:I-A^b tetramers

The aim of this work was to understand how tolerance to a prototypical tissue-restricted antigen shapes the CD4⁺ T cell repertoire; more specifically, how PLP1 drives clonal deletion and clonal diversion on a single-cell level. To track small cohorts of PLP1-specific CD4⁺ T cells in a TCR polyclonal setting we generated I-A^b tetramers in collaboration with Marc Jenkins.

As a prerequisite to synthesize two novel I-A^b tetramers containing the previously fine mapped PLP1₁₁₋₁₉ or PLP1₂₄₀₋₂₄₈ peptides [1, 193], we ranked nonamers within the PLP1 amino acid sequence according to their binding capability for the MHCII I-A^b binding pocket (max. score 146) with an algorithm designed by Marc Jenkins (unpublished). Among the top six binding peptides within the entire protein, we found the previously-identified immunogenic core epitopes PLP1₁₁₋₁₉ (#1, score 124) and PLP1₂₄₀₋₂₄₈ (#6, score 71) (figure 10 A). Both were cloned together with a poly-glycine linker into the pRMHa vector encoding the I-A^b beta chain. Since the overlapping PLP1₂₄₀₋₂₄₈ (#6, score 71) and PLP1₂₄₄₋₂₅₂ (#3, score 86) peptides were predicted to have similar binding affinities to MHCII, we incorporated a “disulphide trap” to force the binding of PLP1₂₄₀₋₂₄₈ in the correct register. Therefore, the second glycine within the linker region C-terminal to the core epitope was exchanged with cysteine so that, together with a modified I-A^b alpha chain containing a cysteine at amino acid position 72, a disulphide bridge stabilized the core epitope PLP1₂₄₀₋₂₄₈ within the MHCII binding pocket.

A

Rank	Position	Score	Nonamer
#1	„11 - 19 aa“	124 (very high)	VGAPFASLV
#2	„187 - 195 aa“	86 (high)	IAFPSKTSA
#3	„244 - 252 aa“	86 (high)	FVGAAATLV
#4	„237 - 245 aa“	78 (high)	FHLFIAAFV
#5	„208 - 216aa“	76 (high)	GVLPWNAFP
#6	„240 - 248 aa“	71 (high)	FIAAFVGAA

B**PLP1₁₁₋₁₉:I-A^b tetramer (Tet-1)****C****PLP1₂₄₀₋₂₄₈:I-A^b tetramer (Tet-3)****Figure 10: PLP1₁₁₋₁₉ and PLP1₂₄₀₋₂₄₈ binding prediction and cloning strategy**

(A) *In silico* binding prediction of nonamers within the PLP1 protein and the peptide-binding groove of I-A^b. The table contains the top six predicted binders, including the position within the entire PLP1 sequence and the respective amino acid sequence. Based on an algorithm provided by Marc Jenkins (not published) a higher score (max. 146) indicates a stronger binding to I-A^b MHCII. Cloning scheme of tetramers specific for the antigenic peptides (B) PLP1₁₁₋₁₉ and (C) PLP1₂₄₀₋₂₄₈. The respective core epitopes (bold letters) are followed by a glycine linker region [in (C) the second glycine was exchanged to cysteine] and flanked by the unique restriction enzymes sequences. Capital letters represent the amino acid sequence and small letters the respective nucleotide sequence.

In order to assess the binding specificity of the newly-generated tetramers within a CD4⁺ T cell population, we immunized C57BL/6 *Plp1*^{WT} and *Plp1*^{KO} (to which PLP1 represents a foreign antigen) mice either with PLP1₁₋₂₄ (peptide#1) or PLP1₂₃₇₋₂₄₈ (peptide#3) peptides. Ten days post-immunization draining and non-draining LNs of two individual mice per group were pooled and pMHCII tetramer positive cells were MACS enriched. Flow-cytometry analysis was used to identify CD44⁺ effector T cells and the specific binding of either PLP1₁₁₋₁₉:I-A^b tetramer (Tet-1) or PLP1₂₄₀₋₂₄₈:I-A^b tetramer (Tet-3). Upon peptide#1 immunization, the proportions of Tet-1⁺ effector T cells were 15-fold higher in the draining LNs compared to the non-draining controls both in the *Plp1*^{KO} and *Plp1*^{WT} animals. Importantly, in the presence of potentially-tolerogenic PLP1, the fraction of Tet-1⁺ T cells was reduced (figure 11 A & B). All other controls immunized with peptide#3 were Tet-1 negative. Similar observations were made for the Tet-3 staining upon peptide#3 immunization: Tet-3⁺ effector T cells were 13-fold higher in the draining LNs of both *Plp1*^{KO} and *Plp1*^{WT} mice compared to the respective non-draining LNs, but the non-tolerant *Plp1*^{KO} mice harboured a higher fraction of Tet-3⁺ T cells

(figure 11 C & D). Overall, the Tet⁺ fractions were less represented in Tet-3 compared to Tet-1 staining (figure 11).

Unspecific staining of CD8⁺ T cells was not observed in any of the described setups (data not shown), underlining the specificity of Tet-1 and Tet-3 for CD4⁺ T cells. In conclusion, we were able to generate two different functional tetramers, which stain PLP1-specific TCRs on CD4⁺ T cells.

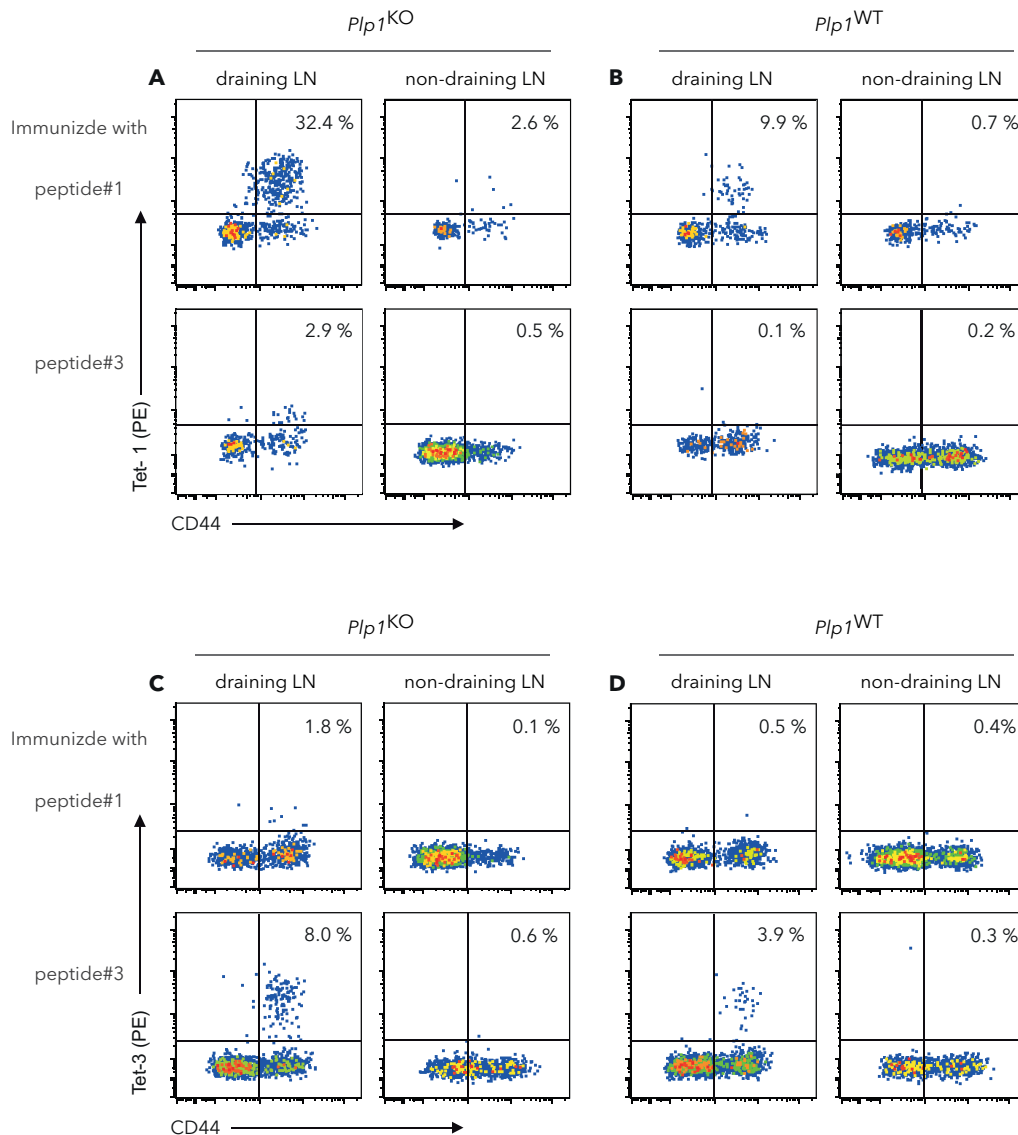


Figure 11: Tetramer functionality upon respective peptide immunization

Fraction of (A) Tet-1 and (C) Tet-3-positive CD44⁺ effector T cells in PLP1 non-tolerant animals and (B) Tet-1 and (D) Tet-3 in PLP1 tolerant animals. The fractions shown represent tetramer positive T cells within pooled (non-) draining LNs from two individual mice 10 days upon immunization with the respective peptide#1 or peptide#3. All dot plots are pre-gated on CD4⁺ CD8⁻ CD11b⁻ CD11c⁻ B220⁻ F4/80⁻ cells.

4.2 PLP1-specific T cells within the polyclonal T cell repertoire

We used the Tet-1 and Tet-3 reagents to identify PLP1-specific CD4⁺ T cells in the native (i.e. non-immunized) repertoire of PLP1-deficient and -sufficient mice. T cells pooled from lymph nodes and spleen of *Plp1*^{KO} animals contained on average 14.0 Tet-1⁺ and 4.4 Tet-3⁺ CD4⁺ T cells (figure 12 A & B). In tolerant *Plp1*^{WT} mice the number of Tet-1⁺ and Tet-3⁺ T cells was not significantly altered. However, differences were detected in the expression pattern of regulatory T cell lineage markers. In the absence of tolerizing self-antigen, essentially all Tet-1- or Tet-3-specific cells were T_{conv} (CD25⁻ Foxp3⁻), whereas in *Plp1*^{WT} mice roughly 35 % of the Tet-1- or Tet-3-specific CD4⁺ T cells expressed CD25 and FoxP3 (figure 12 C & D).

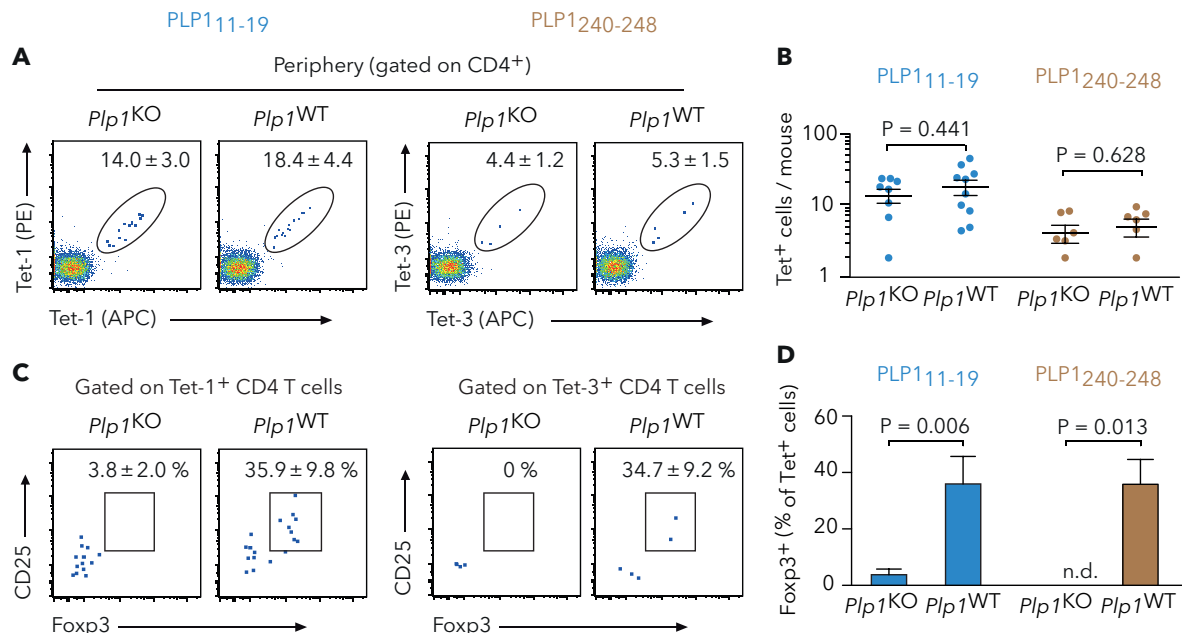


Figure 12: Abundance and phenotype of peripheral PLP1-specific CD4⁺ T cells in the polyclonal repertoire

(A) Abundance of PLP1₁₁₋₁₉- or PLP1₂₄₀₋₂₄₈-specific peripheral T cells in the presence and absence of PLP1. The calculated mean ± SEM represents CD4⁺ Tet-1⁺ or Tet-3⁺ cells/mouse in pooled LNs and spleen after enrichment of tetramer positive cells (n ≥ 6). All dot plots are pre-gated on CD4⁺ CD8⁻ CD11b⁻ CD11c⁻ B220⁻ F4/80⁻. (C) Phenotypical characterization of tetramer positive T cells. Dot plots show mean frequency ± SEM of CD25⁺ Foxp3⁺ peripheral T cells, quantified on the right (D). (A & C) show one representative flow-cytometry plot, while (B & C) represent the overall quantification for all the mice. Statistical significance was calculated using the unpaired two-tailed Student's t-test with Welch's correction for unequal variance.

The thymi of PLP1-sufficient animals comprised a similar number of Tet-1⁺ and Tet-3⁺ CD4 SP T cells compared to the PLP1-deficient mice (figure 13 A & B), and roughly 10 % of these cells expressed CD25 and FoxP3 (figure 13 C & D). Instead, in the absence of PLP1, none of the Tet-1⁺ or Tet-3⁺ thymocytes expressed the regulatory T cell lineage markers (figure 13 C & D), which was reminisced with our observations in the secondary lymphoid organs.

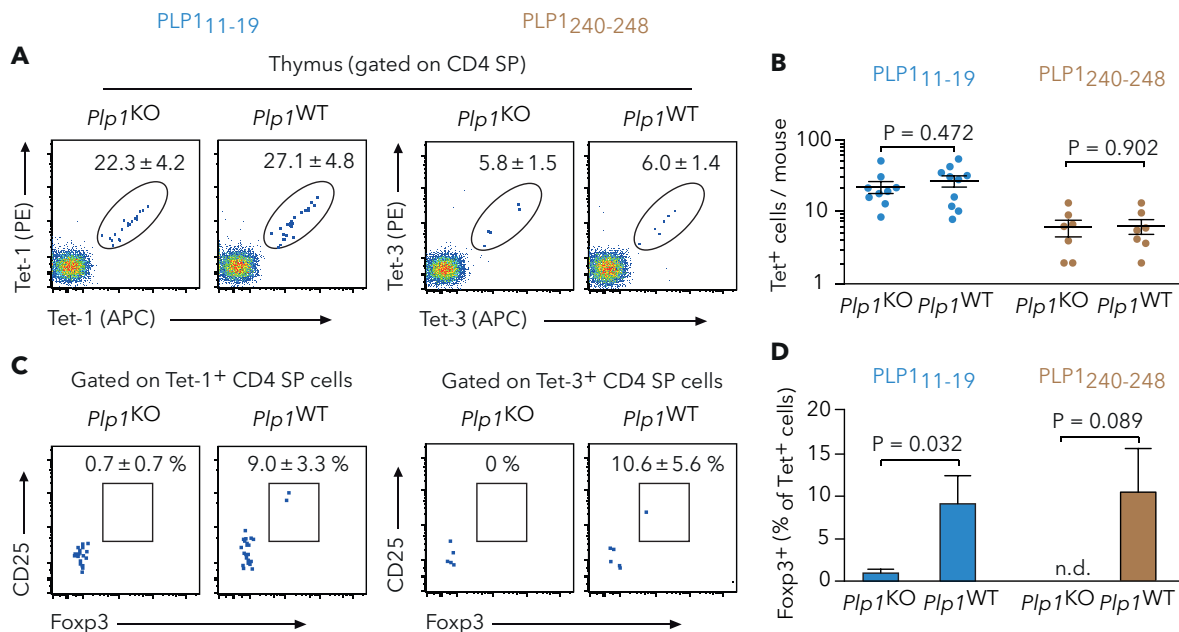


Figure 13: Abundance and phenotype of PLP1-specific CD4 SP thymocytes in the polyclonal repertoire

(A) Abundance of PLP1₁₁₋₁₉- or PLP1₂₄₀₋₂₄₈-specific thymocytes in the presence and absence of PLP1. The calculated mean ± SEM represents CD4 SP Tet-1⁺ or Tet-3⁺ cells/thymi after enrichment of tetramer positive cells (n ≥ 7 mice). All dot plots are pre-gated on CD4⁺ CD8⁻ CD11b⁻ CD11c⁻ B220⁻ F4/80⁻. (C) Phenotypical characterization of tetramer positive thymocytes. Dot plots show mean frequency ± SEM of CD25⁺ FoxP3⁺ thymocytes, quantified on the right (D). (A & C) show one representative flow-cytometry plot, while (B & C) represent the overall quantification for all the mice. Statistical significance was calculated using the unpaired two-tailed Student's test with Welch's correction for unequal variance.

The total number of PLP1₁₁₋₁₉- and PLP1₂₄₀₋₂₄₈-specific CD4⁺ T cells was similar to previously published numbers of anti-foreign Tet⁺ T cells in naïve C57BL/6 mice, which ranged from less than 10 to around 300, depending on the antigen tested [197, 214, 215]. Taken together, these data revealed that clonal diversion substantially contributes to tolerance among PLP1-reactive T cells. This supports the previously published findings of preferred T_{reg} cell induction of polyclonal T cells specific for a neo-self-antigen under the promoters of TRA [86, 87].

4.3 PLP1-specific T cells in a repertoire of reduced diversity

To test if clonal deletion of PLP1-specific T cells happens at all, one would have to compare every Tet⁺ TCR within a non-tolerant naïve repertoire (*Plp1*^{KO}) with the Tet⁺ repertoire in tolerant *Plp1*^{WT} mice. However, due to the theoretical tremendous number of different TCR α / β -chain combinations (in the order of 10¹⁵) [216], which by far exceeds the number of T cells present in the body of a mouse (approx. 6 x 10⁷) [217], we decided to reduce the diversity of the fully polyclonal TCR repertoire. To this purpose, we introduced a TCR β -chain transgene (V β 6) derived from the previously described TCR-PLP1 mouse model and focused on Tet-1⁺ CD4⁺ T cells [193].

To ensure that T cells only express one TCR α -chain and to facilitate the identification of FoxP3 expressing T_{reg} cells, we crossed animals carrying the TCR β -chain transgene with *Tcr α* ^{KO} and FoxP3^{GFP} reporter (Dereg) mice to obtain TCR β -PLP1^{tg/-}::*Tcr α* ^{+/-}::Dereg^{tg/-} mice, in the following referred to as Fixed- β mice.

4.3.1 Characterization of Fixed- β mice

We took advantage of a TCR β -chain transgene originating from a PLP1 specific $\alpha\beta$ TCR with the idea to bias the CD4⁺ T cells towards PLP1 recognition, while maintaining the TCR α -chain polyclonal. Indeed, previous experiments in the lab revealed that the expression of V β 6-chain is up to 3-fold more frequent among *Plp1*^{KO} T cells after multiple rounds of *in vitro* PLP1 stimulation [218].

Compared to an un-manipulated C57BL/6 mouse, the Fixed- β mice harbored three times more CD4 SP T cells. The fraction of CD4 SP T cells expressing CD25 and FoxP3 was around 5 %, independent of PLP1 expression (figure 14 A & B - C57BL/6L *Plp1*^{KO} not shown). More than 97 % of CD4⁺ T cells expressed the V β 6-chain transgene (figure 14 C).

Taken together, the V β 6-chain transgene was efficiently expressed by CD4 T cells, leading to an increased fraction of CD4⁺ T cells without altering the frequency of regulatory T cells.

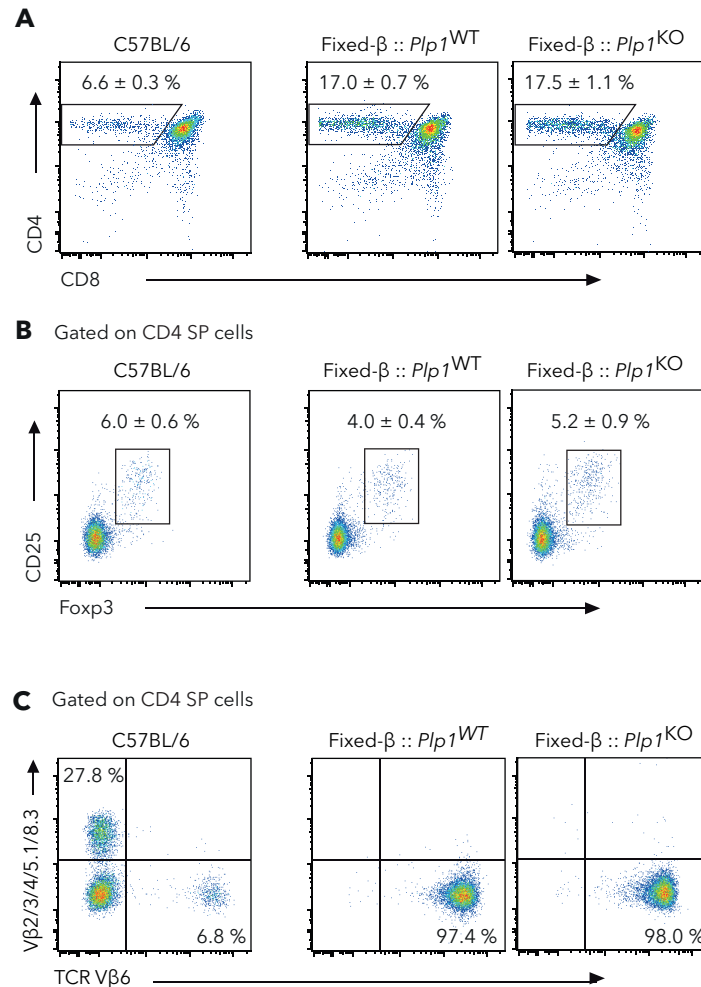


Figure 14: T_{reg} cell induction in C57BL/6 and Fixed-β mice

(A) Thymic CD4/CD8 profiles of C57BL/6 and Fixed-β::*Plp1*^{KO} or *Plp1*^{WT} animals. The calculated mean ± SEM represents the % of CD4 SP/thymus ($n \geq 3$). (B) Phenotypic characterization of CD4 SP cells. Mean frequency ± SEM represents CD25⁺ FoxP3⁺ expressing thymocytes. (C) Expression of either the endogenous (C57BL/6) or the transgenic (Fixed-β) TCR Vβ6-chain among CD4 SP thymocytes, in parallel to the cumulative fraction of endogenous TCR Vβ2/3/4/5.1/5.2 (mean frequency ± SEM).

4.3.2 T_{reg} phenotype of peripheral Tet-1⁺ T cells in PLP1-sufficient mice

We next analyzed the Fixed-β mice in the absence and presence of PLP1 in regard to abundance and phenotype of CD4⁺ Tet-1⁺ T cells. The Fixed-β::*Plp1*^{WT} animals displayed a significantly higher frequency of Tet-1⁺ T cells in secondary lymphoid organs (224 vs. 78 T cells/mouse) (figure 15 A). Importantly, a substantial fraction (57.7 %) of CD4⁺ Tet-1⁺ T cells in Fixed-β::*Plp1*^{WT} mice expressed CD25 and FoxP3, whereas in Fixed-β::*Plp1*^{KO} mice, only 5.8 % of CD4⁺ Tet-1⁺ expressed these T_{reg} cell lineage markers (figure 15 B).

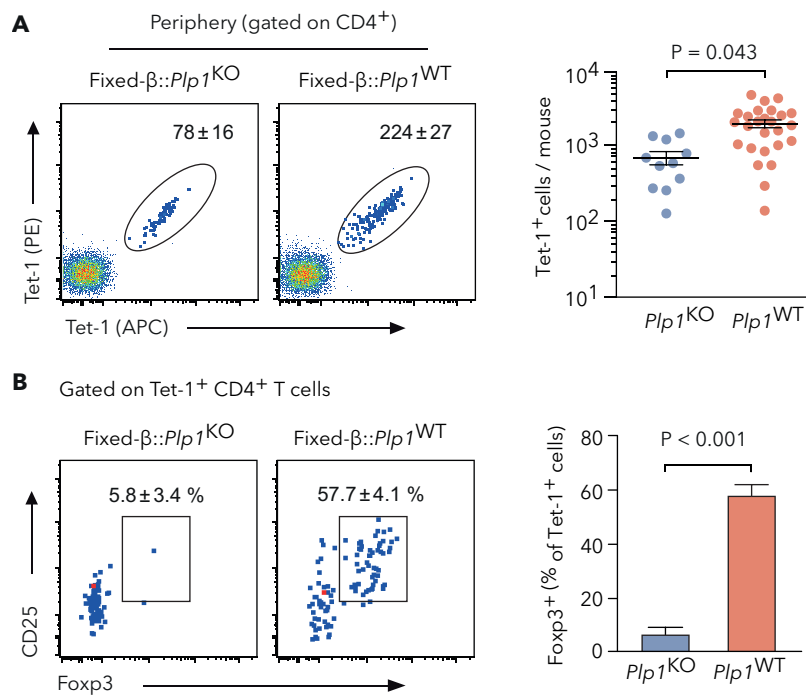


Figure 15: PLP1 specific regulatory T cell in Fixed- $\beta::Plp1^{WT}$ lymph nodes

(A) Abundance of PLP1₁₁₋₁₉-specific peripheral T cells in Fixed- $\beta::Plp1^{WT}$ and Fixed- $\beta::Plp1^{KO}$ animals. The calculated mean \pm SEM represents the absolute number of Tet-1⁺ cells/mouse in pooled LNs and spleen ($n \geq 11$). On the left, representative dot plots are pre-gated on CD4⁺ CD8⁻ CD11b⁻, CD11c⁻, B220⁻ and F4/80⁻ and show MACS-enriched tetramer positive cells. On the right, data points are representative of one mouse each. (B) Phenotypical characterization of tetramer positive CD4⁺ T cells. Mean frequency \pm SEM represents CD25⁺ FoxP3⁺ peripheral T cells. Statistical significance was calculated using the unpaired two-tailed Student's t-test with the Welch's correction for unequal variance.

In sum, although we detected an increase in PLP1-specific T cells of 4 to 10-fold compared to the polyclonal setting, these numbers were still in the described physiological range of naïve CD4⁺ T cells specific for anti-foreign antigens [197, 214, 215]. Additionally, the Fixed- $\beta::Plp1^{WT}$ mice mirrored with a robust T_{reg} cell induction the results of the fully polyclonal repertoire.

4.3.3 Anergic phenotype within the Tet-1⁺ T cell population in the presence of tolerizing-antigen

A substantial fraction of Tet-1⁺ T cells in Fixed- $\beta::Plp1^{WT}$ animals were CD25 and FoxP3 negative (figure 15 B & 16 A). We therefore asked whether these cells were truly naïve or displayed phenotypic hallmarks of being tolerized by mechanisms other than T_{reg} cell diversion, for instance anergy.

Indeed, in Fixed- $\beta::Plp1^{WT}$ mice, around 60 % of CD4⁺ Tet-1⁺ CD25⁻ FoxP3⁻ T cells expressed the T cell anergy markers FR4 and CD73 [171], whereas in Fixed- $\beta::PLP1^{KO}$ mice, only a minor fraction of CD4⁺ Tet-1⁺ CD25⁻ FoxP3⁻ T cells expressed FR4 and CD73 (figure 16 B). On these seemingly anergic T cells in Fixed- $\beta::Plp1^{WT}$ animals, we also observed an increase in CD44 expression equal to the level of Fixed- $\beta::Plp1^{WT}$ T_{reg} cells (figure 16 C). The fraction of CD44⁺ cells was seven times higher within CD4⁺ Tet-1⁺ CD25⁻ FoxP3⁻ Fixed- $\beta::Plp1^{WT}$ compared to CD4⁺ Tet-1⁺ CD25⁻ FoxP3⁻ Fixed- $\beta::Plp1^{KO}$ T cells.

Altogether, compared to Fixed- $\beta::Plp1^{KO}$ mice peripheral tetramer positive cells in PLP1 tolerant Fixed- β animals are not reduced, but consist of either regulatory T cells or anergic lymphocytes.

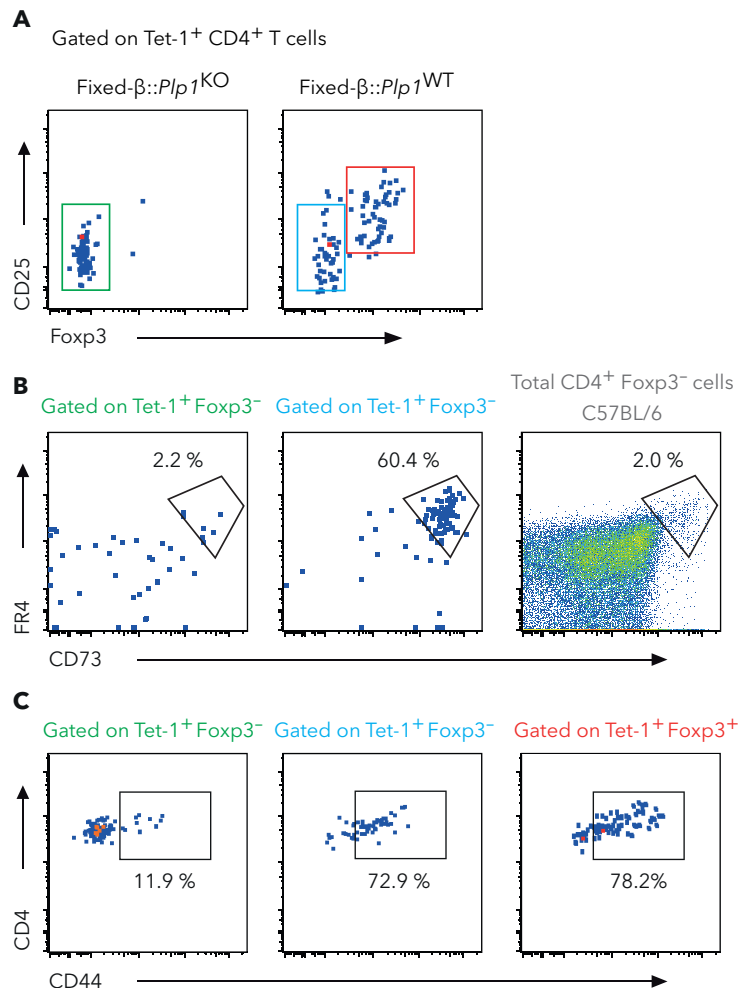


Figure 16: Peripheral Tet-1⁺ CD4⁺ T cells display an activated and anergic phenotype in the presence of antigen

(A) CD25 and FoxP3 expression on PLP1₁₁₋₁₉-specific peripheral T cells from Fixed-β::*Plp1*^{WT} or Fixed-β::*Plp1*^{KO} mice. (B) FR4 and CD73 or (C) CD44 staining and calculated mean of CD4⁺ CD25⁻ FoxP3⁻ Tet-1⁺ peripheral T cells of Fixed-β::*Plp1*^{KO} (green) and Fixed-β::*Plp1*^{WT} (blue) from at least 6 mice each, compared to either bulk C57BL/6L CD4⁺ CD25⁻ FoxP3⁻ T cells (gray in B) or to CD4⁺ Tet-1⁺ CD25⁻ FoxP3⁺ T cells from Fixed-β::*Plp1*^{WT} animals (red in C).

4.3.4 Central tolerance clonally diverts and deletes self-reactive T cells

We next characterized abundance and phenotype of CD4 SP Tet-1⁺ thymocytes. In Fixed-β::*Plp1*^{KO} mice, we identified on average 746 CD4 SP Tet-1⁺ T cells. None of these were CD25 and FoxP3 positive (figure 17). In contrast, CD4 SP Tet-1⁺ thymocytes of Fixed-β::*Plp1*^{WT} animals were significantly reduced (310 cells) and 11.1 % displayed the regulatory T cell lineage markers CD25 and FoxP3.

It was recently demonstrated that in C57BL/6 mice under steady state conditions around 30 % of the thymic T_{reg} cells consist of immigrants from the periphery [219]. These lack the expression of CCR7 [220]. To define the quantity of re-immigrated regulatory T cells in Fixed-β::*Plp1*^{WT} animals, we assessed the CCR7 expression on CD4 SP CD25⁺ FoxP3⁺ T cells, revealing that more than 80 % of the cells expressed CCR 7 (figure 17 C).

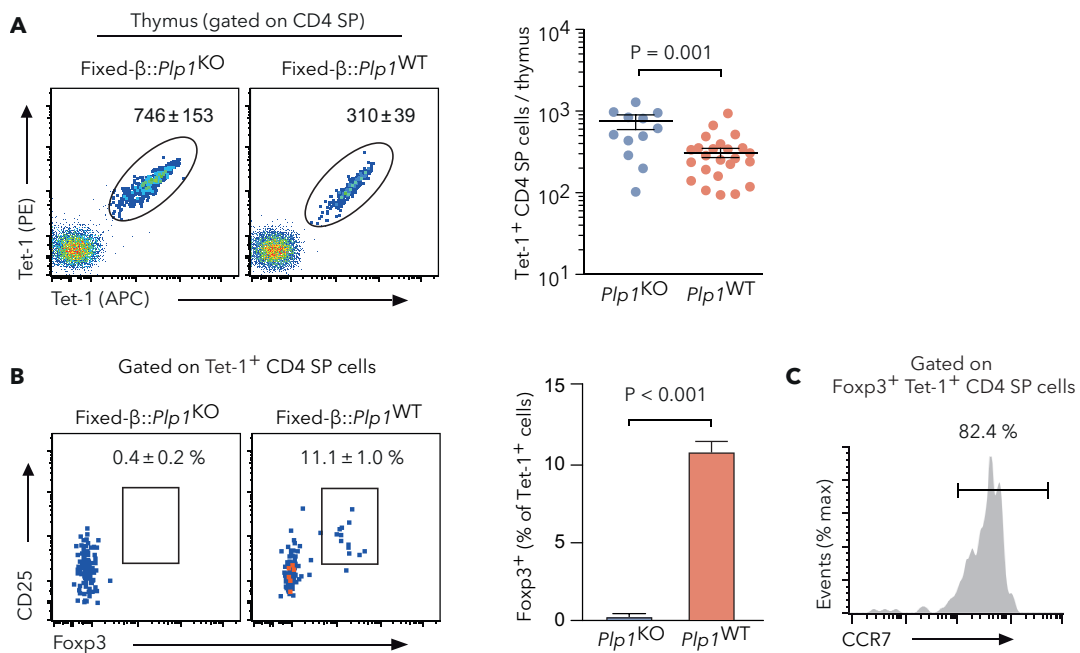


Figure 17: Deletion and T_{reg} cell diversion of autoreactive CD4 SP Tet-1⁺ thymocytes in PLP1-sufficient mice

(A) Abundance of Tet-1⁺ thymocytes in Fixed-β::Plp1^{WT} and Fixed-β::Plp1^{KO} mice. The calculated mean ± SEM represents Tet-1⁺ thymocytes/thymus after MACS-enrichment of tetramer positive cells (n ≥ 11). All dot plots are pre-gated on CD4⁺ CD8⁻ CD11b⁻, CD11c⁻, B220⁻ and F4/80⁻. (B) Phenotypical characterization of tetramer positive thymocytes. Mean frequency ± SEM represents CD25⁺ FoxP3⁺ thymocytes. (C) Expression level of CCR7 on regulatory T cells (CD4⁺ CD25⁺ FoxP3⁺) in Fixed-β::Plp1^{WT} thymi, as indication of non-recirculating T_{reg} cells. Staining and calculated mean of pooled thymi (n = 6). Where indicated, p-values were calculated using the unpaired two-tailed Student's t-test with Welch's correction for unequal variance.

These data are consistent with negative selection and diversion of autoreactive thymocytes occurring concomitantly. While the reduced number of CD4 SP T cells speaks for itself, the appearance of a high fraction of CCR7 expressing regulatory T cells strongly suggests the generation of those in the thymus.

4.3.5 Mature autoreactive thymocytes express anergy markers

It is conceivable that the expression of PLP1 in the thymus not only deletes and diverts self-reactive thymocytes, but also induces anergy of a fraction of cells. Therefore, we addressed at which maturation stage CD4 SP T cells get deleted and whether the surviving T cells show an anergic phenotype. Concerning deletion, we took advantage of the maturation-dependent CD69 and MHCII expression. In the medulla CD69⁺ MHCII⁻ convert into CD4 SP CD69⁺ MHCII⁺ and, before emigration into the periphery, to CD69⁻ MHCII⁺ [113].

In the presence of tolerizing antigen, the Tet-1⁺ T cells accumulated in the earliest stage of development (CD69⁺ MHCII⁻) in a PLP1-independent manner (figure 18 B). Over the course of maturation, a small fraction of Tet-1⁺ PLP1 T cells acquired a (mature) regulatory T cell phenotype, whereas the most mature stage showed the strongest reduction in Tet-1⁺ T cells. This is consistent with the idea that PLP1 specific T cells undergo clonal diversion and clonal deletion before reaching the most mature stage (CD69⁻ MHCII⁺) (figure 18 B). Moreover, a fraction of mature non-T_{reg} cells expressed FR4 and CD73, whereas this was not the case in Fixed-β::Plp1^{KO} mice (figure 18 C).

In sum, the appearance of fully mature non-regulatory CD4 SP Tet-1⁺ FR4⁺ CD73⁺ T cells in the thymus suggests that the induction of anergy might be a third central tolerance mechanism within the medulla.

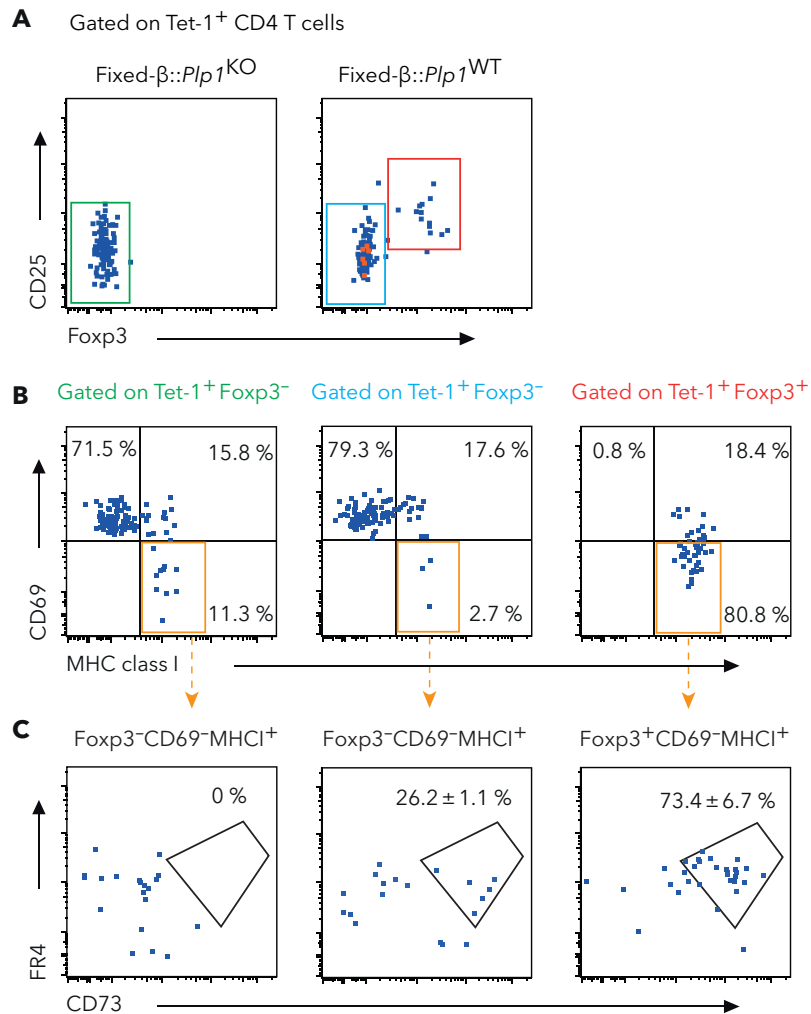


Figure 18: Mature CD4 SP thymocytes express the peripheral energy markers FR4 and CD73

(A) PLP1₁₁₋₁₉-specific thymocytes from Fixed-β::*Plp1*^{WT} or Fixed-β::*Plp1*^{KO} mice (phenotyped in figure 17 B). (B) CD69 and MHC class I staining from pooled CD4 SP CD25⁻ Foxp3⁻ Tet-1⁺ thymocytes of *Plp1*^{KO} (green), *Plp1*^{WT} (blue) and CD4 SP Tet-1⁺ CD25⁺ Foxp3⁺ regulatory T cells of *Plp1*^{WT} (red). (C) FR4 and CD73 staining of the most mature CD4 SP Tet-1⁺. All values calculated from at least 5 mice each.

4.3.6 Clonal deletion and clonal diversion require PLP1 expression by TECs and depend on AIRE

Previous experiments in the lab showed that the expression of PLP1 in the thymic epithelium was sufficient for central tolerance induction. In *Plp1*^{WT} → *Plp1*^{KO} thymus chimeras, irradiated and reconstituted with bone marrow from PLP1-deficient mice, the ability of peripheral T cells to respond to PLP1 was highly reduced [1]. Furthermore, in TCR-PLP1 transgenic mice lacking PLP1 in thymic epithelial cells (TECs) clonal deletion

and diversion of CD4 SP thymocytes was entirely absent [193]. To understand to which extent central tolerance of PLP1-specific polyclonal T cells depends on PLP1 expression by TECs, we crossed the Fixed- $\beta::Plp1^{WT}$ animals with *FoxN1* cre and *Plp1* floxed mice. This conditional knockout mouse model lacks PLP1 expression in TECs, and will in the following be referred to as Fixed- $\beta::Plp1^{\Delta TEC}$. The CD4 SP compartment of these animals contained on average 518 Tet-1⁺ thymocytes and with a barely detectable fraction of CD25⁺ FoxP3⁺, resembling the phenotype of Fixed- $\beta::Plp1^{KO}$ (figure 19 A & B vs. figure 17). Remarkably, despite this apparent lack of thymic T_{reg} cell induction, 60 % of the peripheral Tet-1⁺ T cells were composed of regulatory T cells, mirroring the peripheral regulatory T cell fraction of Fixed- $\beta::Plp1^{WT}$ animals (figure 19 C & D vs. figure 15).

Given the fact that the transcriptional regulator AIRE drives the expression of many TRA in mTECs, our lab had previously examined the effect of an inactive *Aire* gene on central tolerance mechanisms in TCR-PLP1 transgenic mice. In this study the lack of AIRE resulted in the loss of both clonal deletion and diversion of TCR transgenic cells [1, 193]. To evaluate the impact of the transcription factor AIRE on our Fixed- $\beta::Plp1^{WT}$, we bred them to animals carrying a defective *Aire* gene, in the following referred to as Fixed- $\beta::Aire^{KO}$.

The number and phenotype of CD4 SP Tet-1⁺ thymocytes in AIRE-deficient animals differ significantly from Fixed- $\beta::Plp1^{WT}$ and resembled those of Fixed- $\beta::Plp1^{KO}$ and Fixed- $\beta::Plp1^{\Delta TEC}$ mice, in regard to the scarcity of regulatory T cells (figure 19 A & B vs. figure 17). On the contrary, in peripheral lymphoid organs, the higher number of Tet-1⁺ CD25⁺ FoxP3⁺ T cells phenocopied the results from the Fixed- $\beta::Plp1^{\Delta TEC}$ and Fixed- $\beta::Plp1^{WT}$, diverging notably from PLP1-deficient animals (figure 19 C & D vs. figure 15). Taken together, the lack of PLP1 and AIRE expression in TECs leads to a breakdown of central tolerance mechanisms that normally apply to Tet-1⁺ thymocytes. Although we did not find indications for T_{reg} cell induction in the thymus of Fixed- $\beta::Plp1^{\Delta TEC}$ or Fixed- $\beta::Aire^{KO}$ mice, the high fraction of peripheral regulatory T cells - reaching levels comparable to Fixed- $\beta::Plp1^{WT}$ animals - speaks for a potential antigen source driving T_{reg} cell diversion in the periphery.

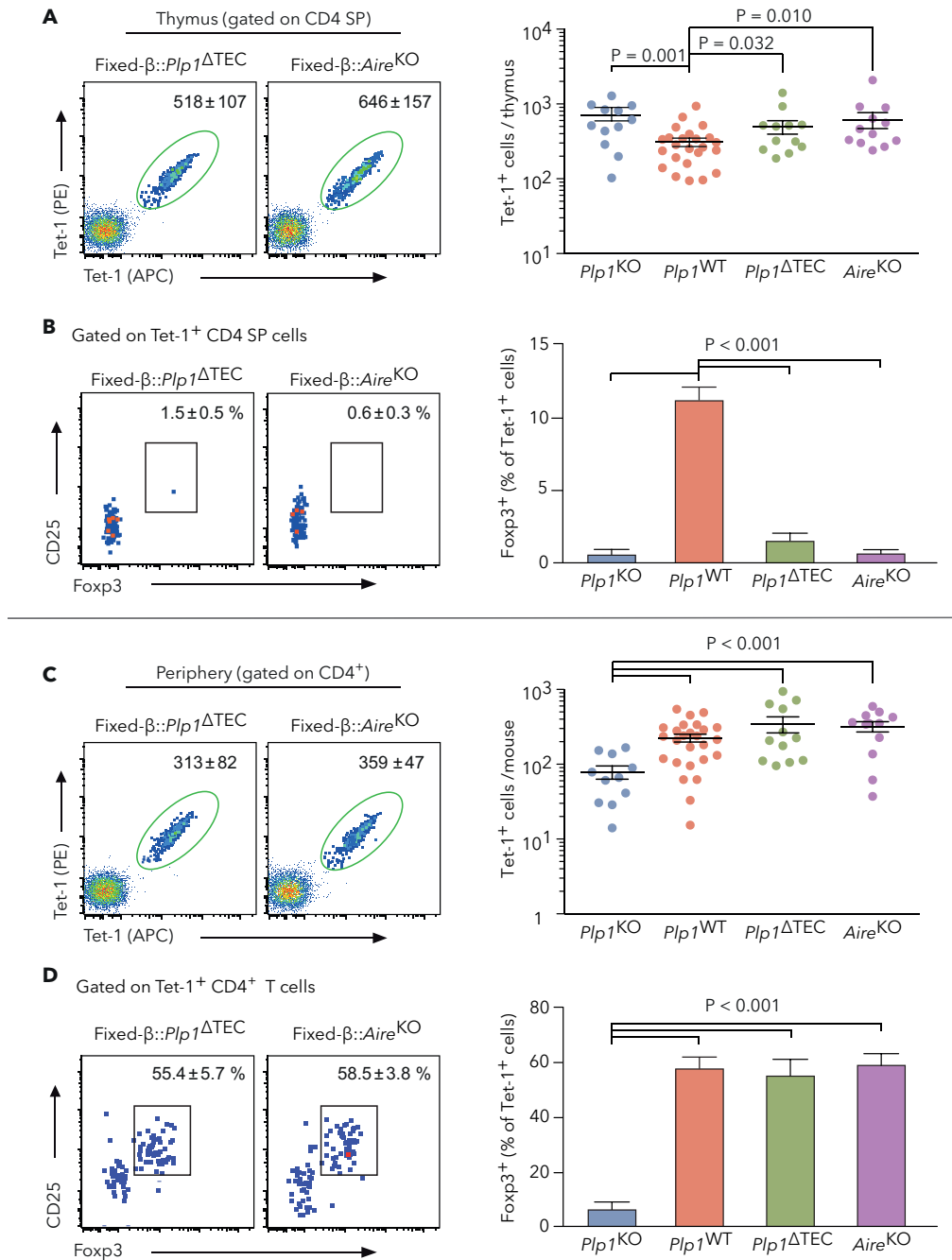


Figure 19: Central tolerance of Tet-1⁺ T cells depends on PLP1 and AIRE expression by TECs

Abundance of Tet-1⁺ T cells in Fixed-β::*Plp1*^{ΔTEC} and Fixed-β::*Aire*^{KO} in the (A) thymus and (C) periphery. The calculated mean ± SEM represents Tet-1⁺ T cells/mouse after enrichment of tetramer positive cells (n ≥ 12). All dot plots are pre-gated on CD4⁺ CD8⁻ CD11b⁻, CD11c⁻, B220⁻ and F4/80⁻. Phenotypical characterization of regulatory T cells among tetramer positive T cells (B) in the thymus and (D) in the periphery. Mean frequency ± SEM represents CD25⁺ Fopx3⁺ thymocytes. Where indicated, p-values were calculated using the unpaired two-tailed Student's test with the Welch's correction for unequal variances.

4.3.7 CD11c expressing cells are responsible for peripheral T_{reg} cell induction

In order to find the APCs inducing PLP1-specific tolerance in the periphery of mice lacking PLP1 in the thymus, we took advantage of DC-deficient mice. Additionally, an inactive *Aire* gene was introduced to prevent thymus-derived regulatory T cells. The mouse model will be in the following referred to as Fixed-β::ΔDC::*Aire*^{KO}.

Compared to the tolerant Fixed-β::*Plp1*^{WT} animals, the ablation of DCs (Fixed-β::ΔDC) did not significantly alter the T_{reg} cell compartment, neither in the thymus nor in the periphery it seems that the generation of thymic regulatory T cells is independent of DCs (figure 20). In combination with an inactive *Aire* gene, the thymocytes in the Fixed-β::ΔDC::*Aire*^{KO} animals escaped clonal diversion and contained exclusively Tet-1⁺ CD25⁻ FoxP3⁻ thymocytes. The fraction of regulatory T cells was very low also in the periphery, resembling the phenotype of Fixed-β::*Plp1*^{KO} mice. In Fixed-β::ΔDC mice, thymic regulatory T cells are able to further migrate into the periphery and fill up the regulatory T cell niche to Fixed-β::*Plp1*^{WT} levels. On the contrary, the lack of AIRE in Fixed-β::ΔDC::*Aire*^{KO} mice prevents the intra-thymic PLP1 encounter and, as a consequence, the generation of thymic-derived T_{reg} cells. In the periphery, the absence of antigen-presenting DCs abolishes diversion of potential PLP1-reactive T cells. This is consistent with previously studies in our lab in which PLP1-specific T cells from TCR-PLP1 tg mice failed to proliferate when injected into DC-deficient animals [221].

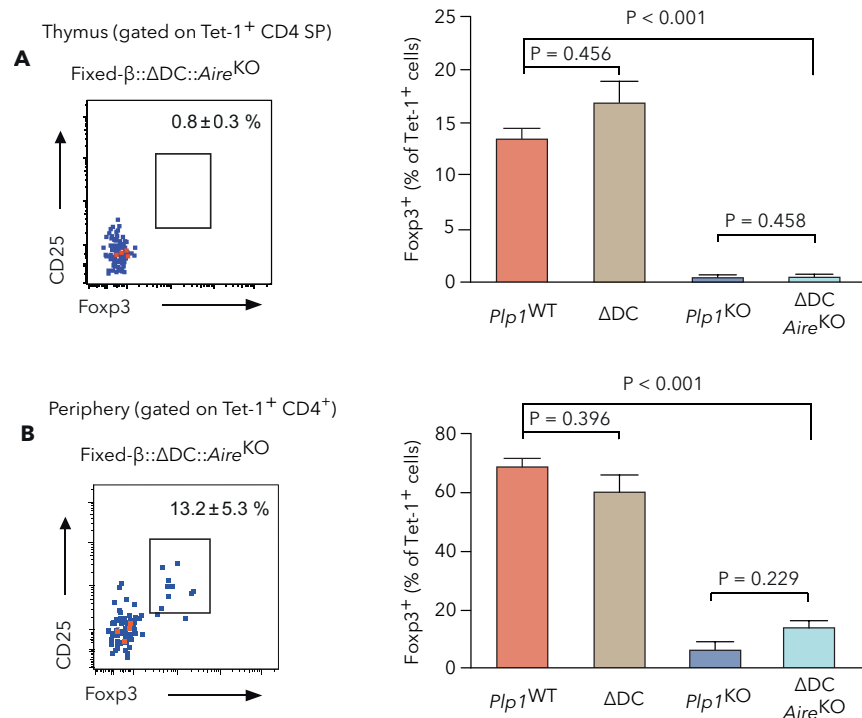


Figure 20: Peripheral tolerance of Tet-1⁺ T cells depends on cd11c expressing cells

CD25⁺ FoxP3⁺ expressing cells among Tet-1⁺ T cells in Fixed-β::ΔDC::Aire^{KO} in the (A) thymus and (B) periphery (red = Fixed-β::*Plp1*^{WT}, brown = Fixed-β::ΔDC, gray-blue = Fixed-β::*Plp1*^{KO} and turquoise = Fixed-β::ΔDC::Aire^{KO}). Mean frequency ± SEM represents CD25⁺ FoxP3⁺ among Tet-1⁺ cells (n ≥ 3 mice). All dot plots are pre-gated on CD4⁺ CD8⁻ CD11b⁻, CD11c⁻, B220⁻ and F4/80⁻ Tet-1⁺. Significance was calculated using the unpaired two-tailed Student's test and the Welch's correction.

4.4 TCR repertoire of Tet-1⁺ T cells

So far, our data suggest that clonal deletion and clonal diversion into regulatory T cells operate in parallel as central tolerance mechanisms of PLP1₁₁₋₁₉-specific T cells. To understand to which extent the presence of PLP1 shapes the CD4⁺ Tet-1⁺ TCR repertoire and to address whether these alternative fates selectively apply to cells bearing different TCRs, we analyzed the TCR repertoire in the absence and presence of PLP1. In order to define a naïve reference repertoire, we single-cell sorted and sequenced the TCR α-chain of CD4 SP Tet-1⁺ thymocytes from non-tolerant Fixed-β::*Plp1*^{KO} thymi and identified on 488 of them eight public TCR α-chains (TCR-A to TCR-H in figure 21 A). Each of these TCRs was expressed by more than 1 % of the sequenced thymocytes (altogether the eight public TCRs represented more than 90 % of all sequences) and were reactive against PLP1₁₋₂₄, as confirmed by stimulating T cell hybridomas expressing the respective TCRs (data not shown). Importantly, different mRNA nucleotide sequences encoded for the same TCR α-chain amino acid sequence, for instance 22 for

TCR-A (figure 21 F). In order to exclude multiple counts of proliferated T cells upon antigen encounter, only one mRNA nucleotide sequence per TCR α -chain and per mouse was considered.

At this point it was impossible to estimate the amount of TCR sequences we would have to analyze to reach the saturation of the naïve repertoire. Therefore, we sequenced in parallel a second PLP1₁₁₋₁₉-specific and naïve TCR repertoire of thymocytes originated from Fixed- β ::*Plp1* ^{Δ TEC} animals. As previously shown (figure 19 A & B), the absence of thymic PLP1 expression was accompanied by the lack of central tolerance among Tet-1⁺ cells. Interestingly, the 167 CD4 SP Tet-1⁺ thymocytes expressed the very same eight public TCRs found in Fixed- β ::*Plp1*^{KO} thymi, confirming that they represented a robust naïve reference repertoire for PLP1₁₁₋₁₉-specific TCRs (figure 21 B).

Focusing on how the encounter of thymic PLP1 shapes the Tet-1⁺ thymocyte repertoire, we analyzed 209 Tet-1⁺ CD25⁻ FoxP3⁻ cells from Fixed- β ::*Plp1*^{WT} thymi. The sequencing revealed the same TCR candidates similarly distributed as in the non-tolerant repertoires (figure 21 C), with the exception of TCR-A, which was slightly more frequent. To determine whether regulatory T cell diversion occurs to the same TCRs, we analyzed in parallel 42 TCRs of Tet-1⁺ CD25⁺ FoxP3⁺ thymic regulatory T cells from Fixed- β ::*PLP1*^{WT} thymi. The composition of the emerging repertoire shared the same expression pattern for TCR-B, TCR-G and TCR-H compared to the non-tolerant Tet-1⁺ CD25⁻ FoxP3⁻ repertoires. On the contrary, the frequency of TCR-F was very low and, more strikingly, TCR-C to TCR-E were entirely missing. The most prominent among T_{reg} cells was receptor TCR-A, which was expressed on 70 % of Tet-1⁺ thymic regulatory T cells (figure 21 C).

To understand to which extent the presence of PLP1 alters the peripheral TCR composition of PLP1₁₁₋₁₉-specific lymphocytes, we evaluated the TCRs of CD4⁺ CD25⁻ FoxP3⁻ lymphocytes and of regulatory T cells from peripheral lymphoid organs of Fixed- β ::*PLP1*^{WT} mice. Interestingly, in spite of displaying completely different T cell phenotypes, peripheral FoxP3⁻ and FoxP3⁺ cells almost entirely overlapped in their TCR composition (figure 21 D). In comparison to the naïve Fixed- β ::*PLP1*^{KO} reference repertoire, receptor A was again strongly overexpressed and took up two-thirds of the whole TCR populations in both FoxP3⁻ and FoxP3⁺ repertoires. Among TCRs from the regulatory T cell repertoire, we found the receptor TCR-H in a higher frequency. Noteworthy, the receptors TCR-F and TCR-E, which were highly present in the non-tolerant repertoire, were almost entirely missing in both peripheral Fixed- β ::*Plp1*^{WT}

repertoires (figure 21 A vs. figure 21 D). Astonishing was also the fact that, despite the different fates, seven out of eight TCRs (except TCR-F) shared an identical TCR α -chain amino acid sequence and differed only in two amino acids in the CDR3 α region (figure 21 E).

In summary, our data showed that in comparison to the naive (Fixed- β ::*P/Ip1*^{KO} or Fixed- β ::*P/Ip1* ^{Δ TEC}) repertoire, some TCRs in the periphery of Fixed- β ::*P/Ip1*^{WT} mice were greatly reduced, consistent with the assumption that T cells expressing these receptors were clonally deleted (TCR-E and TCR-F). Other receptors (TCR-A and TCR-H), which were overexpressed in the regulatory T cell compartment, argue for T_{reg} cell induction instead of deletion as a tolerance pathway. Finally, we noticed a striking similarity among the repertoires of peripheral CD25⁻ FoxP3⁻ T cells and both thymic and peripheral regulatory T cells in Fixed- β ::*P/Ip1*^{WT} animals.

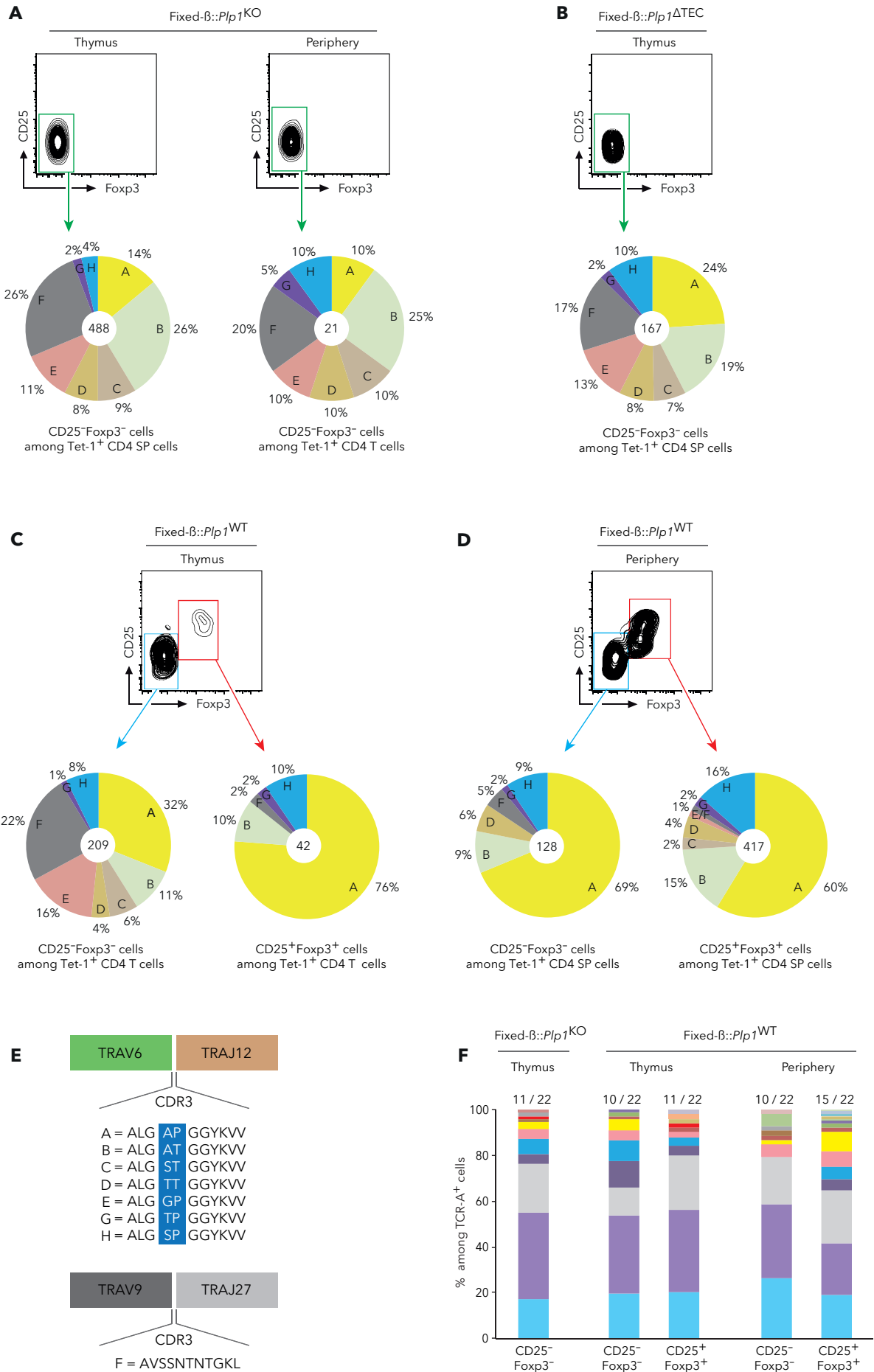


Figure 21: TCR α -chain sequencing of Tet-1⁺ T cells

Frequency of (eight) TCR α -chain candidates among Tet-1⁺ CD4⁺ T cells after sequencing PLP1 tolerant and non-tolerant repertoires. Each color represents a different TCR α -chain amino acid sequence and centered numbers represent the total cells analyzed for the respective chart. All shown TCR α -chain sequences were expressed at a frequency > 1 %. (A) TCRs within the naïve repertoire of both thymus and periphery in Fixed- β ::*Plp1*^{KO} animals. Results represent the sequencing of 111 individual mice. (B) TCRs within a second naïve thymus repertoire of Fixed- β ::*Plp1* ^{Δ TEC} animals. Results represent the sequencing of 47 individual mice. (C) TCRs within the tolerant repertoire of the thymus in Fixed- β ::*Plp1*^{WT} animals. Results represent the sequencing of 114 individual mice. (D) TCRs within the tolerant repertoire of the periphery in Fixed- β ::*Plp1*^{WT} animals. Results represent the sequencing of 132 individual mice. (E) CDR3 α region of all eight TCRs. The blue background highlights the difference among TRAV6 TRAJ12 expressing T cells within the entire TCR α -chain sequences (except TCR-F, which expresses TRAV9 TRAJ27). (F) Variety of 22 mRNA nucleotide sequences exemplified by TCR-A within PLP1-sufficient and -deficient repertoires. Each color represents a different mRNA sequences. Only one mRNA/organ was counted. All sequences were annotated using the IMGT/V-QUEST database.

4.5 Characterization of selected PLP1-specific TCRs in transgenic mice

Next, we aimed to confirm the cell-fate-specifying function of several representative TCRs through re-expression in TCR transgenic mice. For this purpose, we cloned four TCR α -chains of interest (TCR-A and TCR-H both common on CD25⁺ FoxP3⁺ expressing T cells, and TCR-E and TCR-F both strongly reduced in the tolerant repertoire) into a pTa cassette vector [202] and produced, via pronuclear injection into zygotes (performed by Ronald Naumann at the Max-Planck-Institute of Molecular Cell Biology and Genetics Dresden), four TCR α -chain transgenic mice. The respective TCR α -chain transgenic mice were crossed with Fixed- β animals to generate TCR transgenic animals, referred to as TCR-F (gray), TCR-A (yellow), TCR-H (blue) and TCR-E (salmon). The animals were backcrossed on to a *Rag1* knockout background to obtain a monoclonal T cell repertoire.

First, we asked how central tolerance mechanisms affect the fate of our four selected TCRs in the presence and absence of PLP1 (figure 22). No deletion occurred to the CD4 SP TCR-F transgenic cells, but we observed an accumulation of PLP1-dependent regulatory T cells within the thymus. On the other hand, the thymocytes of the three remaining TCR transgenic mice were significantly reduced in *Plp1*^{WT} mice, indication deletion at the most mature stage (CD69⁻ MHCII⁺). Concomitantly, a significant number of PLP1-specific T_{reg} cells were detected among surviving TCR-A and TCR-H CD4 SP thymocytes, whereas no T_{reg} cell diversion was detected in TCR-E thymi.

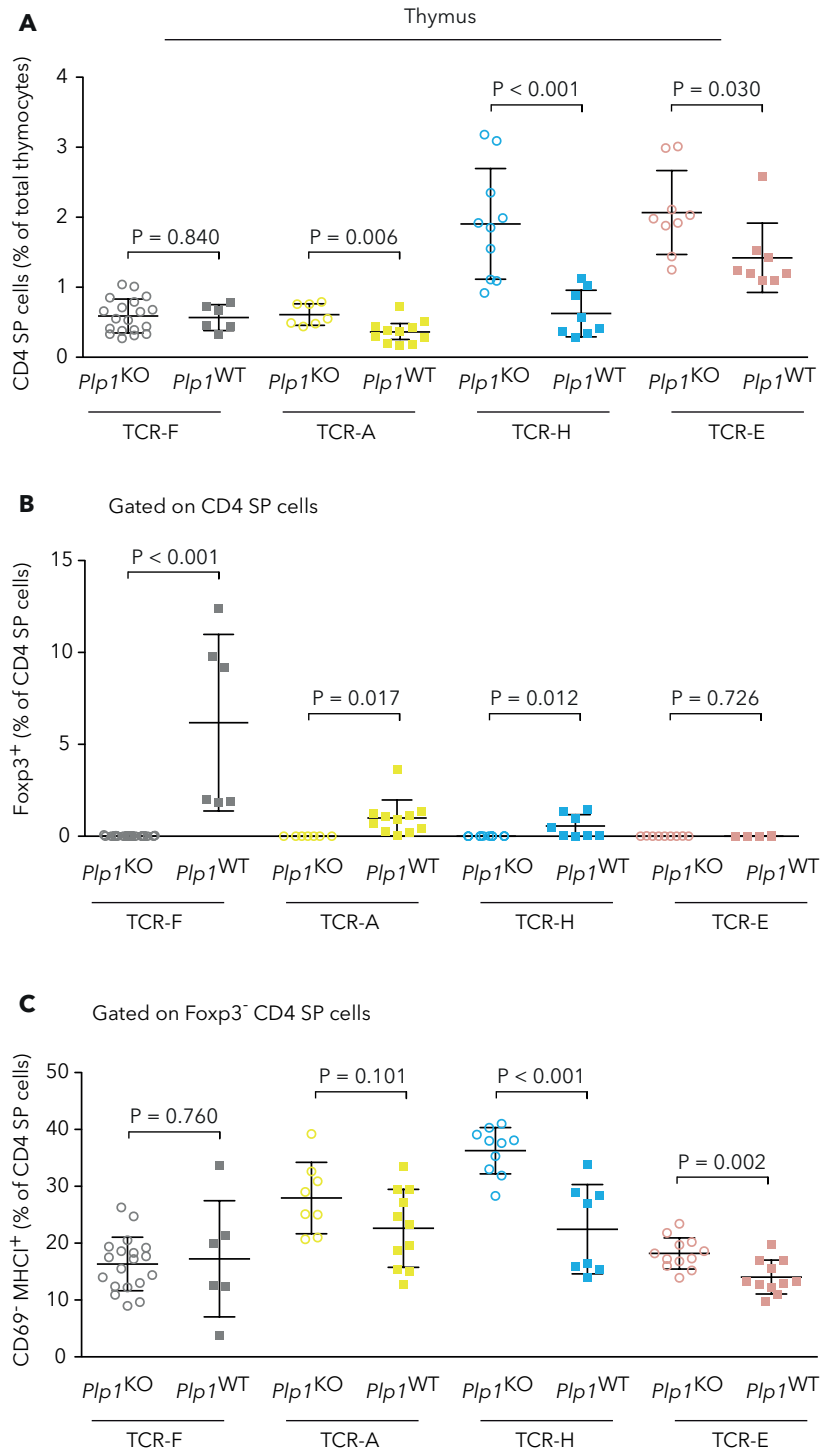
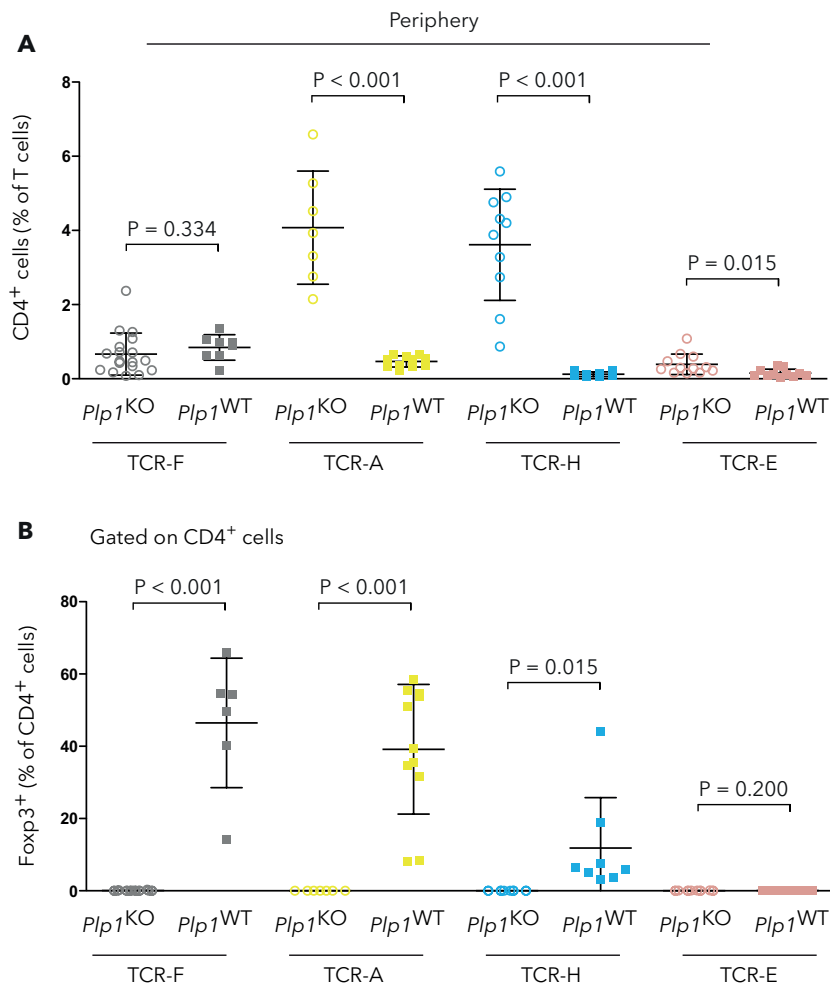


Figure 22: Central tolerance mechanisms in PLP1-specific TCR transgenic mice

CD4 SP thymocytes characterization of TCR transgenic mice - TCR-F (gray), TCR-A (yellow), TCR-H (blue) and TCR-E (salmon) - in the presence and absence of PLP1. (A) Frequency of CD4 SP thymocytes. (B) Percentage of regulatory T cells among CD4 SP T cells. (C) CD69 and MHCII staining of CD4 SP CD25⁻ FoxP3⁻ thymocytes. All statistical significances were calculated using the unpaired two-tailed Student's t-test with the Welch's correction for unequal variance. Data points are pre-gated on CD4⁺ Vβ6⁺ CD8⁻ and are representative of one mouse each (n ≥ 6).

We next analyzed the composition of the peripheral CD4⁺ TCR transgenic T cells (figure 23). Among those of TCR-F transgenic animals, we observed the highest frequency of regulatory T cells. The frequency of CD4⁺ T cells was indistinguishable between *PLP1*^{WT} and *PLP1*^{KO} animals suggesting that deletion does not operate as a tolerance mechanism in this setting. A significant PLP1-dependent decrease of CD4⁺ TCR transgenic T cells was detected in animals expressing the TCR-A, TCR-H and also TCR-E, although less intense for the latter. Furthermore, we could detect regulatory T cells within the surviving population of TCR-F, TCR-A and TCR-H transgenic animals. Noteworthy, besides deviation into regulatory T cells, a minor fraction of the remaining CD25⁻ FoxP3⁻ TCR transgenic T cells displayed an anergic phenotype in TCR-F, TCR-A and TCR-H transgenic mice, but not in TCR-E mice.



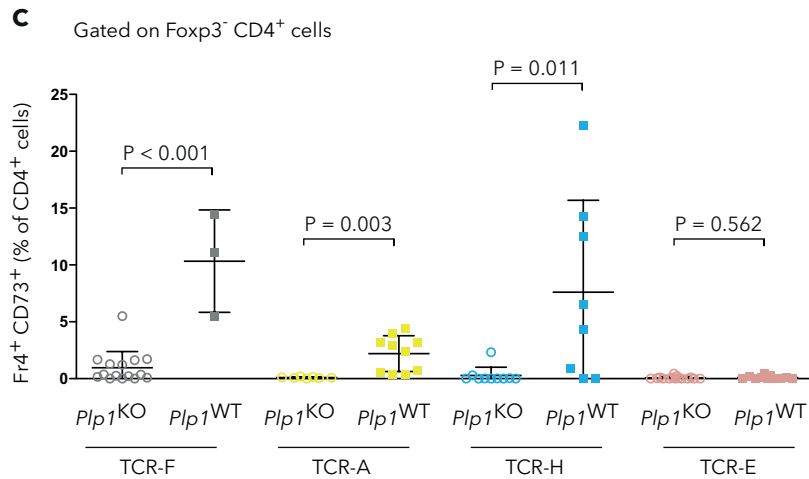


Figure 23: Peripheral TCR transgenic T cells display various cell fates

Characterization of peripheral CD4⁺ T cells from TCR transgenic mice - TCR-F (gray), TCR-A (yellow), TCR-H (blue) and TCR-E (salmon) - in the presence and absence of PLP1. (A) Frequency of CD4⁺ T cells. (B) Percentage of regulatory T cells among CD4⁺ T cells. (C) Expression of FR4 and CD73 anergy markers on CD4⁺ Vβ6⁺ CD25⁻ FoxP3⁻ T cells. All statistical significances were calculated using the unpaired two-tailed Student's t-test with the Welch's correction for unequal variance. Data points are pre-gated on CD4⁺ Vβ6⁺ CD8⁻ and are representative of one mouse each (n ≥ 6).

In summary, the results obtained from TCR transgenic mice reflect only some of the hallmarks described by the previous TCR sequencing experiments. Namely, the TCR-E transgenic CD4⁺ T cells were deleted, and those expressing the receptors TCR-H and TCR-A were converted into regulatory T cells. In addition to T_{reg} cell induction, a large proportion of the CD4⁺ T cells were deleted upon PLP1 antigen encounter in TCR-H and TCR-A transgenic settings. Finally, in contrast to what we inferred from the repertoire inventories, T cells expressing the TCR-F were not deleted but instead displayed the strongest T_{reg} cell induction of all four TCR transgenic animals.

4.5.1 Hierarchy of functional avidity to PLP1

Finally, we wanted to address whether the four receptors described so far respond differently to the cognate antigen PLP1. To do so, we isolated CD4 SP thymocytes from all four *Plp1*^{KO} *Rag1*^{KO} TCR transgenic mice, labeled them with the proliferation dye Cell Trace Violet (CTV) and stimulated them with DCs pulsed with titrated amounts of PLP1₁₋₂₄ peptide (or anti-CD3 as positive control).

The titration of anti-CD3 revealed an equal proliferative response of all four TCR transgenic CD4 SP thymocytes, (figure 24 B). However, upon peptide stimulation with PLP1₁₋₂₄, CD4⁺ T cells expressing TCR-F displayed the highest response, followed by

TCR-A, TCR-H and TCR-E (EC_{50} in the same order, data not shown) (figure 24 A). These data were in line with stimulation assays previously performed in our group on T cell hybridomas expressing the respective TCRs (data not shown). Both studies revealed the same hierarchy of dose-response curves upon stimulation of the four different TCRs with the cognate antigen.

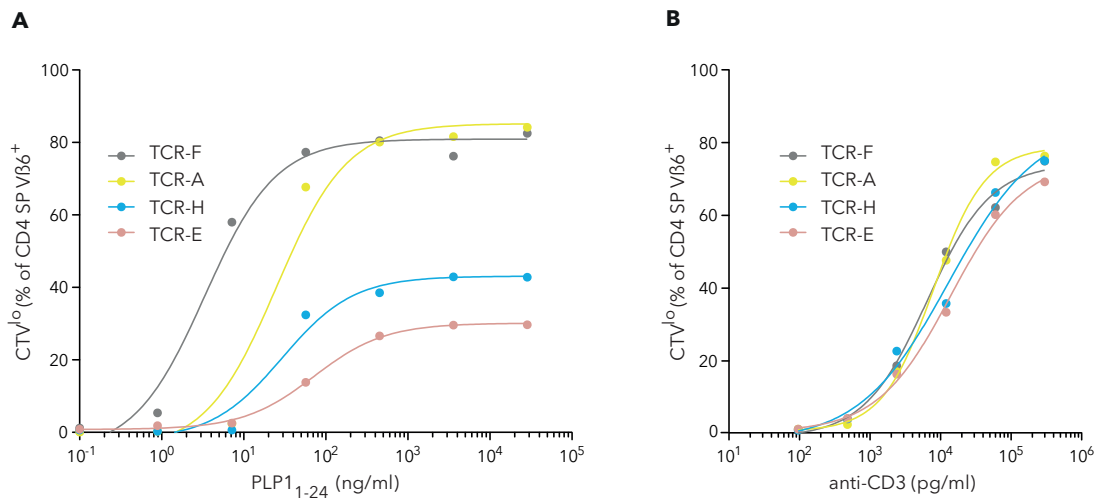


Figure 24: Ex vivo dose-response curves for TCR transgenic thymocytes

Ex vivo stimulation of CD4 SP thymocytes expressing one of the four transgenic TCRs (TCR-H (gray), TCR-A (yellow), TCR-H (blue) or TCR-E (salmon)) with (A) PLP₁₋₂₄ or (B) anti-CD3. Untouched CD4 SP thymocytes were obtained after depletion with anti-CD8⁺ MACS MicroBeads and stimulated for three days in the presence of BM-DCs plus peptide or anti-CD3. Observed values were modeled into a best-fit curve using the nonlinear regression function of Prism 7.

5. Discussion

Despite a growing body of evidence that self-recognition leads to alternative fates following an affinity/avidity-based model of thymocyte selection, we had to question this model, as it is mainly based on TCR transgenics specific for neo-self-antigens [177-180, 184]. With the invaluable help of the I-A^b tetramer technology by Marc Jenkins [197, 213], we set out to study the physiological central tolerance mechanisms that shape the CD4⁺ T cell repertoire specific for the naturally expressed antigen PLP1.

5.1 Establishment of the tetramer technology

Initially, we calculated and ranked *in silico* the potential binding strength of all PLP1 epitopes (nonamers) for the MHCII binding groove, since a strong peptide:MHCII interaction promotes the formation of a functional tetramer. It appeared that, among the previously defined PLP1 immunogenic epitopes (see figure 6), those, which induce robust central tolerance of specific T cells in the thymus (PLP1₁₁₋₁₉ and PLP1₂₄₀₋₂₄₈), are predicted to bind strongly to the MHCII groove (figure 10 A) [1, 193]. On the contrary, PLP1₁₇₄₋₁₈₂ (results not shown) is predicted to bind with a very low strength. Retrospectively, this supports the hypothesis of Wang *et al.* that, due to the low binding strength of PLP1₁₇₄₋₁₈₂ for the MHCII binding groove, the antigen might fail to be presented to the T cells during their development, resulting in incomplete or missing tolerance. Consequently, escaping PLP1₁₇₄₋₁₈₂-specific T cells are able to react even in the seemingly "tolerant" *Plp1*^{WT} system to the PLP1-antigen upon immunization and proliferate [1], or can even induce spontaneous EAE in TCR-PLP2 tg *Rag1*^{KO} mice [193].

The amino acid positions 1, 4, 6 and 9 are considered critical for the stable binding of nonamers embedded in MHCII and thus successful tetramer production (figure 10 B & C). The respective amino acids "anchor" the peptide within the I-A^b MHCII groove, whereas those remaining protrude and interact with the TCR [222]. Nelson *et al.* showed that, by altering the anchor amino acids, one can obtain a higher stability of the nonamers within the groove without affecting the interaction to the TCR [223]. However, the *in silico* calculation and even the production of the most promising mimotopes proved unsuccessful for the epitope PLP1₁₇₄₋₁₈₂ (data not shown). On the other hand, we designed and successfully produced the two tetramers including the PLP1₁₁₋₁₉ (Tet-1) and PLP1₂₄₀₋₂₄₈ (Tet-3) nonamers, in accordance to the predicted strong peptide:MHCII interaction.

We next tested the functionality of Tet-1 and Tet-3 by immunizing *Plp1*^{KO} and *Plp1*^{WT} mice with either PLP1₁₋₂₄ (peptide#1) or PLP1₂₃₇₋₂₄₈ (peptide#3) and by tracking the respective peptide-specific T cells, as previously described by Moon *et al.* [197, 213]. The presence of Tet⁺ CD4⁺ CD44⁺ effector T cells in the draining LNs of mice immunized with the respective peptide showed that both Tet-1 and Tet-3 are functional (figure 11).

5.2 Polyclonal T cell repertoire reveals clonal diversion as major tolerance mechanism

Before the advent of the tetramer technology, the number of endogenous T cells specific for a given antigen was calculated by extrapolation, for instance, by comparing the reaction of transferred TCR tg T cells with that of endogenous T cells upon antigen exposure [224, 225]. Later on, the lab of Marc Jenkins revolutionized the quantification of naturally occurring antigen-specific CD4⁺ T cells in non-immunized mice: they developed a protocol, which includes direct staining with pMHC tetramers followed by magnetic enrichment of tetramer-labeled T cells and allows the detection of as few as 5 antigen-specific T cells per mouse [197, 213]. Employing this strategy, we have calculate the size of the naive and tolerant polyclonal CD4 T cell repertoires specific for two epitopes (PLP1₁₁₋₁₉ and PLP1₂₄₀₋₂₄₈) of the naturally expressed protein PLP1 (figures 12 A & 13 A). These are in line with the previously reported numbers of antigen-specific T cells range from less than 10 to maximally around 300 per mouse in the peripheral lymphoid organs [197, 214, 215]. Interestingly, the tolerant repertoire did not reveal any quantitative evidence of clonal deletion. Instead, we found a solid fraction of regulatory T cells compared to the naïve repertoire, for both Tet-1 and Tet-3 (figures 12 & 13). These findings support the idea of Legoux *et al.* that CD4 T cell tolerance mechanisms to TRAs might operate by T_{reg} cell induction [86]. On the other hand, they are in contrast to the observed negative selection in the TCR-PLP1 tg system [193] and to the findings of Malhotra *et al.*, who, in addition to a preferential T_{reg} cell induction, identified moderate deletion of T cells specific for a model antigen under the control of TRA promoters [87].

Enumeration of Tet⁺ cells may be a poor indicator of whether or not deletion may occur, because deletion might be masked by the simultaneous proliferation of cells with shared antigen specificity but possibly different TCRs. Therefore, based on our findings in the truly polyclonal setting, we cannot make a conclusive statement on whether

tolerance to PLP1 operates only via regulatory T cell induction or in parallel via deletion. This would require the identification of the fate of distinct TCRs.

In order to follow the fate of individual TCR candidates, we needed to generate a database of all naïve and tolerant PLP1-specific TCRs. However, sequencing experiments performed on antigen-specific CD4⁺ T cells, found in similarly limited numbers as our PLP1-specific polyclonal cells, revealed that TCRs recognizing the same antigen had almost no overlap in their TCR sequence [214, 215]. This is easily interpretable, if we think that theoretically 10^{15} different TCR combinations can be generated [216], while each mouse has only about 6×10^7 T cells [217], which makes it almost impossible to find the same TCR clones in different mice. Keeping in mind this limitation, we decided to introduce the TCR β -chain tg (originated from TCR-PLP1 transgenic mouse) [193], with the aim of reducing the TCR diversity and possibly increasing the amount of PLP1-specific CD4⁺ T cells. The approach of reducing the TCR complexity by fixing the TCR β -chain and sequencing the polyclonal TCR α -chain has been successfully applied in the characterization of thymic selection mechanisms previously [187, 226-229].

5.3 Tolerance mechanisms in a repertoire of reduced complexity

From this point on we focused on Tet-1 (PLP1₁₁₋₁₉)-specific CD4 T cells only.

It is impossible to predict in which structural conformation the TCRs bind to PLP1 embedded in the I-A^b tetramer. Usually both TCR-chains bind the pMHCII via their CDR3 loops and are therefore jointly responsible for antigen recognition and the following outcome [222]. However, we cannot guarantee that this is always the case. An preferred binding of the transgenic TCR β -chain might cause an imbalanced distribution of the TCR:pMHCII interaction and an excessive skewing towards PLP1 recognition, resulting rather in a TCR transgenic system than in one with reduced TCR diversity. First of all, we ruled out this possibility by comparing the size of the naive and tolerant peripheral Tet-1⁺ populations in Fixed- β animals (figure 15 A), which appeared to be within the aforementioned natural range of T cells specific for a single antigen in the polyclonal TCR repertoire [197, 214, 215]. Furthermore, the Fixed- β mice reproduced the main tolerance hallmark observed in the fully polyclonal system, i. e. a significant fraction of T_{reg} cells within the *Plp1*^{WT} tolerant CD4 T cell repertoire in both the periphery and the thymus (figures 12 vs. 15 & figures 13 vs. 17).

Fixed- β ::*Plp1*^{WT} mice displayed a decreased number of Tet-1-specific CD4 SP cells in the thymus as compared to Fixed- β ::*Plp1*^{KO} mice (figure 17 A), which suggested that a fraction of PLP1 reactive T cells was negatively selected. This phenomenon might have been masked in the fully polyclonal repertoire owing to the small number of Tet⁺ cells (figure 13 A & B). In peripheral lymphoid organs of Fixed- β mice, instead, we found more PLP1-specific T cells in the presence of PLP1, whereby the majority of them display the suppressive T_{reg} cell phenotype (figure 15 B). Whether this population consists mainly of thymus-derived T_{reg} cells or whether a certain proportion is peripherally induced is not clear. Indeed, although the access to neuronal antigens is at least in part regulated by the blood-brain barrier, naïve T cells from TCR-PLP1 tg *Plp1*^{KO} mice do proliferate upon adoptive transfer into *Plp1*^{WT} animals, which indicates draining of PLP1 or PLP1-presenting cells in the lymphoid tissues [193]. Interestingly, PLP1-specific T cells circulate not only in mice, but also in healthy humans and therefore possess the potential to induce a spontaneous neuronal autoimmune reaction [230]. Regardless of their origin, it appears likely that PLP1-specific T_{reg} cells (figures 12 & 15) fulfill an important function in T cell immune homeostasis by suppressing escaped PLP1-autoreactive T cells, as suggested by experiments showing increased EAE susceptibility or increased activity of effector T cells after successful depletion of T_{reg} cells [86, 231].

Besides regulatory T cells, we identified a large fraction of anergic FoxP3⁻ CD25⁻ Tet-1-specific CD4 T cells within the lymphoid tissues of Fixed- β ::*Plp1*^{WT} mice, providing evidence for a third tolerance mechanism (figure 16 B). The induction of CD4 T cell anergy has been described in the literature as a peripheral tolerance mechanism triggered by the chronic recognition of self-pMHCII in the absence of infection or inflammation in various mouse strains [171, 232]. In fact, next to the previously identified anergy markers FR4 and CD73, the tolerant T cells showed an increased expression of the activation marker CD44, indicating a persistent interaction with the cognate antigen within the lymphoid tissue (figure 16 C). This piece of evidence would support the notion that PLP1 is accessible in the lymphoid tissue and that T cell anergy is a peripheral tolerance mechanism for Tet-1-specific T cells. Recently, it has been speculated that anergic T cells, at least in part, may be precursors of peripheral T_{reg} cells [170, 171]. Since the majority of T_{reg} cells are thymus-derived, we hypothesized that T cell anergy can be induced next to T_{reg} cells also in the thymus as a third and previously undiscovered central tolerance mechanism.

In order to analyze thymocytes that already underwent central tolerance, we first had to identify the mature SP T cells in the thymus. To our surprise, after gating on CD4 SP Tet-1⁺ CD25⁻ FoxP3⁻ CD69⁻ MHC1⁺ cells (figure 18 B), we discovered a distinct population expressing the alleged anergic markers FR4 and CD73 (figure 18 C). Anergy as a third central tolerance mechanism for T cells have not been described yet, but our results suggest that they might be converted already before entering the periphery. This could relativize the number of potentially self-reactive T cells escaping central tolerance, as they could migrate as “harmless” anergic cells into the periphery. Therefore, it is tempting to speculate that the in one particular model described 30% of CD4 T cells specific for a ubiquitously expressed antigen, which according to Moon *et al.* escape the central selection mechanisms [214], exhibit an anergic phenotype. It is especially exciting since it is precisely this population that does not respond upon immunization attempts [214]. To what extent or whether this depends on thymic and/or peripherally-induced anergy remains to be addressed, as well as to what degree T cell anergy might be induced in the thymus by other TRAs or ubiquitous antigens.

5.4 Tolerance-inducing factors in a repertoire with reduced diversity

TRAs are usually expressed by mTEC^{hi} cells. The intrathymic expression pattern of PLP1 is rather atypical with its mRNA expression in cTECs, mTEC^{hi}, mTEC^{lo} and thymic DCs [80, 193].

Our results show that both deletion and diversion of PLP1-specific thymocytes depend on the expression of PLP1 by TECs, as conditional deletion of PLP1 under the FoxN1 promoter abolishes the manifestation of central tolerance phenotype (figure 19 A & B left). The same holds true when AIRE is knocked out, as the thymi of these mice look exactly like the *Plp1*^{KO} thymi, which lack tolerance induction towards PLP1 (figure 19 A & B right). These results are consistent with the findings of Wang *et al.* using the TCR-PLP1 tg system [193]. Given that AIRE, selectively expressed by mTECs, but not cTECs, it is likely that central tolerance is mediated by PLP1-expression in mTECs. Why mRNA expression in cTECs appears not to lead to tolerance remains to be investigated.

At this point, we reasoned that mTEC^{hi} could be the most likely source of tolerizing antigen of central tolerance to PLP1, as the expression of PLP1 on TECs and the crucial role of AIRE in this process would point out. Nevertheless, AIRE does not only induce the expression of TRAs, but also influences tolerance through other mechanisms, such as adaptation of chemokine expression or antigen transfer to DCs (reviewed in [233]). For

this reason, we directly addressed the role of DCs by deleting CD11c expressing cells. We found that Fixed- β mice lacking DCs are able to induce thymic T_{reg} cells (figure 20 A) and display similar amounts of Tet-1⁺ thymocytes (data not shown). Unfortunately, due to the low amount of biological replicates and the need for fixation and intracellular FoxP3 staining, we cannot exclude the involvement of thymic DCs in deletion of PLP1-specific thymocytes, as the quantification of Tet-1⁺ cells is not reliable for fixed samples.

Our data from the lymphoid tissues of Fixed- β animals suggest that DCs are capable of peripheral T_{reg} cell induction. Indeed, when we eliminated thymic-derived PLP1-specific T_{reg} cells by either deleting PLP1 in TECs or by knocking out *Aire*, we still observed a similar frequency of peripheral T_{reg} cells as in the *Plp1*^{WT} controls (figure 19 D vs. figure 15). These peripheral T_{reg} cells were absent in mice simultaneously lacking DCs and AIRE (Fixed- β :: Δ DC::*Aire*^{KO} mice), arguing that DCs are responsible for the peripheral T_{reg} cell phenotype (figure 20 B). This is of particular interest as pT_{reg} cells have so far only been observed at mucosal barriers such as the gut [234, 235], the lungs [236] and the placenta [237], so in association with the presentation of “foreign” (commensal-derived) antigens, whereas thymus-derived T_{reg} cells are believed to control immune homeostasis to self-antigens [238].

Interestingly, Wang *et al.* did not report compensatory pT_{reg} cell induction in the TCR-PLP1 transgenic system, whenever they abolished central tolerance to PLP1, but only a partial peripheral deletion of PLP1-specific CD4 T cells [193]. Vice versa, we did not observe any peripheral deletion, although it could have been masked by the proliferation of T_{reg} cells. Overall, these apparent contradictions can be explained by the fact that monoclonal TCR repertoires, by focusing on a single TCR candidate, lose information on the fate of all other antigen-specific TCRs, whereas the bulk analysis of a polyclonal repertoire of a given specificity oversees what happens at the level of a single TCR clone.

5.5 How central tolerance affects individual PLP1-specific T cell clones

In order to understand if individual PLP1-specific TCRs undergo different fates upon antigen encounter in the thymus, we proceeded with single cell sequencing of the TCR α -chain in the Fixed- β setting.

We initially sequenced a naive reference repertoire, to create a comprehensive database of all Tet-1⁺ TCRs. Of note, we identified the very same eight public TCR α -chains in the thymus and periphery of Fixed- $\beta::Plp1^{KO}$ as well as in the thymus of Fixed- $\beta::Plp1^{ATEC}$ mice (figure 21 A & B). Since the relative distribution of these eight public TCR clones did not change when increasing the number of sequenced TCRs in both settings, we were confident that we reached saturation of our reference repertoire.

After defining the naïve PLP1-specific reference TCRs, we sequenced the thymocytes of the tolerant $Plp1^{WT}$ animals, which consisted of both regulatory and non regulatory T cells. The majority of non regulatory PLP1-specific cells seem to be in an immature state (figure 18 B). Given the limited concentration of PLP1 in the medulla, it is likely that they have not encountered the PLP1 antigen yet. Consequently, it is reasonable to assume that the majority of our sequenced thymocytes were in a "naive" state. In light of this, we were not surprised to see an almost perfect overlap between the TCRs expressed by the non regulatory Fixed- $\beta::Plp1^{WT}$ thymocytes and the truly naive reference TCRs (figure 21 C left pie chart vs. figure 21 A & B).

We next focused on the TCRs of antigen-experienced T cells, which include those expressed by T_{reg} thymocytes as well as by peripheral regulatory and non regulatory T cells in Fixed- $\beta::Plp1^{WT}$ mice. The latter are indeed mainly anergic (figure 16 B). These three TCR repertoires strongly differed from all the previously described "naïve" TCR compartments and at the same time were almost identical to one another (figure 21 A & B & C & D). After we collected all the data, we needed to identify deleter and diverter TCRs, thus to define criteria for such identification. We defined as "deleter" a TCR that is present in the naïve reference compartment, but is lost or strongly reduced in the periphery of tolerant $Plp1^{WT}$ mice. A "diverter" is instead a TCR that is expressed by T_{reg} cells.

Applying these criteria, it seems that clonal diversion only affects some of the public TCR candidates. Besides the receptors TCR-B and TCR-H, which are expressed by roughly 10 % of T_{reg} cells each, it is TCR-A, which is present on the vast majority of T_{reg} cells (figure 21 C & D). As for clonal deletion, the receptors TCR-E and TCR-F are totally absent or strongly reduced in their frequency in the tolerant repertoires compared to the naïve repertoires, thus classifying as deleter TCRs (figure 21 A & B & C & D).

One could argue that our definition of deleter TCRs also include TCRs that are deleted by peripheral tolerance mechanisms. However, in case of preferential deletion of TCR-E

and TCR-F in the periphery, we would have expected to find them at a higher frequency in the non regulatory peripheral T cell fraction of Fixed- β ::*Plp1*^{WT}, i.e. after thymic emigration but before the peripheral deletion actually happened. Since our sequencing data represent a snapshot of TCRs expressed by T cells of different “ages”.

Concerning clonal diversion, we think that the majority of our diverter TCRs are converted in the thymus, as more than 80 % of CD4 SP FoxP3⁺ CD25⁺ T cells in Fixed- β ::*Plp1*^{WT} thymi are non recirculating CCR7⁺ (figure 17 C). This hypothesis is supported by the fact that more than 70% of polyclonal peripheral T_{reg} cells seem to have thymic origin [140, 142, 239].

One last interesting aspect that deserves attention is the similarity in the TCR distribution between the T_{reg} cells and the non regulatory - mostly anergic - T cells in the periphery of *Plp1*^{WT} animals. This is reminiscent of the “buddy hypothesis”, which suggested that the release of every potential autoreactive T cell is kept in check by a regulatory buddy T cell of equal antigen specificity [239]. However, this theory does not take into account that the majority of the remaining non regulatory T cells have an anergic phenotype. Given the limited space and resources for T_{reg} cell induction in the thymus (e. g. limited cytokine availability), the anergic cells could act as a backup for a possible renewal of T_{reg} cells. Whether and to what extent anergic and regulatory T cells cooperate together as buddies to suppress escaped autoreactive T cells is an interesting aspect that has yet to be demonstrated.

5.6 Characterization of selected TCR candidates

In order to test whether the fate of our PLP1-specific TCRs is related to their affinity/avidity to PLP1, we selected the four most frequent among the eight TCRs reported in figure 21, two of which described as deleter (TCR-E & TCR-F) and two as diverter (TCR-A & TCR-H) TCRs. We then generated the respective TCR a-chain tg mice and bred them to the Fixed- β , *Plp1*^{KO} and *Rag1*^{KO} animals, to obtain a TCR monoclonal systems. We isolated CD4 SP thymocytes from each of the four TCR tg *Plp1*^{KO} animals and checked their proliferation *ex vivo* upon stimulation with DCs and titrated amounts of PLP1₁₋₂₄ (figure 24), as a readout of functional avidity. To our surprise and in contradiction with the classical affinity/avidity model (figure 5), we found that deleter TCRs have either the highest (TCR-F) or the lowest (TCR-E) functional avidity to PLP1₁₋₂₄, whereas diverter TCRs have an intermediate one, with TCR-A proliferating more than TCR-H.

Next, we wanted to verify in the monoclonal system if each TCR candidate recapitulates the cell fate identified by the sequencing experiments, upon PLP1 encounter *in vivo*. The comparison of the respective TCR tg CD4 T cell compartments between PLP1-deficient and -sufficient mice showed a positive correlation between the TCRs' functional avidity and the frequency of T_{reg} cells in both the thymus (figure 22 B) and the periphery (figure 23 B).

The effect was extreme for TCR-E, the receptor with the lowest functional avidity, which did not get diverted into the T_{reg} cell lineage at all. On the contrary, we saw a significantly reduced number of CD4 T cells in the thymus (figure 22 A & C) and periphery (figure 23 A) of TCR-E tg mice, which is in agreement with the aforementioned sequencing data (figure 21) and the definition of a truly deleter TCR. This is of particular interest since clonal deletion of self-reactive T cells has always been associated with TCRs that possess high affinity/avidity to pMHCII and thus theoretically possess an enormous potential to trigger autoimmunity [240, 241]. In contrast, low affinity/avidity TCRs have been associated with incomplete central tolerance induction, resulting in an escape of the respective TCRs and a related autoimmune reaction [229, 242, 243]. Our TCR-E represents an exception to the broadly accepted affinity/avidity model, as it undergoes deletion in spite of relatively low functional avidity to PLP1. However, it is worth mentioning that pMHCII tetramers fail to bind TCRs on the lowest range of affinity/avidity [244], so in our analysis we lack the TCRs with truly low affinity/avidity to PLP1. To understand the necessity to remove TCR-E, it would be interesting to test if PLP1 immunization of TCR-E::*Plp1*^{WT} mice, or the transfer of naïve TCR-E tg CD4 T cells into *Plp1*^{WT} animals, induces EAE.

Also very interesting are the data we obtained from the other TCR tg mice. The two diverter TCRs (TCR-A & TCR-H), for example, differ in their functional avidity to PLP1 (figure 24), which correlated with their frequency in the T_{reg} cell compartment of Fixed-β mice (figure 21 C & D). It appears as if T_{reg} cells with a high self-pMHCII recognition potential possess a selection advantage over "weaker" TCRs and thus outcompete them. One reason might be that T_{reg} cells need to establish a high affinity/avidity interaction with self-pMHCII in order to properly suppress a possible autoimmune reaction. Alternatively, higher affinity/avidity to self-pMHCII might guarantee a faster access to resources for the diversion process. In case access to T_{reg} cell niches is the limiting factor, it would be interesting to test whether an excess of TCR-A expressing thymocytes could hinder the ability of TCR-H to divert into T_{reg} cells. Besides clonal diversion, we

simultaneously observed clonal deletion of the two “diverter” TCRs (figure 22 A & C & figure 23 A). Based on the previously discussed evidence for DC-dependent peripheral tolerance induction to PLP1 (paragraph 5.4), we cannot exclude that deletion of the TCR-A and TCR-H happens preferentially in the periphery (figure 23 A). However, the analysis of CD4 SP thymocytes of the respective TCR tg mice indicated that central tolerance is also acting through deletion. It was probably not possible to capture the concomitant diversion and deletion of TCR-A and TCR-H by sequencing the polyclonal PLP1-specific T cells, because the peripheral FoxP3⁺ compartment, which we expected to be “naïve”, in fact expressed the same TCRs we found on T_{reg} cells and displayed mainly an anergic phenotype (figure 21 D). For this reason, TCRs that are very prominent in the T_{reg} cell compartment are also equally prominent in the FoxP3⁺ peripheral compartment, to the point that deletion might not be visible. Similarly, in neo-antigen-driven T_{reg} TCR tg mice, it was observed that deletion occurs in addition to T_{reg} cell induction [177, 178, 183, 245].

Finally, the TCR-F tg mice - which express the TCR with the highest functional avidity to PLP1 - revealed the largest T_{reg} cell fraction within the CD4⁺ T cells in both the thymus and the periphery, compared to the other three TCR tg (figure 22 B & figure 23 B). This finding is in contrast to the results from our sequencing experiments, which made us define TCR-F as a deleter TCR. However, as we know from the history of the affinity/avidity model, based on the study of TCR tg mice, thymocytes expressing a potential deleter TCR specific for a neo-antigen can be “converted” into T_{reg} cells by reducing the concentration of the cognate antigen in the thymus [74, 183] (figure 25 A). The other way around, thymocytes expressing a potential diverter TCR of unknown specificity did not show any conversion in the monoclonal repertoire until the authors titrated down the amount of TCR tg T cells in bone marrow chimeras [185, 186] (figure 25 B). In both cases it seems there is an optimal TCR:pMHCII ratio for T_{reg} cell induction. We reasoned that a similar shift in this ratio could have happened in our setting, where, compared to the low frequency of TCR-F in the Fixed-β repertoire, we overloaded the thymus with TCR tg T cells of the same specificity, without altering the PLP1 expression (Figure 25 C). This resulted in TCR-F, previously described as deleter TCR, appearing as a diverter TCR.

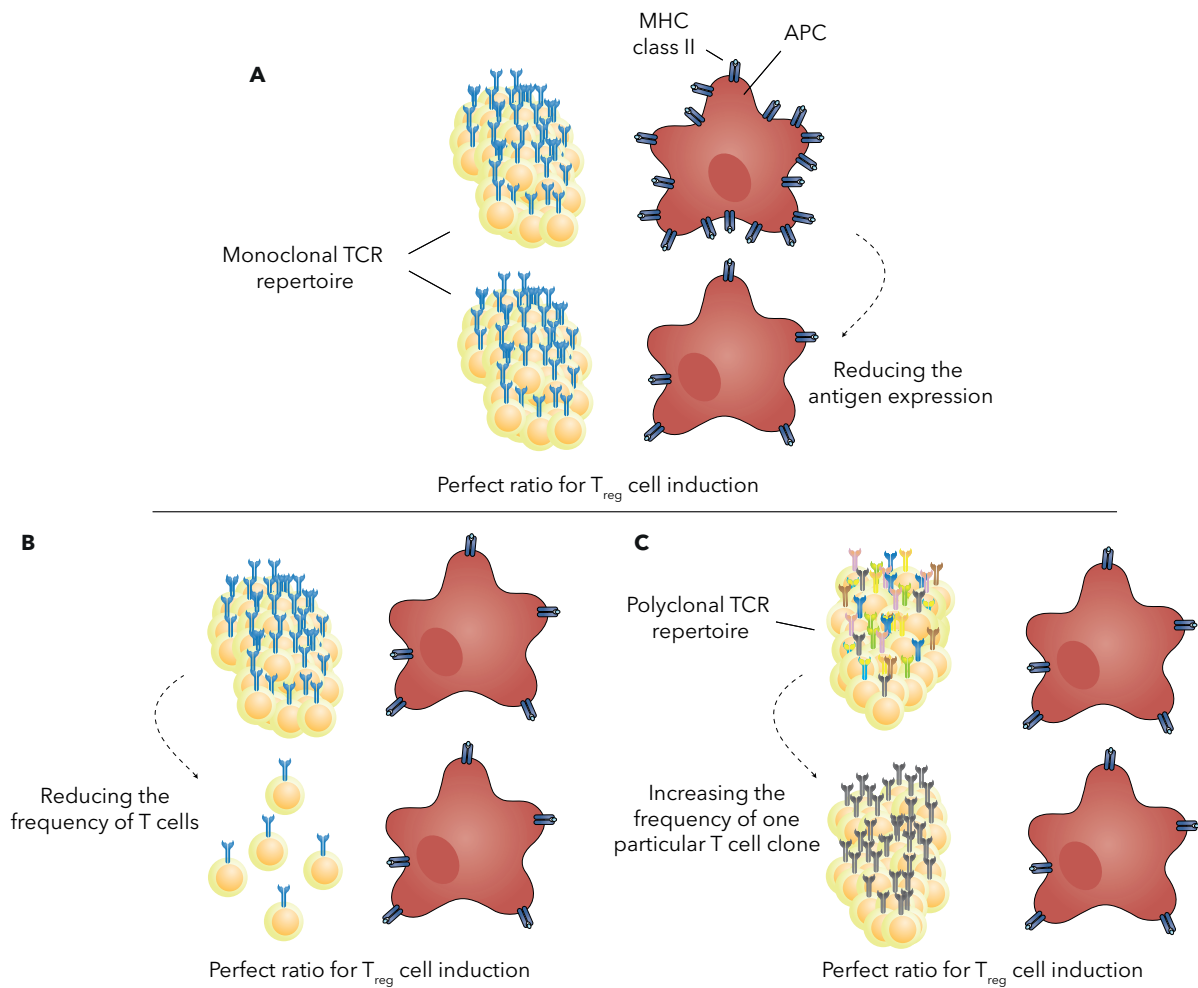


Figure 25: Changing the TCR:pMHCII ratio uncovers a window for T_{reg} cell induction

(A) In two independent TCR tg systems, reducing the amount of pMHCII on mTECs [74] or changing the pattern of thymic antigen expression through the use of different promoters [183] shifts the fate of the thymocytes from being deleted to diverted into T_{reg} cells. (B) In BM-chimera experiments, titrating down the amount of thymocytes expressing a monoclonal TCR derived from a T_{reg} cell clone revealed a threshold, below which conversion into T_{reg} cells could take place [185, 186]. (C) The “deleter” TCR-F (gray) that we identified in the Fixed- β repertoire (figure 21) became a “diverter” TCR when expressed in a monoclonal TCR tg system (figure 22 & figure 23), where the thymus was overloaded with T cells of the same specificity.

It is possible that intraclonal competition might be the reason for the observed phenotype. In a TCR tg system all the thymocytes compete for interaction with the very same epitope of the cognate antigen, which, in case of PLP1 or other TRAs, is expressed at low levels. This may result in limited accessibility of PLP1, leading to decreased occupancy of the TCRs on the surface of each thymocyte, and/or shorter interaction times with APCs, deriving from the physical displacement by other TCR tg T cells. For instance, in a Fixed- β setting similar to ours, Stadinski *et al.* recently demonstrated that

polyclonal thymocytes that engaged in TCR:self-pMHCII interactions with long dwell times underwent deletion, whereas those interacting with shorter dwell times were converted into T_{reg} cells [246]. Furthermore, the competition happening in the thymus of a TCR tg mouse resembles in some way that of peripheral T cells competing during an anti-foreign response [247]. Since the latter was described to act also through the "sequestration" of pMHCII from the surface of APCs [248], we can speculate that the high-affinity TCR-F tg thymocytes might be directly responsible for reducing the amount of PLP1. All in all, the example of TCR-F reminds us once more of the caveats of the TCR tg systems. To test this, one could try to re-establish a physiological TCR:pMHCII by titrating down the amount of TCR tg cells in BM chimeras.

6. Conclusion

Our findings in repertoire inventories support the affinity/avidity model of thymocyte selection. As a proxy of affinity it should be mentioned that the data shown here all refer to functional avidity. To what extent the actual affinity of an individual TCR:pMHCII interaction influences the T cells fate is beyond the scope of this thesis. Our proposed model is shown in figure 26, differing from the classical affinity/avidity model in that it shows a deletion window that spans a wider region than the T_{reg} cell induction window. The T cell fate, which is exemplified by TCR-E (salmon), displayed the lowest functional avidity to PLP1 and yet was deleted in both the Fixed- β and TCR tg settings. According to our data, the induction of T_{reg} cells takes place in a window of higher TCR:pMHCII strength, which might concomitantly lead to deletion and the expression of the anergy markers FR4 and CD73. This is represented by TCR-H (blue) and TCR-A (yellow), whose functional avidity to PLP1 positively correlated to their respective frequency in the T_{reg} cell compartment of Fixed- β mice, as well as to the frequency of T_{reg} cells in the TCR tg scenarios. Finally, we described the upper part of the deletion window at the higher end of TCR:pMHCII strength, demonstrated by TCR-F (gray).

Our interpretation favors the idea that thymocytes bearing autoreactive TCRs with an optimal affinity/avidity to their cognate self-antigen are retained in the mature CD4 T cell repertoire as T_{reg} cells, whereas the ones expressing TCRs of too low or too high affinity/avidity to self-pMHCII are deleted because considered useless or dangerous, respectively. Deletion might also happen in parallel to T_{reg} cell induction, probably when the T_{reg} cell niches are saturated. Furthermore, the induction of anergy seems to be a third option of central tolerance induction, although we could only describe the phenotype, due to the extremely low amount of $CD4^+ Tet-1^+ FoxP3^- CD25^-$ T cells in Fixed- $\beta::Plp1^{WT}$ mice.

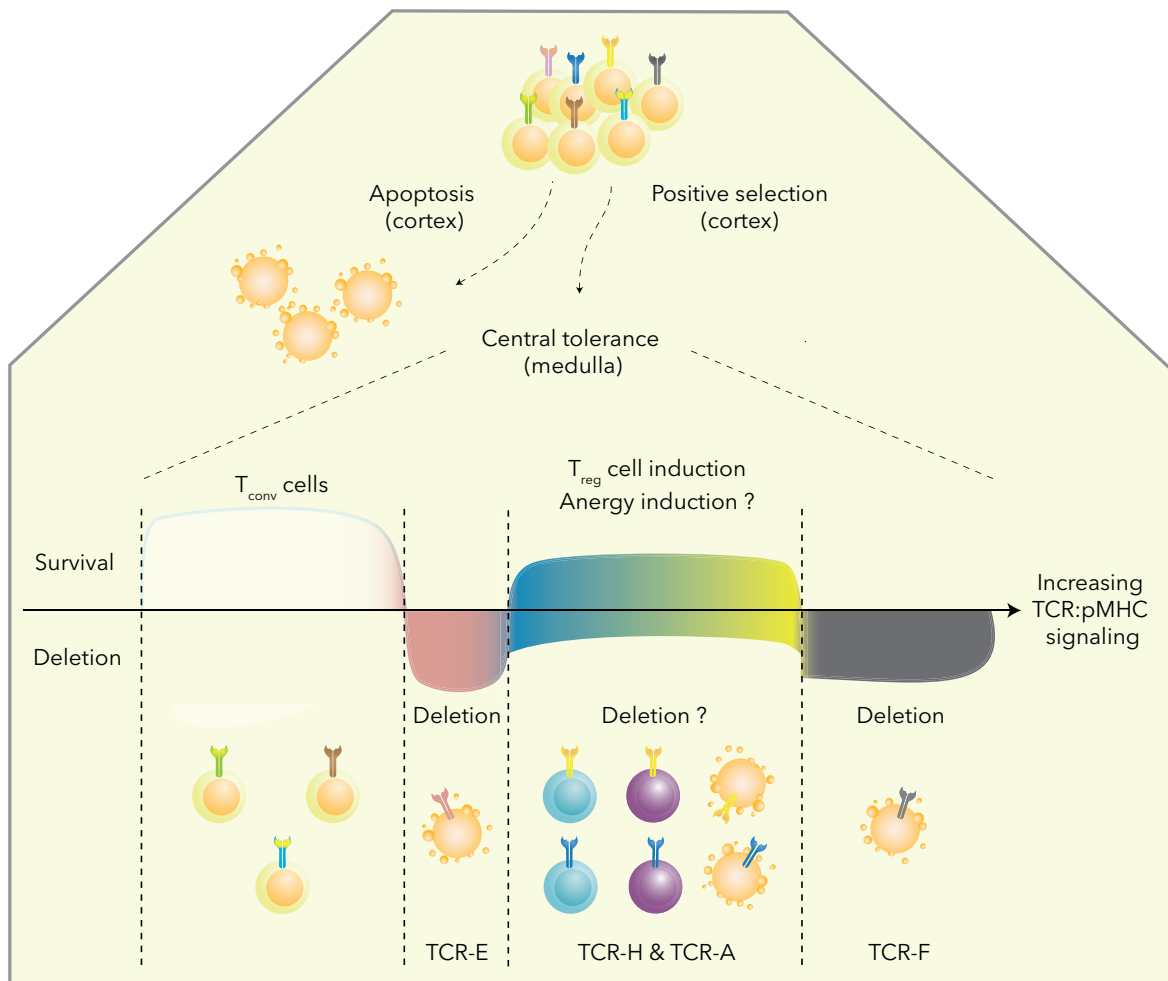


Figure 26: Our proposed model of thymocyte selection

Thymocytes that survive positive selection and enter the medulla are subjected to the central tolerance checkpoint. The T cell fate is determined by the intensity of the TCR:pMHC interactions, which is influenced by both the TCR affinity for the cognate self-antigen and the avidity established by the total TCR:pMHC connections. When the signaling strength of TCR:pMHC is relatively low, thymocytes are allowed to mature and leave the thymus as T_{conv} cells. When the TCR:pMHC interact more strongly, the thymocytes are considered mildly autoreactive, but not enough to be converted into useful T_{reg} cells, and are therefore deleted from the repertoire, as exemplified by TCR-E (salmon). When the TCR:pMHC establish even stronger connections, as in the case of TCR-H (blue) and even more of TCR-A (yellow), the thymocytes are in the perfect window of autoreactivity for the conversion into T_{reg} cells. If enough T_{reg} cells of a given specificity are generated, the redundant thymocytes might be deleted and/or turned into seemingly anergic cells that escape in the periphery. Finally, at the highest strength of TCR:pMHC interaction thymocytes are considered too dangerous and deleted from the repertoire, as shown for TCR-F (gray). Perturbing the ratio of TCR:pMHC can shift the T cell fate, as explained in figure 25, so for instance TCR-F can become a diverter TCR when the TCR:pMHC interactions are not fully established due to excessive intraclonal competition.

1. Klein, L., et al., *Shaping of the autoreactive T-cell repertoire by a splice variant of self protein expressed in thymic epithelial cells*. *Nat Med*, 2000. **6** (1): p. 56-61.
2. Cairns, D., *Ψυχή, Θυμός, and Metaphor in Homer and Plato Etudes Platoniciennes*, 2014.
3. Miller, J.F., *Influence of Thymectomy on Tumor Induction by Polyoma Virus in C57bl Mice*. *Proc Soc Exp Biol Med*, 1964. **116**: p. 323-7.
4. McIntire, K.R., S. Sell, and J.F. Miller, *Pathogenesis of the Post-Neonatal Thymectomy Wasting Syndrome*. *Nature*, 1964. **204**: p. 151-5.
5. Miller, J.F., *Effect of neonatal thymectomy on the immunological responsiveness of the mouse*. *Royal Society*, 1962. **156** (964).
6. Miller, J.F., *Immunological function of the thymus*. *Lancet*, 1961. **2** (7205): p. 748-9.
7. Corbeaux, T., et al., *Thymopoiesis in mice depends on a Foxn1-positive thymic epithelial cell lineage*. *Proc Natl Acad Sci U S A*, 2010. **107** (38): p. 16613-8.
8. Gordon, J., et al., *Gcm2 and Foxn1 mark early parathyroid- and thymus-specific domains in the developing third pharyngeal pouch*. *Mech Dev*, 2001. **103** (1-2): p. 141-3.
9. Manley, N.R., *Thymus organogenesis and molecular mechanisms of thymic epithelial cell differentiation*. *Semin Immunol*, 2000. **12** (5): p. 421-8.
10. Bodey, B., et al., *Involution of the mammalian thymus, one of the leading regulators of aging*. *In Vivo*, 1997. **11** (5): p. 421-40.
11. Hollander, G., et al., *Cellular and molecular events during early thymus development*. *Immunol Rev*, 2006. **209**: p. 28-46.
12. Takahama, Y., et al., *Generation of diversity in thymic epithelial cells*. *Nat Rev Immunol*, 2017. **17** (5): p. 295-305.
13. Gossens, K., et al., *Thymic progenitor homing and lymphocyte homeostasis are linked via S1P-controlled expression of thymic P-selectin/CCL25*. *J Exp Med*, 2009. **206** (4): p. 761-78.
14. Plotkin, J., et al., *Critical role for CXCR4 signaling in progenitor localization and T cell differentiation in the postnatal thymus*. *J Immunol*, 2003. **171** (9): p. 4521-7.
15. Zuniga-Pflucker, J.C., *T-cell development made simple*. *Nat Rev Immunol*, 2004. **4** (1): p. 67-72.
16. Bell, J.J. and A. Bhandoola, *The earliest thymic progenitors for T cells possess myeloid lineage potential*. *Nature*, 2008. **452** (7188): p. 764-7.
17. Ceredig, R., N. Bosco, and A.G. Rolink, *The B lineage potential of thymus settling progenitors is critically dependent on mouse age*. *Eur J Immunol*, 2007. **37** (3): p. 830-7.

18. Luc, S., et al., *The earliest thymic T cell progenitors sustain B cell and myeloid lineage potential*. *Nat Immunol*, 2012. 13 (4): p. 412-9.
19. Shen, H.Q., et al., *T/NK bipotent progenitors in the thymus retain the potential to generate dendritic cells*. *J Immunol*, 2003. 171 (7): p. 3401-6.
20. Zhou, W., et al., *Single-Cell Analysis Reveals Regulatory Gene Expression Dynamics Leading to Lineage Commitment in Early T Cell Development*. *Cell Syst*, 2019. 9 (4): p. 321-337 e9.
21. Koch, U., et al., *Delta-like 4 is the essential, nonredundant ligand for Notch1 during thymic T cell lineage commitment*. *J Exp Med*, 2008. 205 (11): p. 2515-23.
22. Feyerabend, T.B., et al., *Deletion of Notch1 converts pro-T cells to dendritic cells and promotes thymic B cells by cell-extrinsic and cell-intrinsic mechanisms*. *Immunity*, 2009. 30 (1): p. 67-79.
23. von Freeden-Jeffry, U., et al., *The earliest T lineage-committed cells depend on IL-7 for Bcl-2 expression and normal cell cycle progression*. *Immunity*, 1997. 7 (1): p. 147-54.
24. Zamisch, M., et al., *Ontogeny and regulation of IL-7-expressing thymic epithelial cells*. *J Immunol*, 2005. 174 (1): p. 60-7.
25. Buono, M., et al., *Bi-directional signaling by membrane-bound KitL induces proliferation and coordinates thymic endothelial cell and thymocyte expansion*. *Nat Commun*, 2018. 9 (1): p. 4685.
26. Porritt, H.E., K. Gordon, and H.T. Petrie, *Kinetics of steady-state differentiation and mapping of intrathymic-signaling environments by stem cell transplantation in nonirradiated mice*. *J Exp Med*, 2003. 198 (6): p. 957-62.
27. Shortman, K., et al., *The generation and fate of thymocytes*. *Semin Immunol*, 1990. 2 (1): p. 3-12.
28. Sambandam, A., et al., *Notch signaling controls the generation and differentiation of early T lineage progenitors*. *Nat Immunol*, 2005. 6 (7): p. 663-70.
29. Oettinger, M.A., et al., *RAG-1 and RAG-2, adjacent genes that synergistically activate V(D)J recombination*. *Science*, 1990. 248 (4962): p. 1517-23.
30. Kueh, H.Y., et al., *Asynchronous combinatorial action of four regulatory factors activates Bcl11b for T cell commitment*. *Nat Immunol*, 2016. 17 (8): p. 956-65.
31. Yui, M.A., N. Feng, and E.V. Rothenberg, *Fine-scale staging of T cell lineage commitment in adult mouse thymus*. *J Immunol*, 2010. 185 (1): p. 284-93.
32. Akamatsu, Y. and M.A. Oettinger, *Distinct roles of RAG1 and RAG2 in binding the V(D)J recombination signal sequences*. *Mol Cell Biol*, 1998. 18 (8): p. 4670-8.
33. Carpenter, A.C. and R. Bosselut, *Decision checkpoints in the thymus*. *Nat Immunol*, 2010. 11 (8): p. 666-73.

34. von Boehmer, H., *Unique features of the pre-T-cell receptor alpha-chain: not just a surrogate*. *Nat Rev Immunol*, 2005. 5 (7): p. 571-7.
35. Heath, W.R., et al., *Expression of two T cell receptor alpha chains on the surface of normal murine T cells*. *Eur J Immunol*, 1995. 25 (6): p. 1617-23.
36. Turner, S.J., et al., *Structural determinants of T-cell receptor bias in immunity*. *Nat Rev Immunol*, 2006. 6 (12): p. 883-94.
37. Kyewski, B. and L. Klein, *A central role for central tolerance*. *Annu Rev Immunol*, 2006. 24: p. 571-606.
38. Florea, B.I., et al., *Activity-based profiling reveals reactivity of the murine thymoproteasome-specific subunit beta5t*. *Chem Biol*, 2010. 17 (8): p. 795-801.
39. Gommeaux, J., et al., *Thymus-specific serine protease regulates positive selection of a subset of CD4+ thymocytes*. *Eur J Immunol*, 2009. 39 (4): p. 956-64.
40. Nakagawa, T., et al., *Cathepsin L: critical role in li degradation and CD4 T cell selection in the thymus*. *Science*, 1998. 280 (5362): p. 450-3.
41. Nedjic, J., et al., *Autophagy in thymic epithelium shapes the T-cell repertoire and is essential for tolerance*. *Nature*, 2008. 455 (7211): p. 396-400.
42. Breed, E.R., M. Watanabe, and K.A. Hogquist, *Measuring Thymic Clonal Deletion at the Population Level*. *J Immunol*, 2019. 202 (11): p. 3226-3233.
43. McDonald, B.D., et al., *Crossreactive alphabeta T Cell Receptors Are the Predominant Targets of Thymocyte Negative Selection*. *Immunity*, 2015. 43 (5): p. 859-69.
44. Baba, T., Y. Nakamoto, and N. Mukaida, *Crucial contribution of thymic Sirp alpha+ conventional dendritic cells to central tolerance against blood-borne antigens in a CCR2-dependent manner*. *J Immunol*, 2009. 183 (5): p. 3053-63.
45. McCaughy, T.M., et al., *Clonal deletion of thymocytes can occur in the cortex with no involvement of the medulla*. *J Exp Med*, 2008. 205 (11): p. 2575-84.
46. Klein, L., et al., *Positive and negative selection of the T cell repertoire: what thymocytes see (and don't see)*. *Nat Rev Immunol*, 2014. 14 (6): p. 377-91.
47. von Boehmer, H., et al., *Thymic selection revisited: how essential is it?* *Immunol Rev*, 2003. 191: p. 62-78.
48. Davey, G.M., et al., *Preselection thymocytes are more sensitive to T cell receptor stimulation than mature T cells*. *J Exp Med*, 1998. 188 (10): p. 1867-74.
49. Choi, S., et al., *Erratum: THEMIS enhances TCR signaling and enables positive selection by selective inhibition of the phosphatase SHP-1*. *Nat Immunol*, 2017. 18 (6): p. 705.
50. Johnson, A.L., et al., *Themis is a member of a new metazoan gene family and is required for the completion of thymocyte positive selection*. *Nat Immunol*, 2009. 10 (8): p. 831-9.

51. Li, Q.J., et al., *miR-181a is an intrinsic modulator of T cell sensitivity and selection*. Cell, 2007. 129 (1): p. 147-61.
52. Lo, W.L., D.L. Donermeyer, and P.M. Allen, *A voltage-gated sodium channel is essential for the positive selection of CD4(+) T cells*. Nat Immunol, 2012. 13 (9): p. 880-7.
53. Wang, D., et al., *Tespa1 is involved in late thymocyte development through the regulation of TCR-mediated signaling*. Nat Immunol, 2012. 13 (6): p. 560-8.
54. Mick, V.E., et al., *The regulated expression of a diverse set of genes during thymocyte positive selection in vivo*. J Immunol, 2004. 173 (9): p. 5434-44.
55. Testi, R., et al., *The CD69 receptor: a multipurpose cell-surface trigger for hematopoietic cells*. Immunol Today, 1994. 15 (10): p. 479-83.
56. Brugnera, E., et al., *Coreceptor reversal in the thymus: signaled CD4+8+ thymocytes initially terminate CD8 transcription even when differentiating into CD8+ T cells*. Immunity, 2000. 13 (1): p. 59-71.
57. Lundberg, K., et al., *Intermediate steps in positive selection: differentiation of CD4+8int TCRint thymocytes into CD4-8+TCRhi thymocytes*. J Exp Med, 1995. 181 (5): p. 1643-51.
58. He, X., et al., *The zinc finger transcription factor Th-POK regulates CD4 versus CD8 T-cell lineage commitment*. Nature, 2005. 433 (7028): p. 826-33.
59. Etzensperger, R., et al., *Identification of lineage-specifying cytokines that signal all CD8(+)-cytotoxic-lineage-fate 'decisions' in the thymus*. Nat Immunol, 2017. 18 (11): p. 1218-1227.
60. Issuree, P.D., C.P. Ng, and D.R. Littman, *Heritable Gene Regulation in the CD4:CD8 T Cell Lineage Choice*. Front Immunol, 2017. 8: p. 291.
61. Kadouri, N., et al., *Thymic epithelial cell heterogeneity: TEC by TEC*. Nat Rev Immunol, 2020. 20 (4): p. 239-253.
62. Ehrlich, L.I., et al., *Differential contribution of chemotaxis and substrate restriction to segregation of immature and mature thymocytes*. Immunity, 2009. 31 (6): p. 986-98.
63. Hu, Z., et al., *CCR4 promotes medullary entry and thymocyte-dendritic cell interactions required for central tolerance*. J Exp Med, 2015. 212 (11): p. 1947-65.
64. Kozai, M., et al., *Essential role of CCL21 in establishment of central self-tolerance in T cells*. J Exp Med, 2017. 214 (7): p. 1925-1935.
65. Ueno, T., et al., *CCR7 signals are essential for cortex-medulla migration of developing thymocytes*. J Exp Med, 2004. 200 (4): p. 493-505.
66. Fontenot, J.D., M.A. Gavin, and A.Y. Rudensky, *Foxp3 programs the development and function of CD4+CD25+ regulatory T cells*. Nat Immunol, 2003. 4 (4): p. 330-6.

67. Hori, S., T. Nomura, and S. Sakaguchi, *Control of regulatory T cell development by the transcription factor Foxp3*. *Science*, 2003. **299** (5609): p. 1057-61.
68. Khattri, R., et al., *An essential role for Scurfin in CD4+CD25+ T regulatory cells*. *Nat Immunol*, 2003. **4** (4): p. 337-42.
69. Lio, C.W. and C.S. Hsieh, *A two-step process for thymic regulatory T cell development*. *Immunity*, 2008. **28** (1): p. 100-11.
70. Liu, Y., et al., *A critical function for TGF-beta signaling in the development of natural CD4+CD25+Foxp3+ regulatory T cells*. *Nat Immunol*, 2008. **9** (6): p. 632-40.
71. Sakaguchi, S., et al., *Immunologic self-tolerance maintained by activated T cells expressing IL-2 receptor alpha-chains (CD25). Breakdown of a single mechanism of self-tolerance causes various autoimmune diseases*. *J Immunol*, 1995. **155** (3): p. 1151-64.
72. Ohnmacht, C., et al., *Constitutive ablation of dendritic cells breaks self-tolerance of CD4 T cells and results in spontaneous fatal autoimmunity*. *J Exp Med*, 2009. **206** (3): p. 549-59.
73. van Meerwijk, J.P., et al., *Quantitative impact of thymic clonal deletion on the T cell repertoire*. *J Exp Med*, 1997. **185** (3): p. 377-83.
74. Hinterberger, M., et al., *Autonomous role of medullary thymic epithelial cells in central CD4(+) T cell tolerance*. *Nat Immunol*, 2010. **11** (6): p. 512-9.
75. Perry, J.S.A., et al., *Distinct contributions of Aire and antigen-presenting-cell subsets to the generation of self-tolerance in the thymus*. *Immunity*, 2014. **41** (3): p. 414-426.
76. Perry, J.S. and C.S. Hsieh, *Development of T-cell tolerance utilizes both cell-autonomous and cooperative presentation of self-antigen*. *Immunol Rev*, 2016. **271** (1): p. 141-55.
77. Sansom, S.N., et al., *Population and single-cell genomics reveal the Aire dependency, relief from Polycomb silencing, and distribution of self-antigen expression in thymic epithelia*. *Genome Res*, 2014. **24** (12): p. 1918-31.
78. Aichinger, M., et al., *Macroautophagy substrates are loaded onto MHC class II of medullary thymic epithelial cells for central tolerance*. *J Exp Med*, 2013. **210** (2): p. 287-300.
79. Danan-Gotthold, M., et al., *Extensive RNA editing and splicing increase immune self-representation diversity in medullary thymic epithelial cells*. *Genome Biol*, 2016. **17** (1): p. 219.
80. Derbinski, J., et al., *Promiscuous gene expression in medullary thymic epithelial cells mirrors the peripheral self*. *Nat Immunol*, 2001. **2** (11): p. 1032-9.
81. Colobran, R., et al., *Association of an SNP with intrathymic transcription of TSHR and Graves' disease: a role for defective thymic tolerance*. *Hum Mol Genet*, 2011. **20** (17): p. 3415-23.

82. Durinovic-Bello, I., et al., *Insulin gene VNTR genotype associates with frequency and phenotype of the autoimmune response to proinsulin*. *Genes Immun*, 2010. 11 (2): p. 188-93.
83. Cloosen, S., et al., *Expression of tumor-associated differentiation antigens, MUC1 glycoforms and CEA, in human thymic epithelial cells: implications for self-tolerance and tumor therapy*. *Cancer Res*, 2007. 67 (8): p. 3919-26.
84. Derbinski, J., et al., *Promiscuous gene expression patterns in single medullary thymic epithelial cells argue for a stochastic mechanism*. *Proc Natl Acad Sci U S A*, 2008. 105 (2): p. 657-62.
85. Klein, L., B. Roettinger, and B. Kyewski, *Sampling of complementing self-antigen pools by thymic stromal cells maximizes the scope of central T cell tolerance*. *Eur J Immunol*, 2001. 31 (8): p. 2476-86.
86. Legoux, F.P., et al., *CD4+ T Cell Tolerance to Tissue-Restricted Self Antigens Is Mediated by Antigen-Specific Regulatory T Cells Rather Than Deletion*. *Immunity*, 2015. 43 (5): p. 896-908.
87. Malhotra, D., et al., *Tolerance is established in polyclonal CD4(+) T cells by distinct mechanisms, according to self-peptide expression patterns*. *Nat Immunol*, 2016. 17 (2): p. 187-95.
88. Anderson, M.S., et al., *Projection of an immunological self shadow within the thymus by the aire protein*. *Science*, 2002. 298 (5597): p. 1395-401.
89. DeVoss, J., et al., *Spontaneous autoimmunity prevented by thymic expression of a single self-antigen*. *J Exp Med*, 2006. 203 (12): p. 2727-35.
90. Gavanescu, I., et al., *Loss of Aire-dependent thymic expression of a peripheral tissue antigen renders it a target of autoimmunity*. *Proc Natl Acad Sci U S A*, 2007. 104 (11): p. 4583-7.
91. Betterle, C., et al., *Autoimmune adrenal insufficiency and autoimmune polyendocrine syndromes: autoantibodies, autoantigens, and their applicability in diagnosis and disease prediction*. *Endocr Rev*, 2002. 23 (3): p. 327-64.
92. Nagamine, K., et al., *Positional cloning of the APECED gene*. *Nat Genet*, 1997. 17 (4): p. 393-8.
93. Anderson, M.S., et al., *The cellular mechanism of Aire control of T cell tolerance*. *Immunity*, 2005. 23 (2): p. 227-39.
94. Liston, A., et al., *Gene dosage--limiting role of Aire in thymic expression, clonal deletion, and organ-specific autoimmunity*. *J Exp Med*, 2004. 200 (8): p. 1015-26.
95. Liston, A., et al., *Aire regulates negative selection of organ-specific T cells*. *Nat Immunol*, 2003. 4 (4): p. 350-4.
96. Taniguchi, R.T., et al., *Detection of an autoreactive T-cell population within the polyclonal repertoire that undergoes distinct autoimmune regulator (Aire)-mediated selection*. *Proc Natl Acad Sci U S A*, 2012. 109 (20): p. 7847-52.

97. Kekalainen, E., et al., *A defect of regulatory T cells in patients with autoimmune polyendocrinopathy-candidiasis-ectodermal dystrophy*. *J Immunol*, 2007. **178** (2): p. 1208-15.
98. Aschenbrenner, K., et al., *Selection of Foxp3+ regulatory T cells specific for self antigen expressed and presented by Aire+ medullary thymic epithelial cells*. *Nat Immunol*, 2007. **8** (4): p. 351-8.
99. Malchow, S., et al., *Aire Enforces Immune Tolerance by Directing Autoreactive T Cells into the Regulatory T Cell Lineage*. *Immunity*, 2016. **44** (5): p. 1102-13.
100. Takaba, H., et al., *Fezf2 Orchestrates a Thymic Program of Self-Antigen Expression for Immune Tolerance*. *Cell*, 2015. **163** (4): p. 975-87.
101. Tomofuji, Y., et al., *Chd4 choreographs self-antigen expression for central immune tolerance*. *Nat Immunol*, 2020.
102. Wu, L. and K. Shortman, *Heterogeneity of thymic dendritic cells*. *Semin Immunol*, 2005. **17** (4): p. 304-12.
103. Lei, Y., et al., *Aire-dependent production of XCL1 mediates medullary accumulation of thymic dendritic cells and contributes to regulatory T cell development*. *J Exp Med*, 2011. **208** (2): p. 383-94.
104. Ardouin, L., et al., *Broad and Largely Concordant Molecular Changes Characterize Tolerogenic and Immunogenic Dendritic Cell Maturation in Thymus and Periphery*. *Immunity*, 2016. **45** (2): p. 305-18.
105. Gallegos, A.M. and M.J. Bevan, *Central tolerance to tissue-specific antigens mediated by direct and indirect antigen presentation*. *J Exp Med*, 2004. **200** (8): p. 1039-49.
106. Hubert, F.X., et al., *Aire regulates the transfer of antigen from mTECs to dendritic cells for induction of thymic tolerance*. *Blood*, 2011. **118** (9): p. 2462-72.
107. Perry, J.S.A., et al., *Transfer of Cell-Surface Antigens by Scavenger Receptor CD36 Promotes Thymic Regulatory T Cell Receptor Repertoire Development and Allo-tolerance*. *Immunity*, 2018. **48** (5): p. 923-936 e4.
108. Hadeiba, H., et al., *Plasmacytoid dendritic cells transport peripheral antigens to the thymus to promote central tolerance*. *Immunity*, 2012. **36** (3): p. 438-50.
109. Cosway, E.J., et al., *Redefining thymus medulla specialization for central tolerance*. *J Exp Med*, 2017. **214** (11): p. 3183-3195.
110. Perera, J., et al., *Autoreactive thymic B cells are efficient antigen-presenting cells of cognate self-antigens for T cell negative selection*. *Proc Natl Acad Sci U S A*, 2013. **110** (42): p. 17011-6.
111. Yamano, T., et al., *Thymic B Cells Are Licensed to Present Self Antigens for Central T Cell Tolerance Induction*. *Immunity*, 2015. **42** (6): p. 1048-61.

112. Lu, F.T., et al., *Thymic B cells promote thymus-derived regulatory T cell development and proliferation*. *J Autoimmun*, 2015. **61**: p. 62-72.
113. Xing, Y., et al., *Late stages of T cell maturation in the thymus involve NF-kappaB and tonic type I interferon signaling*. *Nat Immunol*, 2016. **17** (5): p. 565-73.
114. Bankovich, A.J., L.R. Shioy, and J.G. Cyster, *CD69 suppresses sphingosine 1-phosphate receptor-1 (S1P1) function through interaction with membrane helix 4*. *J Biol Chem*, 2010. **285** (29): p. 22328-37.
115. Kumar, A., et al., *S1P Lyase Regulation of Thymic Egress and Oncogenic Inflammatory Signaling*. *Mediators Inflamm*, 2017. **2017**: p. 7685142.
116. Liu, B., et al., *A Hybrid Insulin Epitope Maintains High 2D Affinity for Diabetogenic T Cells in the Periphery*. *Diabetes*, 2020. **69** (3): p. 381-391.
117. Raposo, B., et al., *T cells specific for post-translational modifications escape intrathymic tolerance induction*. *Nat Commun*, 2018. **9** (1): p. 353.
118. Mundt, S., et al., *The CNS Immune Landscape from the Viewpoint of a T Cell*. *Trends Neurosci*, 2019. **42** (10): p. 667-679.
119. Qu, N., et al., *Immunological microenvironment in the testis*. *Reprod Med Biol*, 2020. **19** (1): p. 24-31.
120. Keino, H., S. Horie, and S. Sugita, *Immune Privilege and Eye-Derived T-Regulatory Cells*. *J Immunol Res*, 2018. **2018**: p. 1679197.
121. Liu, S., et al., *The role of decidual immune cells on human pregnancy*. *J Reprod Immunol*, 2017. **124**: p. 44-53.
122. Hawiger, D., et al., *Dendritic cells induce peripheral T cell unresponsiveness under steady state conditions in vivo*. *J Exp Med*, 2001. **194** (6): p. 769-79.
123. Loschko, J., et al., *Antigen targeting to plasmacytoid dendritic cells via Siglec-H inhibits Th cell-dependent autoimmunity*. *J Immunol*, 2011. **187** (12): p. 6346-56.
124. Wu, J. and A. Horuzsko, *Expression and function of immunoglobulin-like transcripts on tolerogenic dendritic cells*. *Hum Immunol*, 2009. **70** (5): p. 353-6.
125. Sun, C.M., et al., *Small intestine lamina propria dendritic cells promote de novo generation of Foxp3 T reg cells via retinoic acid*. *J Exp Med*, 2007. **204** (8): p. 1775-85.
126. Zheng, S.G., et al., *IL-2 is essential for TGF-beta to convert naive CD4+CD25- cells to CD25+Foxp3+ regulatory T cells and for expansion of these cells*. *J Immunol*, 2007. **178** (4): p. 2018-27.
127. Bourque, J. and D. Hawiger, *The BTLA-HVEM-CD5 Immunoregulatory Axis-An Instructive Mechanism Governing pTreg Cell Differentiation*. *Front Immunol*, 2019. **10**: p. 1163.

128. Salomon, B., et al., *B7/CD28 costimulation is essential for the homeostasis of the CD4+CD25+ immunoregulatory T cells that control autoimmune diabetes*. *Immunity*, 2000. 12 (4): p. 431-40.
129. Akbari, O., et al., *Antigen-specific regulatory T cells develop via the ICOS-ICOS-ligand pathway and inhibit allergen-induced airway hyperreactivity*. *Nat Med*, 2002. 8 (9): p. 1024-32.
130. Francisco, L.M., et al., *PD-L1 regulates the development, maintenance, and function of induced regulatory T cells*. *J Exp Med*, 2009. 206 (13): p. 3015-29.
131. Schulke, S., *Induction of Interleukin-10 Producing Dendritic Cells As a Tool to Suppress Allergen-Specific T Helper 2 Responses*. *Front Immunol*, 2018. 9: p. 455.
132. Mascanfroni, I.D., et al., *IL-27 acts on DCs to suppress the T cell response and autoimmunity by inducing expression of the immunoregulatory molecule CD39*. *Nat Immunol*, 2013. 14 (10): p. 1054-63.
133. Collison, L.W., et al., *The inhibitory cytokine IL-35 contributes to regulatory T-cell function*. *Nature*, 2007. 450 (7169): p. 566-9.
134. Mucida, D., et al., *Reciprocal TH17 and regulatory T cell differentiation mediated by retinoic acid*. *Science*, 2007. 317 (5835): p. 256-60.
135. Sakaguchi, S., et al., *Regulatory T cells and immune tolerance*. *Cell*, 2008. 133 (5): p. 775-87.
136. Godfrey, V.L., et al., *Fatal lymphoreticular disease in the scurfy (sf) mouse requires T cells that mature in a sf thymic environment: potential model for thymic education*. *Proc Natl Acad Sci U S A*, 1991. 88 (13): p. 5528-32.
137. Toomer, K.H., et al., *Essential and non-overlapping IL-2Ralpha-dependent processes for thymic development and peripheral homeostasis of regulatory T cells*. *Nat Commun*, 2019. 10 (1): p. 1037.
138. Bennett, C.L., et al., *The immune dysregulation, polyendocrinopathy, enteropathy, X-linked syndrome (IPEX) is caused by mutations of FOXP3*. *Nat Genet*, 2001. 27 (1): p. 20-1.
139. Goudy, K., et al., *Human IL2RA null mutation mediates immunodeficiency with lymphoproliferation and autoimmunity*. *Clin Immunol*, 2013. 146 (3): p. 248-61.
140. Weiss, J.M., et al., *Neuropilin 1 is expressed on thymus-derived natural regulatory T cells, but not mucosa-generated induced Foxp3+ T reg cells*. *J Exp Med*, 2012. 209 (10): p. 1723-42, S1.
141. Yadav, M., et al., *Neuropilin-1 distinguishes natural and inducible regulatory T cells among regulatory T cell subsets in vivo*. *J Exp Med*, 2012. 209 (10): p. 1713-22, S1-19.
142. Thornton, A.M., et al., *Expression of Helios, an Ikaros transcription factor family member, differentiates thymic-derived from peripherally induced Foxp3+ T regulatory cells*. *J Immunol*, 2010. 184 (7): p. 3433-41.

143. Zheng, Y., et al., *Role of conserved non-coding DNA elements in the Foxp3 gene in regulatory T-cell fate*. Nature, 2010. 463 (7282): p. 808-12.
144. Yadav, M., S. Stephan, and J.A. Bluestone, *Peripherally induced tregs - role in immune homeostasis and autoimmunity*. Front Immunol, 2013. 4: p. 232.
145. O'Garra, A., et al., *IL-10-producing and naturally occurring CD4+ Tregs: limiting collateral damage*. J Clin Invest, 2004. 114 (10): p. 1372-8.
146. Tran, D.Q., *TGF-beta: the sword, the wand, and the shield of FOXP3(+) regulatory T cells*. J Mol Cell Biol, 2012. 4 (1): p. 29-37.
147. de la Rosa, M., et al., *Interleukin-2 is essential for CD4+CD25+ regulatory T cell function*. Eur J Immunol, 2004. 34 (9): p. 2480-8.
148. Deaglio, S., et al., *Adenosine generation catalyzed by CD39 and CD73 expressed on regulatory T cells mediates immune suppression*. J Exp Med, 2007. 204 (6): p. 1257-65.
149. Leone, R.D., Y.C. Lo, and J.D. Powell, *A2aR antagonists: Next generation checkpoint blockade for cancer immunotherapy*. Comput Struct Biotechnol J, 2015. 13: p. 265-72.
150. Ngoenkam, J., W.W. Schamel, and S. Pongcharoen, *Selected signalling proteins recruited to the T-cell receptor-CD3 complex*. Immunology, 2018. 153 (1): p. 42-50.
151. Kong, K.F., et al., *Protein kinase C-eta controls CTLA-4-mediated regulatory T cell function*. Nat Immunol, 2014. 15 (5): p. 465-72.
152. Wing, K., et al., *CTLA-4 control over Foxp3+ regulatory T cell function*. Science, 2008. 322 (5899): p. 271-5.
153. Cribbs, A.P., et al., *Treg cell function in rheumatoid arthritis is compromised by ctla-4 promoter methylation resulting in a failure to activate the indoleamine 2,3-dioxygenase pathway*. Arthritis Rheumatol, 2014. 66 (9): p. 2344-54.
154. Pallotta, M.T., et al., *Indoleamine 2,3-dioxygenase is a signaling protein in long-term tolerance by dendritic cells*. Nat Immunol, 2011. 12 (9): p. 870-8.
155. Wu, H., J. Gong, and Y. Liu, *Indoleamine 2, 3-dioxygenase regulation of immune response (Review)*. Mol Med Rep, 2018. 17 (4): p. 4867-4873.
156. Mahnke, K., et al., *Tolerogenic dendritic cells and regulatory T cells: a two-way relationship*. J Dermatol Sci, 2007. 46 (3): p. 159-67.
157. Watanabe, N., et al., *BTLA is a lymphocyte inhibitory receptor with similarities to CTLA-4 and PD-1*. Nat Immunol, 2003. 4 (7): p. 670-9.
158. Leach, D.R., M.F. Krummel, and J.P. Allison, *Enhancement of antitumor immunity by CTLA-4 blockade*. Science, 1996. 271 (5256): p. 1734-6.
159. Goldberg, M.V. and C.G. Drake, *LAG-3 in Cancer Immunotherapy*. Curr Top Microbiol Immunol, 2011. 344: p. 269-78.

160. Krueger, J., et al., *CD28 family of receptors inter-connect in the regulation of T-cells*. *Receptors Clin Investig*, 2017. 4.
161. Joller, N., et al., *Cutting edge: TIGIT has T cell-intrinsic inhibitory functions*. *J Immunol*, 2011. 186 (3): p. 1338-42.
162. Du, W., et al., *TIM-3 as a Target for Cancer Immunotherapy and Mechanisms of Action*. *Int J Mol Sci*, 2017. 18 (3).
163. Wang, L., et al., *VISTA, a novel mouse Ig superfamily ligand that negatively regulates T cell responses*. *J Exp Med*, 2011. 208 (3): p. 577-92.
164. Golden-Mason, L., et al., *Negative immune regulator Tim-3 is overexpressed on T cells in hepatitis C virus infection and its blockade rescues dysfunctional CD4+ and CD8+ T cells*. *J Virol*, 2009. 83 (18): p. 9122-30.
165. Jovasevic, V.M., et al., *Importance of IL-10 for CTLA-4-mediated inhibition of tumor-eradicating immunity*. *J Immunol*, 2004. 172 (3): p. 1449-54.
166. Chen, W., W. Jin, and S.M. Wahl, *Engagement of cytotoxic T lymphocyte-associated antigen 4 (CTLA-4) induces transforming growth factor beta (TGF-beta) production by murine CD4(+) T cells*. *J Exp Med*, 1998. 188 (10): p. 1849-57.
167. Keir, M.E., et al., *PD-1 and its ligands in tolerance and immunity*. *Annu Rev Immunol*, 2008. 26: p. 677-704.
168. Macon-Lemaitre, L. and F. Triebel, *The negative regulatory function of the lymphocyte-activation gene-3 co-receptor (CD223) on human T cells*. *Immunology*, 2005. 115 (2): p. 170-8.
169. Schorer, M., et al., *TIGIT limits immune pathology during viral infections*. *Nat Commun*, 2020. 11 (1): p. 1288.
170. Kalekar, L.A. and D.L. Mueller, *Relationship between CD4 Regulatory T Cells and Anergy In Vivo*. *J Immunol*, 2017. 198 (7): p. 2527-2533.
171. Kalekar, L.A., et al., *CD4(+) T cell anergy prevents autoimmunity and generates regulatory T cell precursors*. *Nat Immunol*, 2016. 17 (3): p. 304-14.
172. Pletinckx, K., et al., *Immature dendritic cells convert anergic nonregulatory T cells into Foxp3- IL-10+ regulatory T cells by engaging CD28 and CTLA-4*. *Eur J Immunol*, 2015. 45 (2): p. 480-91.
173. Suss, G. and K. Shortman, *A subclass of dendritic cells kills CD4 T cells via Fas/Fas-ligand-induced apoptosis*. *J Exp Med*, 1996. 183 (4): p. 1789-96.
174. Grossman, W.J., et al., *Differential expression of granzymes A and B in human cytotoxic lymphocyte subsets and T regulatory cells*. *Blood*, 2004. 104 (9): p. 2840-8.
175. Gondek, D.C., et al., *Cutting edge: contact-mediated suppression by CD4+CD25+ regulatory cells involves a granzyme B-dependent, perforin-independent mechanism*. *J Immunol*, 2005. 174 (4): p. 1783-6.

176. Klein, L., E.A. Robey, and C.S. Hsieh, *Central CD4(+) T cell tolerance: deletion versus regulatory T cell differentiation*. *Nat Rev Immunol*, 2019. **19** (1): p. 7-18.
177. Apostolou, I., et al., *Origin of regulatory T cells with known specificity for antigen*. *Nat Immunol*, 2002. **3** (8): p. 756-63.
178. Jordan, M.S., et al., *Thymic selection of CD4+CD25+ regulatory T cells induced by an agonist self-peptide*. *Nat Immunol*, 2001. **2** (4): p. 301-6.
179. Kappler, J.W., N. Roehm, and P. Marrack, *T cell tolerance by clonal elimination in the thymus*. *Cell*, 1987. **49** (2): p. 273-80.
180. Kieselow, P., et al., *Tolerance in T-cell-receptor transgenic mice involves deletion of nonmature CD4+8+ thymocytes*. *Nature*, 1988. **333** (6175): p. 742-6.
181. Sebзда, E., et al., *Positive and negative thymocyte selection induced by different concentrations of a single peptide*. *Science*, 1994. **263** (5153): p. 1615-8.
182. Feuerer, M., et al., *Enhanced thymic selection of FoxP3+ regulatory T cells in the NOD mouse model of autoimmune diabetes*. *Proc Natl Acad Sci U S A*, 2007. **104** (46): p. 18181-6.
183. Picca, C.C., et al., *Thymocyte deletion can bias Treg formation toward low-abundance self-peptide*. *Eur J Immunol*, 2009. **39** (12): p. 3301-6.
184. Lee, H.M., et al., *A broad range of self-reactivity drives thymic regulatory T cell selection to limit responses to self*. *Immunity*, 2012. **37** (3): p. 475-86.
185. Bautista, J.L., et al., *Intraclonal competition limits the fate determination of regulatory T cells in the thymus*. *Nat Immunol*, 2009. **10** (6): p. 610-7.
186. Leung, M.W., S. Shen, and J.J. Lafaille, *TCR-dependent differentiation of thymic Foxp3+ cells is limited to small clonal sizes*. *J Exp Med*, 2009. **206** (10): p. 2121-30.
187. Kieback, E., et al., *Thymus-Derived Regulatory T Cells Are Positively Selected on Natural Self-Antigen through Cognate Interactions of High Functional Avidity*. *Immunity*, 2016. **44** (5): p. 1114-26.
188. Greer, J.M. and M.B. Lees, *Myelin proteolipid protein--the first 50 years*. *Int J Biochem Cell Biol*, 2002. **34** (3): p. 211-5.
189. Hellings, N., et al., *Longitudinal study of antimyelin T-cell reactivity in relapsing-remitting multiple sclerosis: association with clinical and MRI activity*. *J Neuroimmunol*, 2002. **126** (1-2): p. 143-60.
190. Simmons, S.B., et al., *Modeling the heterogeneity of multiple sclerosis in animals*. *Trends Immunol*, 2013. **34** (8): p. 410-22.
191. Tuohy, V.K., et al., *Identification of an encephalitogenic determinant of myelin proteolipid protein for SJL mice*. *J Immunol*, 1989. **142** (5): p. 1523-7.

192. Tuohy, V.K., R.A. Sobel, and M.B. Lees, *Myelin proteolipid protein-induced experimental allergic encephalomyelitis. Variations of disease expression in different strains of mice.* J Immunol, 1988. **140** (6): p. 1868-73.
193. Wang, L., et al., *Epitope-Specific Tolerance Modes Differentially Specify Susceptibility to Proteolipid Protein-Induced Experimental Autoimmune Encephalomyelitis.* Front Immunol, 2017. **8**: p. 1511.
194. Greer, J.M., et al., *Identification and characterization of a second encephalitogenic determinant of myelin proteolipid protein (residues 178-191) for SJL mice.* J Immunol, 1992. **149** (3): p. 783-8.
195. Tuohy, V.K. and D.M. Thomas, *Sequence 104-117 of myelin proteolipid protein is a cryptic encephalitogenic T cell determinant for SJL/J mice.* J Neuroimmunol, 1995. **56** (2): p. 161-70.
196. Voskuhl, R.R., *Myelin protein expression in lymphoid tissues: implications for peripheral tolerance.* Immunol Rev, 1998. **164**: p. 81-92.
197. Moon, J.J., et al., *Naive CD4(+) T cell frequency varies for different epitopes and predicts repertoire diversity and response magnitude.* Immunity, 2007. **27** (2): p. 203-13.
198. Scott, C.A., et al., *Role of chain pairing for the production of functional soluble IA major histocompatibility complex class II molecules.* J Exp Med, 1996. **183** (5): p. 2087-95.
199. Beckett, D., E. Kovaleva, and P.J. Schatz, *A minimal peptide substrate in biotin holoenzyme synthetase-catalyzed biotinylation.* Protein Sci, 1999. **8** (4): p. 921-9.
200. Yang, J., et al., *In vivo biotinylation of the major histocompatibility complex (MHC) class II/peptide complex by coexpression of BirA enzyme for the generation of MHC class II/tetramers.* Hum Immunol, 2004. **65** (7): p. 692-9.
201. Kozono, H., et al., *Production of soluble MHC class II proteins with covalently bound single peptides.* Nature, 1994. **369** (6476): p. 151-4.
202. Kouskoff, V., et al., *Cassette vectors directing expression of T cell receptor genes in transgenic mice.* J Immunol Methods, 1995. **180** (2): p. 273-80.
203. Klugmann, M., et al., *Assembly of CNS myelin in the absence of proteolipid protein.* Neuron, 1997. **18** (1): p. 59-70.
204. Ramsey C, W.O., Puhakka L, Halonen M, Moro A, Kampe O, et al., *Aire deficient mice develop multiple features of APECED phenotype and show altered immune response.* Hum Mol Genet, 2002.
205. Rossi, S.W., et al., *Keratinocyte growth factor (KGF) enhances postnatal T-cell development via enhancements in proliferation and function of thymic epithelial cells.* Blood, 2007. **109** (9): p. 3803-11.
206. Luders, K.A., et al., *Genetic dissection of oligodendroglial and neuronal Plp1 function in a novel mouse model of spastic paraplegia type 2.* Glia, 2017. **65** (11): p. 1762-1776.

207. Fontenot, J.D., et al., *Regulatory T cell lineage specification by the forkhead transcription factor foxp3*. *Immunity*, 2005. 22 (3): p. 329-41.
208. Lahl, K., et al., *Selective depletion of Foxp3+ regulatory T cells induces a scurfy-like disease*. *J Exp Med*, 2007. 204 (1): p. 57-63.
209. Mombaerts, P., et al., *RAG-1-deficient mice have no mature B and T lymphocytes*. *Cell*, 1992. 68 (5): p. 869-77.
210. Mombaerts, P., et al., *Mutations in T-cell antigen receptor genes alpha and beta block thymocyte development at different stages*. *Nature*, 1992. 360 (6401): p. 225-31.
211. Alamyar, E., et al., *IMGT((R)) tools for the nucleotide analysis of immunoglobulin (IG) and T cell receptor (TR) V-(D)-J repertoires, polymorphisms, and IG mutations: IMGT/V-QUEST and IMGT/HighV-QUEST for NGS*. *Methods Mol Biol*, 2012. 882: p. 569-604.
212. Dossinger, G., et al., *MHC multimer-guided and cell culture-independent isolation of functional T cell receptors from single cells facilitates TCR identification for immunotherapy*. *PLoS One*, 2013. 8 (4): p. e61384.
213. Moon, J.J., et al., *Tracking epitope-specific T cells*. *Nat Protoc*, 2009. 4 (4): p. 565-81.
214. Moon, J.J., et al., *Quantitative impact of thymic selection on Foxp3+ and Foxp3- subsets of self-peptide/MHC class II-specific CD4+ T cells*. *Proc Natl Acad Sci U S A*, 2011. 108 (35): p. 14602-7.
215. Tubo, N.J., et al., *Single naive CD4+ T cells from a diverse repertoire produce different effector cell types during infection*. *Cell*, 2013. 153 (4): p. 785-96.
216. Davis, M.M. and P.J. Bjorkman, *T-cell antigen receptor genes and T-cell recognition*. *Nature*, 1988. 334 (6181): p. 395-402.
217. Jenkins, M.K., et al., *On the composition of the preimmune repertoire of T cells specific for Peptide-major histocompatibility complex ligands*. *Annu Rev Immunol*, 2010. 28: p. 275-94.
218. Winnewisser, J., *Central tolerance induction to the self-antigen PLP*. Dissertation, 2015.
219. Thiault, N., et al., *Peripheral regulatory T lymphocytes recirculating to the thymus suppress the development of their precursors*. *Nat Immunol*, 2015. 16 (6): p. 628-34.
220. Cowan, J.E., N.I. McCarthy, and G. Anderson, *CCR7 Controls Thymus Recirculation, but Not Production and Emigration, of Foxp3(+) T Cells*. *Cell Rep*, 2016. 14 (5): p. 1041-1048.
221. Wang, L., *Mechanisms of central and peripheral T cell tolerance to an antigen of the central nervous system*. Dissertation, 2017.
222. Painter, C.A. and L.J. Stern, *Conformational variation in structures of classical and non-classical MHCII proteins and functional implications*. *Immunol Rev*, 2012. 250 (1): p. 144-57.

223. Nelson, R.W., et al., *T cell receptor cross-reactivity between similar foreign and self peptides influences naive cell population size and autoimmunity*. *Immunity*, 2015. **42** (1): p. 95-107.
224. Blattman, J.N., et al., *Estimating the precursor frequency of naive antigen-specific CD8 T cells*. *J Exp Med*, 2002. **195** (5): p. 657-64.
225. Whitmire, J.K., N. Benning, and J.L. Whitton, *Precursor frequency, nonlinear proliferation, and functional maturation of virus-specific CD4+ T cells*. *J Immunol*, 2006. **176** (5): p. 3028-36.
226. Bouneaud, C., P. Kourilsky, and P. Bousso, *Impact of negative selection on the T cell repertoire reactive to a self-peptide: a large fraction of T cell clones escapes clonal deletion*. *Immunity*, 2000. **13** (6): p. 829-40.
227. Malchow, S., et al., *Aire-dependent thymic development of tumor-associated regulatory T cells*. *Science*, 2013. **339** (6124): p. 1219-24.
228. Malherbe, L., et al., *Clonal selection of helper T cells is determined by an affinity threshold with no further skewing of TCR binding properties*. *Immunity*, 2004. **21** (5): p. 669-79.
229. Zehn, D. and M.J. Bevan, *T cells with low avidity for a tissue-restricted antigen routinely evade central and peripheral tolerance and cause autoimmunity*. *Immunity*, 2006. **25** (2): p. 261-70.
230. Zhang, J., et al., *Increased frequency of interleukin 2-responsive T cells specific for myelin basic protein and proteolipid protein in peripheral blood and cerebrospinal fluid of patients with multiple sclerosis*. *J Exp Med*, 1994. **179** (3): p. 973-84.
231. Koutrolos, M., et al., *Treg cells mediate recovery from EAE by controlling effector T cell proliferation and motility in the CNS*. *Acta Neuropathol Commun*, 2014. **2**: p. 163.
232. Chappert, P. and R.H. Schwartz, *Induction of T cell anergy: integration of environmental cues and infectious tolerance*. *Curr Opin Immunol*, 2010. **22** (5): p. 552-9.
233. Perniola, R., *Twenty Years of AIRE*. *Front Immunol*, 2018. **9**: p. 98.
234. Arpaia, N., et al., *Metabolites produced by commensal bacteria promote peripheral regulatory T-cell generation*. *Nature*, 2013. **504** (7480): p. 451-5.
235. Lathrop, S.K., et al., *Peripheral education of the immune system by colonic commensal microbiota*. *Nature*, 2011. **478** (7368): p. 250-4.
236. Josefowicz, S.Z., et al., *Extrathymically generated regulatory T cells control mucosal TH2 inflammation*. *Nature*, 2012. **482** (7385): p. 395-9.
237. Samstein, R.M., et al., *Extrathymic generation of regulatory T cells in placental mammals mitigates maternal-fetal conflict*. *Cell*, 2012. **150** (1): p. 29-38.
238. Josefowicz, S.Z., L.F. Lu, and A.Y. Rudensky, *Regulatory T cells: mechanisms of differentiation and function*. *Annu Rev Immunol*, 2012. **30**: p. 531-64.

239. Hsieh, C.S., H.M. Lee, and C.W. Lio, *Selection of regulatory T cells in the thymus*. *Nat Rev Immunol*, 2012. **12** (3): p. 157-67.
240. Palmer, E., *Negative selection--clearing out the bad apples from the T-cell repertoire*. *Nat Rev Immunol*, 2003. **3** (5): p. 383-91.
241. von Boehmer, H., H.S. Teh, and P. Kisielow, *The thymus selects the useful, neglects the useless and destroys the harmful*. *Immunol Today*, 1989. **10** (2): p. 57-61.
242. Enouz, S., et al., *Autoreactive T cells bypass negative selection and respond to self-antigen stimulation during infection*. *J Exp Med*, 2012. **209** (10): p. 1769-79.
243. Koehli, S., et al., *Optimal T-cell receptor affinity for inducing autoimmunity*. *Proc Natl Acad Sci U S A*, 2014. **111** (48): p. 17248-53.
244. Wooldridge, L., et al., *Tricks with tetramers: how to get the most from multimeric peptide-MHC*. *Immunology*, 2009. **126** (2): p. 147-64.
245. Klein, L., K. Khazaie, and H. von Boehmer, *In vivo dynamics of antigen-specific regulatory T cells not predicted from behavior in vitro*. *Proc Natl Acad Sci U S A*, 2003. **100** (15): p. 8886-91.
246. Stadinski, B.D., et al., *A temporal thymic selection switch and ligand binding kinetics constrain neonatal Foxp3(+) Treg cell development*. *Nat Immunol*, 2019. **20** (8): p. 1046-1058.
247. Kedl, R.M., et al., *T cells compete for access to antigen-bearing antigen-presenting cells*. *J Exp Med*, 2000. **192** (8): p. 1105-13.
248. Kedl, R.M., et al., *T cells down-modulate peptide-MHC complexes on APCs in vivo*. *Nat Immunol*, 2002. **3** (1): p. 27-32.

7. Appendix

7.1 Table of figures

Figure 1: V(D)J recombination of TCR loci in developing thymocytes.....	14
Figure 2: Role of cTECs in T cell development.....	16
Figure 3: Medullary thymic epithelia cells (mTECs) and their function in central tolerance	20
Figure 4: Peripheral tolerance mechanisms	25
Figure 5: Affinity and avidity-dependent models of thymocyte selection	26
Figure 6: T cell epitopes of PLP1 in C57BL/6 and SJL mouse strains	29
Figure 7: Schematic overview of single cell TCR α -chain sequencing.....	42
Figure 8: TCR-A, TCR-H and TCR-E gene fragment.....	45
Figure 9: TCR-F gene fragment.....	45
Figure 10: PLP1 ₁₁₋₁₉ and PLP1 ₂₄₀₋₂₄₈ binding prediction and cloning strategy	50
Figure 11: Tetramer functionality upon respective peptide immunization	51
Figure 12: Abundance and phenotype of peripheral PLP1-specific CD4 ⁺ T cells in the polyclonal repertoire	52
Figure 13: Abundance and phenotype of PLP1-specific CD4 SP thymocytes in the polyclonal repertoire	53
Figure 14: T _{reg} cell induction in C57BL/6 and Fixed- β mice.....	55
Figure 15: PLP1 specific regulatory T cell in Fixed- β :: <i>Plp1</i> ^{WT} lymph nodes	56
Figure 16: Peripheral Tet-1 ⁺ CD4 ⁺ T cells display an activated and anergic phenotype in the presence of antigen	58
Figure 17: Deletion and T _{reg} cell diversion of autoreactive CD4 SP Tet-1 ⁺ thymocytes in PLP1-sufficient mice	59
Figure 18: Mature CD4 SP thymocytes express the peripheral anergy markers FR4 and CD73	60

Figure 19: Central tolerance of Tet-1⁺ T cells depends on PLP1 and AIRE expression by
TECs62

Figure 20: Peripheral tolerance of Tet-1⁺ T cells depends on cd11c expressing cells.....64

Figure 21: TCR α-chain sequencing of Tet-1⁺ T cells.....68

Figure 22: Central tolerance mechanisms in PLP1-specific TCR transgenic mice.....69

Figure 23: Peripheral TCR transgenic T cells display various cell fates71

Figure 24: *Ex vivo* dose-response curves for TCR transgenic thymocytes.....72

Figure 25: Changing the TCR:pMHCII ratio uncovers a window for T_{reg} cell induction ...83

Figure 26: Our proposed model of thymocyte selection86

7.2 Abbreviations

aa	amino acid
Aire	autoimmune regulator
APC	antigen-presenting cell
APECED	autoimmune polyendocrinopathy, candidiasis and ectodermal dystrophy
A(M/D/T)P	adenosin (mono/di/tri) phosphate
BM	bone marrow
CMJ	cortico-medullary junction
CD	cluster of differentiation
cDC/pDC	conventional/plasmacytoid dendritic cell
CNS	central nerve system
cTEC	cortical thymic epithelia cell
CTSL	cathepsin L
CTV	cell trace violet
DN/DP	double negative / double positive
EAE	experimental autoimmune encephalomyelitis
FoxP3	forkhead box P3
FoxN1	forkhead box N1
FR4	folate receptor 4
GFP	green fluorescent protein
HEL	hen egg lysozyme
IDO1	indoleamine 2,3-dioxygenase-1
IFN	Interferon
IL	interleukine
IRBP	interphotoreceptor retinoid-binding protein
KO	knockout
MACS	magnetic-activated cell sorting
MBP	myelin basic protein

MHCI/II	major histocompatibility complex class 1/2
MOG	myelin oligodendrocyte glycoprotein
mTEC	medular thymic epithelia cell
NFAT	nuclear factor of activated T cells
Nrp1	Neuropilin-1
NOD	non-obese diabetic
PGE	promiscuous gene expression
PLP1	proteolipid protein 1
RAG	recombination activating gen
S1P(R)	sphingosine-1-phosphate (receptor)
SP	single positive
TCR	T cell receptor
Tg	transgenic
TdT	terminal deoxynucleotidyl transferase
TGF-β	tumor growth factor β
TRA	tissue restricted antigen
TSSP	thymus specific serine protease
OVA	ovalbumin
VDJ	variable diversity joining
WT	wild type
A2aR	Adenosine A2a receptor
BTLA	B- and T-lymphocyte attenuator
CTLA-4	cytotoxic T-lymphocyte-associated protein 4
LAG3	lymphocyte activating 3
PD-1	programmed cell death protein 1
TIM-3	T-cell immunoglobulin mucin-3
VISTA	V-domain Ig suppressor of T cell activation

7.3 Eidesstattliche Versicherung



LUDWIG-
MAXIMILIANS-
UNIVERSITÄT
MÜNCHEN

Promotionsbüro
Medizinische Fakultät



Eidesstattliche Versicherung

Name, Vorname

Ich erkläre hiermit an Eides statt,
dass ich die vorliegende Dissertation mit dem Titel

selbständig verfasst, mich außer der angegebenen keiner weiteren Hilfsmittel bedient und alle Erkenntnisse, die aus dem Schrifttum ganz oder annähernd übernommen sind, als solche kenntlich gemacht und nach ihrer Herkunft unter Bezeichnung der Fundstelle einzeln nachgewiesen habe.

Ich erkläre des Weiteren, dass die hier vorgelegte Dissertation nicht in gleicher oder in ähnlicher Form bei einer anderen Stelle zur Erlangung eines akademischen Grades eingereicht wurde.

Ort, Datum

Tobias Johannes Haßler

Unterschrift Doktorandin bzw. Doktorand